ADDIS ABABA UNIVERSITY

ADDIS ABABA INSTITUTE OF TECHNOLOGY

SCHOOL OF CIVIL AND ENVIRONMENTAL ENGINEERING

EFFECT OF LAYERED REINFORCEMENT ARRANGEMENT ON DEFORMATION AND CRACKING OF REINFORCED CONCRETE BEAMS

A Thesis in Structural Engineering

By Eden Shiferaw Weyessa

Addis Ababa

A Thesis

Submitted in Partial Fulfillment of the Requirements for the Degree of Master of Science

The undersigned have examined the thesis entitled '**Effect of layered reinforcement arrangement on deformation and cracking of reinforced concrete beams**' presented by **Eden Shiferaw Weyessa**, a candidate for the degree of **Master of Science** and hereby certify that it is worthy of acceptance.

Dr. Bedilu Habte		
Advisor	Signature	Date
Dr. Shifferaw Taye		
Internal Examiner	Signature	Date
Dr. Abraham Gebre		
External Examiner	Signature	Date
Dr. Ing. Mebruk Mohammed		
Chair person	Signature	Date

UNDERTAKING

I certify that research work titled “Effect of layered reinforcement arrangement on deformation and cracking of reinforced concrete beams” is my own work. The work has not been presented elsewhere for assessment. Where material has been used from other sources it has been properly acknowledged / referred.

Signature ……...

Eden Shiferaw

September/2020

ABSTRACT

The purpose of this work is to study the effect of layered reinforcement arrangement on the deformation and cracking of reinforced concrete beams in both flexural and tensile loading. The study is based on analytical simulation of four flexural beams and eleven tensile beams in objective of studying the response and behavior of concrete and reinforcement with different arrangements of reinforcements.

Even though experiments observed in different literatures show a good agreement with code predictions, there are still inadequacies in predicting reinforced concrete elements cracking behavior with different arrangements of reinforcement bars. In order to increase adequacy of serviceability results related with effect of reinforcement bar arrangement on reinforced concrete elements cracking behavior, detailed assessment is required.

The analytical simulation was attempted using a non-linear finite element tool called ABAQUS CAE for beams with different arrangement of reinforcement bars and different concrete grades.

Results of simulation from flexural elements showed that different reinforcement layouts show correlation with flexural stiffness and do not show direct relationship with reinforced concrete structures cracking behavior.

Considering the tensile members, the strain observed in the specimens varies not only along the bar but also with in the surface of the concrete section. Adequacy of evaluating the cracking behavior in the members is closely associated with assessing the strain in the concrete since the strain in the reinforcements is similar in the cases considered.

Key words: - Cracking, finite element

ACKNOWLEDGMENTS

First and foremost, praises and thanks be to God, the almighty, for his showers of blessings throughout my research work to complete the research successfully.

I would also like to express my sincere gratitude to my advisor Dr. Bedilu Habte, Addis Ababa university, Institute of technology, for his supervision, comments and guidance throughout this research work.

I am extremely grateful to my parents for their love, prayers, caring and sacrifices for educating and preparing me for my future. I cannot thank you enough.

My special thanks goes to my uncle Engineer Endale (PEng) for his encouragement and motivation throughout the class time and the research work.

I also like to thank Eyerusalem Haile and her beloved family for encouraging and supporting me throughout this study.

Last but not least, I would also like to pass my appreciation towards my friends and all my family who in one way or the other helped me to accomplish this study.

Thank you!

TABLE OF CONTENTS

LIST OF TABLES

LIST OF FIGURES

LIST OF SYMBOLS AND ABBREVIATIONS

Notations

A_c	area of concrete
A_{ce}	effective area of concrete
A_s	area of reinforcement
c_o	minimum cover to the longitudinal reinforcement
d_c	compressive damage of concrete
d_t	tensile damage
E_c	young's modulus of the concrete section
E'_c	secant deformation modulus of the concrete
E_s	modulus of elasticity of the reinforcement
f_{bo}	biaxial compressive yield stress
f_{cm}	mean compressive strength
f_{co}	uniaxial compressive yield stress
f_{ct}	tensile strength of concrete
f_t	axial tensile strength
G_f	fracture energy
$h_{c,eff}$	effective height of concrete in the tension zone
h_o	height of crack
I	moment of inertia of the section
k_1	curvature in uncracked region
k_2	curvature in cracked region
M	moment
M_{cr}	cracking moment
N	Axial load
N_c	internal force induced in the concrete
N_{cr}	cracking force
Ns	internal force induced in the reinforcement
P	external load
$S_{r,\,max}$	maximum crack spacing
u_t^{ck}	cracking displacement
u_t^{pl}	plastic cracking displacement
w	crack opening displacement

W_1 section modulus of uncracked region

wc crack opening displacement at which stress can no longer be transferred

W_k crack width

α mean value of the parameter of interest (strain, curvature, or deflection)

α_1 value computed in the uncracked section

α_2 value computed in the cracked section

α_e ratio between elastic modulus of reinforcement and concrete

β factor that takes into account long term effects

ε_c strain of concrete

ε_{c1} strain of concrete at peak stress

εc^{in} inelastic strain of concrete

εc^{pl} plastic strain of concrete

ε_{cm} mean strain of concrete

ε_{cu1} nominal ultimate strain

ε_m average strain of a section

$\varepsilon_{oc}{}^{el}$ elastic strain corresponding undamaged material

ε_s strain of reinforcement

ε_{sm} mean strain of reinforcement

σ_c stress in concrete

σ_S stress in the tension reinforcement calculated on the basis of a cracked section

σ_{SR} stress in the tension reinforcement under a loading causing first cracking

σt tensile stress

η ratio between strains of concrete at normal and peak stress

$\rho_{s,eff}$ ratio between area of reinforcement and effective area of concrete in tension zone

ζ distribution coefficient

τ Bond stress

Abbreviations

RC	reinforced concrete
HSC	high strength concrete
NSC	normal strength concrete
FRC	fiber reinforced concrete
EBCS	Ethiopian building code of standard
FE	finite element
FEM	finite element model
CDP	concrete damaged plasticity model
C3D8R	three dimensional 8-noded hexahedral element with reduced integration
T3D2	three dimensional linear truss element
NLGEOM	nonlinear geometry

CHAPTER 1 INTRODUCTION

1.1 Background

Reinforced concrete beams are flexural members which are used in most of civil engineering constructions. These members are designed to allow a certain local damage to occur in the ultimate limit state, assuming all the tensile forces are carried by the steel bars. In a cross-sectional design process, the ultimate compressive concrete strain may control the limit of the damage so as to prevent crushing when yielding of reinforcement bars occur. The occurrence of cracking in concrete is an expected phenomenon for relatively high load. It should be noted however, that cracks, in cases where no pre-stressing is applied, are expected to form even for a small portion of the ultimate load, i.e. already in the service state. In addition to the ultimate limit state considerations, in structural elements design considering serviceability limit state cracks and flexural deflections in reinforced concrete beams, according to a sound design, should be controlled with respect to crack width and should be well distributed over the length of the member.

Cracking in concrete is accompanied by overall stiffness reduction, larger deflections, lack of homogeneity of the cross-section, and it is also aesthetically undesired. In addition, large cracks contribute to the structural member's increased permeability which, under extreme environmental conditions, may enhance corrosion in reinforcement, spalling of cover and bond degradation at the interface between the constituent materials [1].

Thus, crack in reinforced concrete beams might be harmful, but on the other hand in most structural engineering applications it cannot be totally avoided. Such considerations stress the significance in structural engineering for accurate measurement of crack widths and crack pattern [1].

1.2 Statement of the problem

Reinforced Concrete (RC) is a composite construction material made up of concrete and reinforcing steel. The constitutive materials have different mechanical behavior and physical features and also behave differently in their structural response.

Cracking is an important feature of the behavior of concrete structures. The concrete structures are usually full of cracks even under service loads. Obviously, cracking should be taken into account when forecasting ultimate load capacity as well as service behavior [4].

In design of structural elements considering serviceability limit state, limitation of crack width and deformation become the governing criterions. However, such designs are difficult problems in engineering since they are usually done at design stages. Serviceability behavior depends mostly on the concrete properties, which are often unknown at the design stage. After crack initiation, reinforcement layout plays an important role in cracking performance and deformation behavior of the concrete elements. But there are still inadequacies in predicting reinforced concrete elements cracking behavior with different arrangements of reinforcement bars. In order to increase adequacy of serviceability results related with effect of reinforcement bar arrangement on the reinforced concrete elements cracking behavior, detailed assessment is required.

This thesis tried to study on the cracking and deformation behavior of reinforced concrete beams considering the effect of layered reinforcement bar arrangement.

1.3 Objective

The main objective of this research was to study the cracking and deformation behavior in reinforced concrete beams considering the effect of layered reinforcement bar arrangement.

Specific objectives:-

- To study the behavior of the local damage in the concrete.
- To study the behavior of the reinforcement bars in time of fracture.

- To study the reinforcement arrangement effect on the behavior of the constitutive materials.
- To develop a finite element model of a beam that is able to describe the interaction between reinforcement bars and concrete to study the cracking and deformation behavior considering the effect of reinforcement bar arrangement.

1.4 Significance of the study

This thesis presented the effect of layered reinforcement arrangement on deformation and cracking of reinforced concrete beams. This will help to add knowledge about the behaviour of the constitutive materials and the relation between them in time of fracture considering reinforcement bar arrangement effect. This will also help future researchers practicing in this area of study.

1.5 Methodology

The objectives of this thesis work were achieved by the methods outlined below.

1.5.1 Material property selection

Even if there are different material properties to be adopted for the constitutive materials of a reinforced concrete beam, for the purpose of this thesis work all material properties were taken from the new Ethiopian building code.

1.5.2 Methodology adopted

This thesis tried to study the effect of layered reinforcement arrangement on cracking and deformation of reinforced concrete beams by developing a finite element model of beams which can describe the interaction between the reinforcement and the cracked concrete.

The thesis gave emphasis to the local damage in the concrete and also the behavior in the reinforcement separately and also about the deformation and cracking behavior of the constitutive materials in time of fracture considering reinforcement bar arrangement.

The outputs of the analysis were compared with experimental results from literature. After comparing the results, final conclusion and recommendations are provided.

1.6 Scope and limitations

This thesis focused on immediate/short-term loadings applied on reinforced concrete flexural and tensile elements. This helped to emphasize on the role of concrete in tension for such elements considering different arrangements of reinforcements.

Long term effects resulting from shrinkage and creep were not considered here. In addition, deep beams, pre-stressed beams and beam-columns were not considered in this reference.

1.7 Thesis organization

This thesis is composed of five chapters including this chapter. Chapter 2 is focused on the behavior and effects responsible for the cracking and deformation performance of reinforced concrete members and provides current specification for analysis and design of reinforced concrete elements according to EBCS EN 1992-1-1:2013. Chapter 3 discussed the finite element model and analysis procedures and validation for reinforced concrete beam taking experimental results from literature. Results and discussions considering finite element model outputs for reinforced concrete flexural and tensile elements are summarized and presented in chapter 4. Chapter 5 presented the conclusion and recommendations for the overall thesis work. Analytical calculation results are shown in detail in the appendices.

CHAPTER 2 LITERATURE REVIEW

2.1 Behavior of reinforced concrete structures

2.1.1 Introduction

Reinforced Concrete (RC) is a composite construction material made up of concrete and reinforcing steel. The concrete itself is a composite material which derives its material properties (strength and stiffness) from its constituent elements, i.e. aggregates, cement and their interface. At an elementary level, damage in concrete implies degradation of its constituent elements and weakening of the interaction between them. This could occur due to the external load applied on the structure or the internal stresses developed within the structure due to deterioration of the material (Saurabh, 2017).

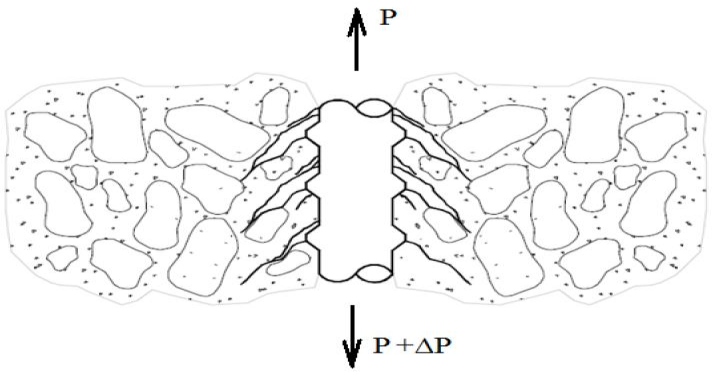

Figure 2- 1 Steel-concrete bond (Yun Lin, 2010)

The stressing and consequent damage of the RC structures is caused by a combination of mechanisms, which may depend on a number of factors like temperature, porosity, water-cement ratio, etc. Hence in reality, it is often difficult to attribute the cause of damage to specific mechanisms and to quantitatively describe the change in material properties. However, due to the fact that the resistance of concrete to tensile load is drastically lower than its strength in compression, damage in concrete is generally accompanied by cracking on the surface (Saurabh, 2017).

Cracks are undesirable in reinforced concrete structures because they:

- look no good
- affect service life of structures

- alter stiffness and change the force distribution in the system
- make sound as if structure is in danger.

Because of the fragile nature of the concrete and the changing loading conditions and other factors not included in design (such as internal casting stresses), cracks in concrete structures can never be completely avoided in practice (Gerd-Jan et al, 2011).

Cracks can occur in a Reinforced Concrete (RC) structure when it is subjected to bending, shear, torsion or tension loading. They may also arise from other phenomena, for example, shrinkage. Some problems such as a leakage from the inside of the structure, an intrusion from the exterior or corrosion in the steel bar may occur because of the cracks. Thus, the crack opening has to be limited in order to maintain the proper functioning or the durability of the structure (Nuraziz, 2017).

For a concrete structure to be serviceable cracking must be controlled and deflection must not be excessive. Service load behavior primarily depends on the concrete properties and these are often not accurately established at the design level. In the design of concrete structures, it is essential to check the serviceability of the structure particularly in the post-cracking range. The behavior in this range is complicated by the effects of several factors which are difficult to assess from purely analytical considerations. The effects of tension stiffening, the spontaneous evolution of primary cracks and secondary cracks in regions between the primary cracks and around the reinforcing bars, and the degree of bond breakdown are of primary importance (R.I. Gilbert, 2017).

2.1.2 Post-Cracking Behavior of Reinforced Concrete Beams

Cracking is recognized as one of the most significant sources of uncertainty in concrete behavior, no predictive accuracy of the concrete behavior can be obtained without a detailed understanding of the concrete post-cracking behavior.

Consider a singly reinforced concrete beam that is subjected to a gradually increasing moment. Prior to cracking, when the applied moment is small, concrete stresses are small and the member behaves in a linear and elastic manner. Concrete stresses and strains on an uncracked section may be considered using the transformed section properties, i.e. an equivalent homogeneous section in which the steel areas are converted into equivalent areas of concrete. However, because steel qualities are typically small, it is usual to ignore

the steel and to calculate stresses and strains prior to cracking using the gross section properties (R.I. Gilbert, 2017).

When the concrete's tensile strength is reached in the extreme tensile fiber cracking occurs. Cracking initiates a marked redistribution of internal stresses and structural behavior becomes nonlinear. As load is gradually increased, the first cracks to form are the primary cracks, which penetrate spontaneously to a height h_o, just below the neutral axis. ho can readily be calculated by standard elastic theory and is the height required to re-establish equilibrium and strain compatibility once cracking has commenced.

The height h_o also governs the crack spacing. The formation of a crack reduces the concrete tensile stresses for a distance of approximately h_o on either side of the crack. In these zones of reduced stress, other cracks are unlikely to form. Therefore, the spacing of the primary cracks is usually between h_o and $2h_o$ (R.I. Gilbert, 2017).

When the primary crack pattern is established, secondary or cover-controlled cracks tend to form in between the primary cracks as the load is increased. They tend to penetrate less deeply and exist only around the reinforcement bars. For perfect 'no-slip' conditions, these cracks form by elastic recovery of the concrete and occur at a spacing of between c_o and $2c_o$, where c_o is the minimum cover to the longitudinal reinforcement (R.I. Gilbert, 2017). After cracking, due to the bond between the steel and the concrete, the intact concrete between adjacent primary cracks carries substantial tensile force, primarily towards the reinforcement. Over a gauge length containing several cracks, the average tensile stress on concrete is a significant percentage of concrete's tensile strength. The stress in the steel is maximum at a crack, carrying the entire tensile force, and drops to a minimum between the cracks. The member's flexural rigidity is substantially greater than that centered on a fully cracked portion, of which tensioned concrete is believed to bear zero stress (R.I. Gilbert, 2017).

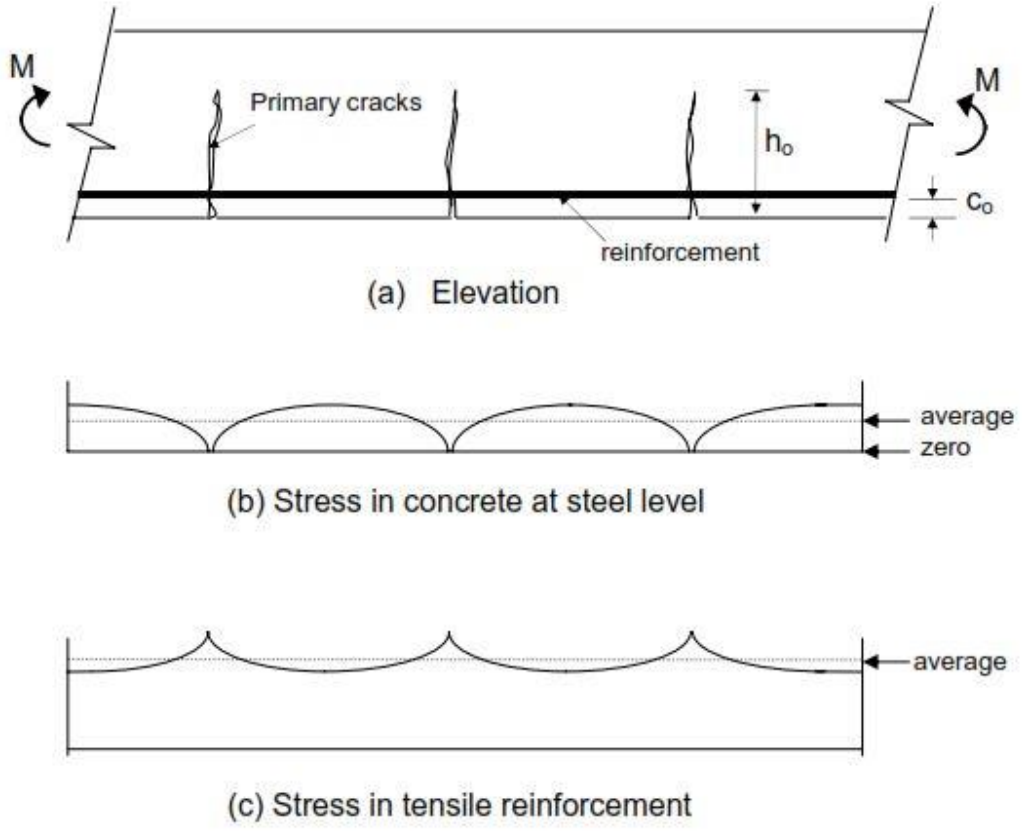

Figure 2- 2 Stresses at steel level in a cracked reinforced concrete member (S. Nejadi, 2017)

2.1.3 Bond-Slip Mechanisms

To predict the cracking and deformation behavior of reinforced concrete members, it is very important to study the transfer of bond stress in the concrete and reinforcement interface zone, which is correlated with studying the bond-slip behavior.

The bond-action of the steel bar interface and surrounding concrete has an important impact on the initiation and distribution of cracks in reinforced concrete members. The bond-action in concrete structures is the key contributing factor to the tension stiffening effect.

A rise in loading can result in an increase in steel strain in a cracked reinforced concrete member, which will cause an extension of the reinforcing bar. Ribs in the bar then appear to move towards the nearest crack relative to the surrounding concrete, i.e. bond-slip is initialized. This will raise the stress on the concrete from the rib bearing and lead to the bond-slip.

2.1.3.1 **Components of Bond-Slip Mechanisms**

The bond-slip mechanism comprises three components, i.e. chemical adhesion, friction and mechanical interlocking of the bar ribs to the concrete. Chemical adhesion depends on the chemical reaction between the reinforcing steel bars and the concrete, friction depends on the surface roughness and the magnitude of friction is related to the normal force to the movement direction, and mechanical interlock depends on the reinforcement geometry and surface deformation. The first two components play a more important and primary role in the bond behavior of plain bars, even though some mechanical interlocking takes place due to the roughness of the bar surface. For deformed bars, mechanical interlock is thought to be the primary mechanism with the others only being secondary effects. However, in spite of acknowledging the three bond components as individual mechanisms, they are not independent. They interact with each other and cannot be analyzed as separated issues. The collective effect of these components leads to different behaviors.

The four general types of bond failure are bar failure, bar pullout, concrete pullout and concrete splitting. Many researchers have contributed to the investigation of bond mechanisms. It is generally accepted that there are different stages of the interaction between steel and concrete when a tensile force is applied to a steel reinforced specimen (Simon Hang Chi chan, 2012).

Several factors affect bonding properties and those who have researched it believe that the bond between steel and concrete in pull-out can be separated into four distinct phases (FIB, 2000).

Stage I is low bond stress values while the concrete is still uncracked, $\tau \leq 0.2\text{-}0.8\ f_{ct}$. The bond is formed mainly by a weak chemical reaction between the steel and the hardened concrete. No bar slip occurs at this stage but extremely localized stresses occur at rib tips on the bar. There may be some relative displacement of the bar but no slip in the bar occurs.

Stage II is when the first crack appears, the stress levels for the bonds are higher, $\tau > 0.2\text{-}0.8\ f_{ct}$. The chemical adhesion breaks down and the bond is provided by friction. High stresses at the top of the ribs cause the concrete to crush locally and micro cracks form. However, the wedge actions, that is the ribs pushing against the surrounding concrete, at the top of the rib remains limited and there are no signs of concrete splitting.

Stage III is for higher bond values, $\tau > 1\text{-}3\ f_{ct}$. The stresses and the wedge action rise. The stress component on the rib can be split into two components, longitudinal bond stress

component causing the transverse cracks and normal stress component causing longitudinal cracks to form; this is the cause of concrete splitting. The tensile force is resisted by circumferential tensile stresses in the concrete. The bond strength and stiffness are assured mostly by interlocking action between the reinforcing bar and the concrete secondly by friction.

Stage IV leads to pull-out or splitting failure. Many factors can influence the type of failure. They can be: the degree of confinement, transverse reinforcements, and size of concrete cover and diameter of reinforcement bars. Splitting failure occurs when radial stresses causes longitudinal cracks that propagate up to the surface, it is typical when bar diameter is large and/or the concrete cover is small. Pull-out failure is initiated by shearing off the concrete keys between the ribs of the reinforcement bars. That usually happens when the concrete cover is thick and/or the transverse reinforcement is not sufficient. Splitting failure is weaker than the pull-out failure.

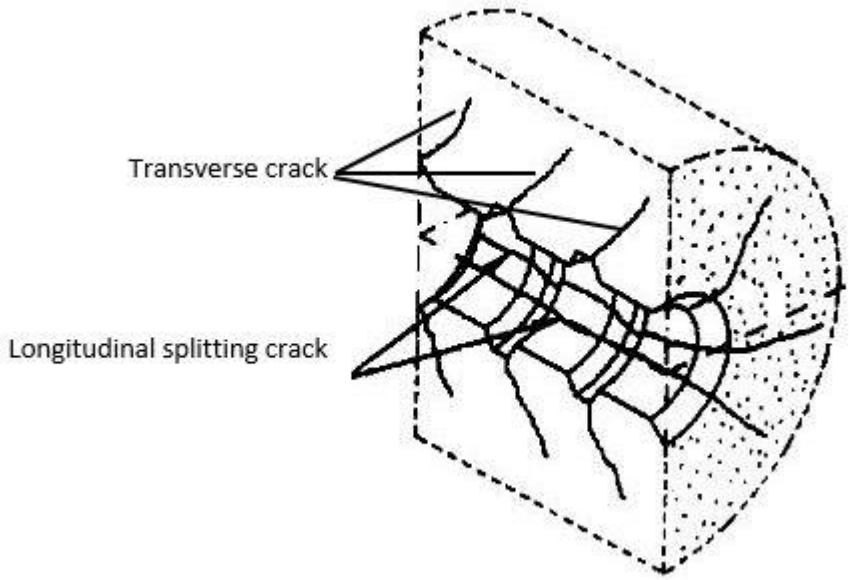

Figure 2- 3 Longitudinal and transverse cracks caused by bond (FIB, 2000)

Secondary internal transverse cracks (radial cracks) are firstly developed at the tips of the ribs to allow slip. Longitudinal cracks are developed and spread, and when further load is applied, the wedging action is enhanced by crushing of the concrete in front of the ribs. Therefore, the component of the wedging action parallel to the reinforcing steel bar

depends on the rib pattern of the reinforcement and the outward component depends on the hoop stress provided by the surrounding confinement (Simon Hang, 2012).

According to (Tepfers R., 1979), as long as there is an undamaged outer concrete ring around the reinforcement, the concrete is capable of exerting a hoop stress around the bar, so that bond strength and stiffness are mostly determined by mechanical interlock.

2.1.4 Factors influencing bond performances

The parameters influencing the bond can be separated into four groups (D. weibe, 2004):

- concrete
    - Concrete composition, E.g. grading curve of the aggregates, binder content
    - Fresh concrete properties, E.g. flow and slump, compatibility
    - Hardened concrete properties, E.g. compressive and tensile strength, modulus of elasticity, fracture characteristics (brittleness)
- properties of the reinforcement
    - Rebar diameter
    - Rib geometry and its arrangement, E.g. high or deep ribbed, orientation and number of rows of the ribs.
    - Relative rib area
- loading regime
    - Short or long term monotonic (static) loading, E.g. loading rate
    - Dynamic loading, E.g. frequency, amplitude
- system parameter
    - Concrete cover, confinement (e.g. due to transverse reinforcement, fibers)
    - Rebar location during casting
    - Rebar Orientation to the way the concrete is casted.

Bond strength is one of the paramount parameters which govern the nature of cracking in concrete structures. This bond will not only depend on concrete strength but also upon the characteristics of the ribs on the reinforcement. A ‘good’ rib pattern, from the serviceability view point, would be expected to have the following characteristics:

- Should provide a strong bond between the rebar and the concrete.
- Should limit width of the concrete cracks to specified limits.

- Should allow ductile RC beam behavior (Simon Hang Chi Chan, 2012).

2.1.5 Influence of bond on structural behavior (ductility)

Bond action is essential not only to guarantee an adequate level of safety, by allowing the two materials (concrete and steel) to work together, but also to control the structural behavior, by providing an adequate level of ductility.

While safety requires bond to have good mechanical properties at the local level, ductility requires bond to withstand large steel strains along the embedded reinforcement, in order to let the strains, spread between two contiguous bending cracks, and to favor the formation of densely-spaced secondary cracks in the concrete (FIB,2000).

2.1.6 Bond models

Bond refers to the interaction between reinforcing steel and the surrounding concrete, which allows transferring of tensile stress from the steel into the concrete. It is a mechanism that permits for reinforcing bar anchorage and affects many other essential structural concrete features such as section stiffness and crack control.

It is well known that the use of deformed bars will significantly improve the bond capacity between steel and concrete. For the satisfactory performance of reinforced concrete structures, adequate bonding between bars and concrete is very important. This is also very important on concrete structures finite element modeling.

Bond models should always include in some way the following topics (FIB, 2000):

- the type of collapse (pull-out and splitting bond failure);
- the reinforcement bar geometry (relative rib area = bond index);
- the type of loading (monotonic/cyclic loads; pulsating/reverse loads);
- the confining action (active/passive confinement);
- the size effects;
- the concrete type (high strength concrete(HSC), normal strength concrete (NSC), fiber reinforced concrete(FRC));
- the environment and its effects on bond (bar corrosion; high/low temperatures);
- the boundary restraints; and
- The specific requirements of RC structures.

There are two main ways to study the cracking and deformation behavior of reinforced concrete.

- Flexural tests of RC beam
- Direct tension tests of RC beams.

The most common way is the beam flexure tests when the beam is exposed to bending by applying either three-point or four-point loading scheme. A shear effect is the main difference between these two flexural tests.

In other way, a direct tension test can be used to analyze reinforced concrete beams cracking and deformation behavior.

2.2 Tension Stiffening Bond Models

2.2.1 Background on tension stiffening bond models

Reinforced concrete members have been commonly used for structural purposes. Tension stiffening refers to tension carrying concrete strength between cracks, which leads to a reinforced concrete member's stability before the reinforcement bar yields. When only concrete is expected to bear stress between the cracks, the reinforcement must hold the entire load at the crack spot. The reinforced concrete component's stiffness influences the efficiency of the member in terms of crack control and deflection. If tension-stiffening effect is neglected, calculated deformation may be overestimated by a large proportion (Yun Lin, 2010).

Concrete cracks when exceeding the tensile stress cap. The cracking in a plain concrete triggers a softening action. Concrete loses its stability at a comparatively high pace as cracking progresses. But the steel reinforcing bars in the tension zone of concrete counteract this softening action. The tensile stress in concrete gradually decreases as cracking develops.

The rigidity of a reinforced concrete (RC) component mounted in axial tension can be regarded as the superposition of the reinforcement stiffness and the stiffness of plain concrete. The steadiness of solid concrete is reduced to that of broken concrete when the RC member is cracked; this is referred to as tension softening. In addition, due to the steel-concrete bond there is a component of stiffness; this is called the tension-stiffening component. Tension softening is a property of plain concrete and model fracture mechanics can be used to simulate that. Tension-stiffening in the presence of

reinforcement bar, is a feature of cracking concrete under tensile stress. The intact cracked concrete between cracks brings a certain amount of tensile force normal to the broken plane due to the reinforcement bond, which contributes to the structure's overall rigidity (Gintaris Kaklauskas et al, 2015)

Crack propagation is a complex phenomenon that relies on the interaction between concrete and reinforcement bar, and plays a significant role in the concrete structure analysis. Tension stiffening models are used to simulate reinforced concrete's post-cracking behavior.

2.2.2 Tension Stiffening Mechanism

To understand true bond stress one must review the process of crack development. When a simply supported beam is loaded past the cracking moment capacity the concrete tensile stress capacity is exceeded which causes cracking. When the beam cracks there are still however portions between the cracks where the concrete still carries tension. As the loading increases, the tensile stress in the concrete between the existing cracks increases until the discrete portion of concrete's tensile capacity is reached and secondary cracks are formed (Graham Dean Roberts, 2015).

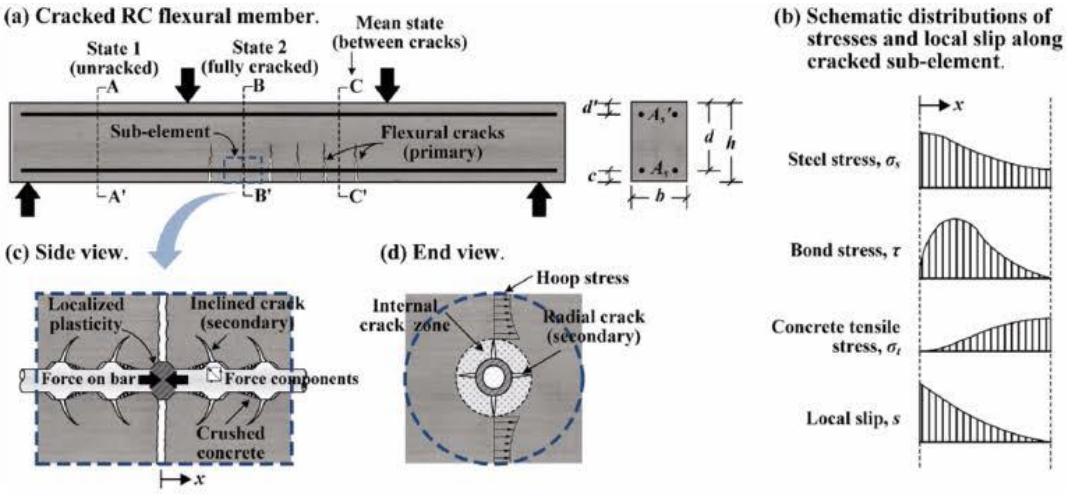

Figure 2- 4 Tension stiffening mechanism [13]

2.3 Design Code Provisions Considering Tension Stiffening

The ES EN 1992-1-1:2013 (Euro code 2) considers tension stiffening in terms of strain, curvature, or deflection, and interpolate the estimated parameter measured on the

uncracked section and on the completely cracked one using the following expressions. The theoretical results from code helps to compare with outputs of simulation.

Considering axial load versus displacement: -

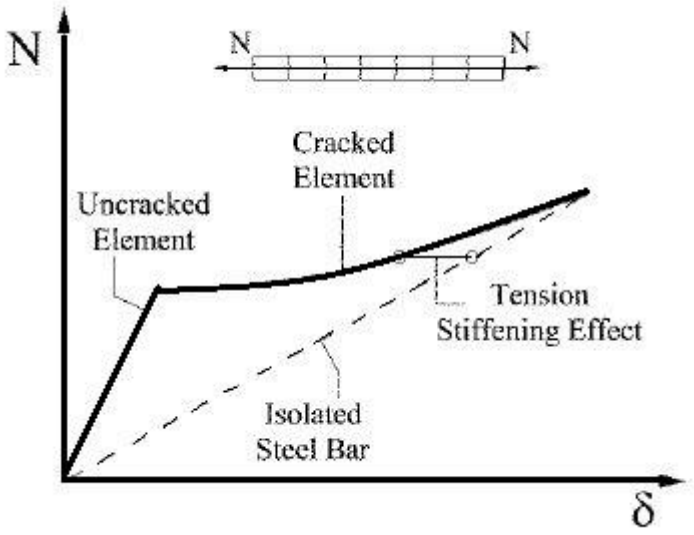

Figure 2- 5 Effects of the tension stiffening on an isolated reinforcing bar (Francesco Morelli et al, 2017)

$$\alpha = \zeta\alpha_2 + (1-\zeta)\alpha_1 \tag{2-1}$$

$$\zeta = 1-\beta\left(\frac{\sigma_{SR}}{\sigma_S}\right)^2 \tag{2-2}$$

Where: -

- α is the mean value of the parameter of interest (strain, curvature, or deflection) of the element segment comprised between two consecutive cracks;
- α_1 and α_2 are the corresponding values computed in the uncracked and fully cracked sections, respectively;
- ζ is the distribution coefficient,
- β is a factor that takes into account long term effects (β = 1.0 for short term effects, β = 0.5 for sustained loads or many cycles of repeated loading);

- σ_S is the stress in the tension reinforcement calculated on the basis of a cracked section and,
- σ_{SR} is the stress in the tension reinforcement calculated on the basis of a cracked section under the loading conditions causing first cracking.

Note: - σ_{SR}/σ_S may be replaced by Mcr/M for flexure or Ncr/N for pure tension, where Mcr is the cracking moment and Ncr is the cracking force.

Considering moment versus curvature:-

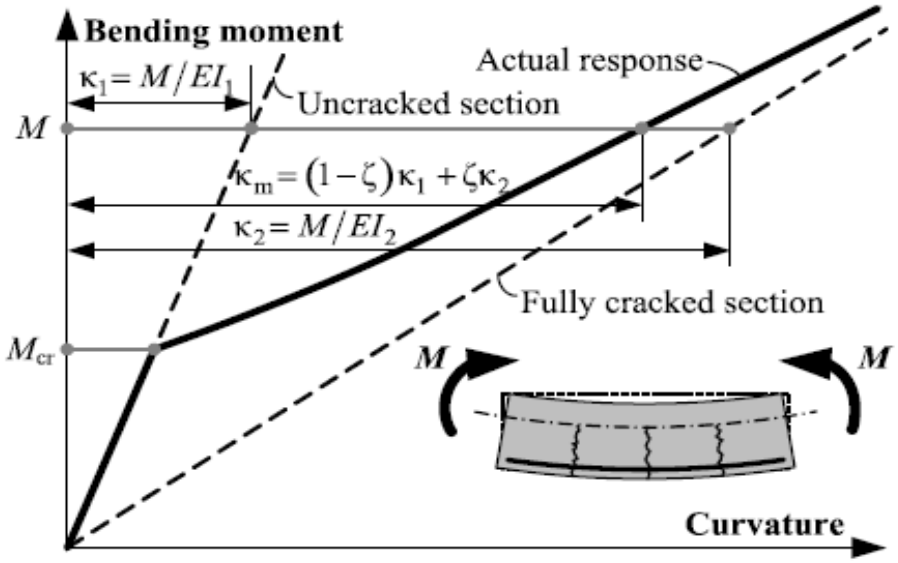

Figure 2- 6 Modeling flexural behavior of RC members (Kaklauskas et al, 2010)

For deformation analysis, two regions can be considered in a reinforced concrete member: *region I*, uncracked, and *region II*, fully cracked. In *region I*, both the concrete as well as the reinforcing steel act elastically, while in *region II after cracking*, the reinforcing steel holds all of the tensile force on the member. The average curvature is expressed as (Kaklauskas et al, 2010): -

$$\kappa = (1-\zeta)\kappa_1 + \zeta\kappa_2 \tag{2-3}$$

Where: -

- κ_1 and κ_2 correspond to the curvatures in *regions I*, and *II*, respectively.

- ζ indicates how close the stress-strain state is to the condition causing cracking. It takes a value of zero at the cracking moment and approaches unity as the loading increases above the cracking moment.

$$\zeta = 1 - \beta\left(\frac{M_{cr}}{M}\right)^2 \tag{2-4}$$

Here β is a factor taken as 1.0 for short-term loading case; M_{cr} and M are the cracking and bending moments applied, respectively. The curvature of uncracked and cracked cross-section of RC member is analyzed using classical material strength formulas, taking into account stiffness of the uncracked and completely cracked cross-section respectively.

$$K_{1(2)} = \frac{M}{E_C I_{1(2)}} \tag{2-5}$$

I_1 and I_2 are the moment of inertia of uncracked and fully cracked states, respectively. Cracking moment of reinforced concrete flexural member is written as:

$$M_{cr} = f_{ct} W_1 \tag{2-6}$$

Where: -

- f_{ct} is concrete tensile strength;
- W_1 is section modulus in region $_{I.}$

2.4 Deformation Behavior of Reinforced Concrete

Given the apparent simplicity of the tensile test system, interpretation of the test results may be inadequate: the experimental data sometimes conflicts with the general assumption of consistency between average reinforcement and concrete strains. This disparity can be due to two well-known, but often ignored issues, namely, the area of concrete effective in tension and the end effect. These two effects are mediated by the bond mechanism and the concrete cover, which can be modeled using the discrete cracking method, but cannot be reflected within the smeared (average) cracking models. The smeared models, accounting for the average deformations of the cracked concrete, do not consider expansion of a specific crack (Arvydas Rimkus, 2017).

Following the load-sharing concept, external load *P* induces two internal forces associated with the reinforcement *Ns* and the concrete *Nc.*

$$P = N_S + N_C \tag{2-7}$$

From the Navier-Bernoulli hypothesis saying the strain profile within a cross-section is represented as a plane, the internal forces are simply related to the average strain of the member, ε_m, assuming same for both the reinforcement and the concrete (Bischoff, 2001).

$$P = A_S E_S \varepsilon_S + A_C E_C^{'} \varepsilon_C = \left(A_S E_S + A_C E_C^{'}\right)\varepsilon_m \tag{2-8}$$

Where: -

A_s and ε_s, and A_c and ε_c are the area and the strain of the reinforcement and concrete, respectively; E_s is the modulus of elasticity of the reinforcement; E'_c is the secant deformation modulus of the concrete.

The reinforced concrete tensile test by (Gudonis et al, 2014) showed that average deformations of steel reinforcement and concrete surfaces differs significantly which disagree with the general assumption of similarity between average strains of the reinforcement and concrete.

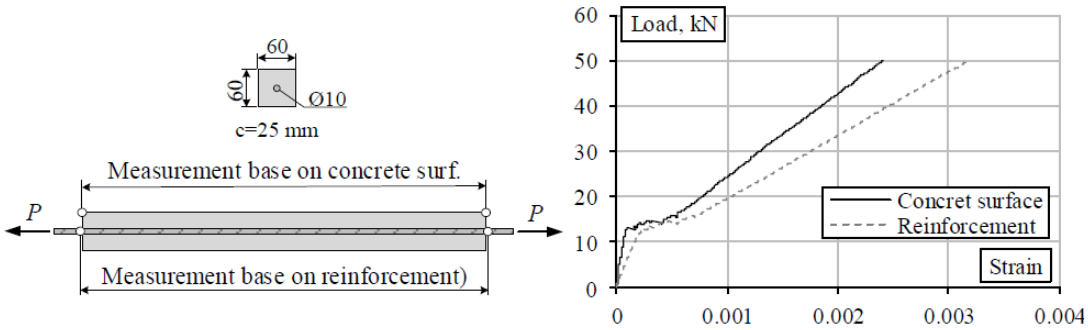

Figure 2- 7 Reinforced concrete tensile test (Gudonis et al, 2014)

It is essential to monitor the deformation of reinforcement and concrete surface in order to study the reinforced concrete structure's structural behavior.

2.5 Code Provision for Crack Width Calculation

Various design provisions predict crack width differently based on different analytical models.

For practical use and design purposes, design codes, such as ES EN 1992-1-1:2013 provide an explicit formulation of crack spacing and average strain in the steel reinforcement and concrete.

For the maximum crack width predictions, the design provisions account for:

- the average strains of the reinforcement bars and the concrete in tension,
- effective area of the concrete in tension,
- modular ratio of reinforcement and concrete
- reinforcement bar diameter,
- concrete cover,
- bond properties of reinforcement bar,
- strain distribution along the cross section of the element and
- Loading conditions.

Influence of these parameters on the predictions of cracking characteristics according to different design provisions is significantly different.

According to ES EN 1992-1-1:2013, crack width can be calculated using: -

$$W_K = S_{r,\max}\left(\varepsilon_{sm} - \varepsilon_{cm}\right) \tag{2-9}$$

Where: -

- $S_{r,\max}$- is the maximum crack spacing
- ε_{sm}- is the mean reinforcement strain under the relevant load combination, including imposed deformations and taking into account the tension stiffness effect. Only the additional tensile strain at the same level beyond the concrete's zero strain state is considered.
- ε_{cm} is the mean strain between crack in the concrete.

$$\varepsilon_{sm} - \varepsilon_{cm} = \sigma_s - \frac{K_t\left(\frac{f_{ct,eff}}{\rho_{p,eff}}\right)\left(1+\alpha_e\rho_{p,eff}\right)}{E_S} \geq 0.6\frac{\sigma_s}{E_s} \tag{2-10}$$

Here: -

- σ_s is the stress in the tensile reinforcement calculated in a cracked section under the applied external load
- α_e is the ratio between E_s and E_c,
- $\rho_{p,eff}$ is the ratio between A_s, that is the whole area of the longitudinal reinforcement, and A_{ce}, that is the concrete effective area in tension.
  A_{ce} is obtained multiplying the width of the section by $h_{c,eff}$.
  $h_{c,eff}$ = the minimum value between 2.5(h - d), (h - x)/3 and h/2

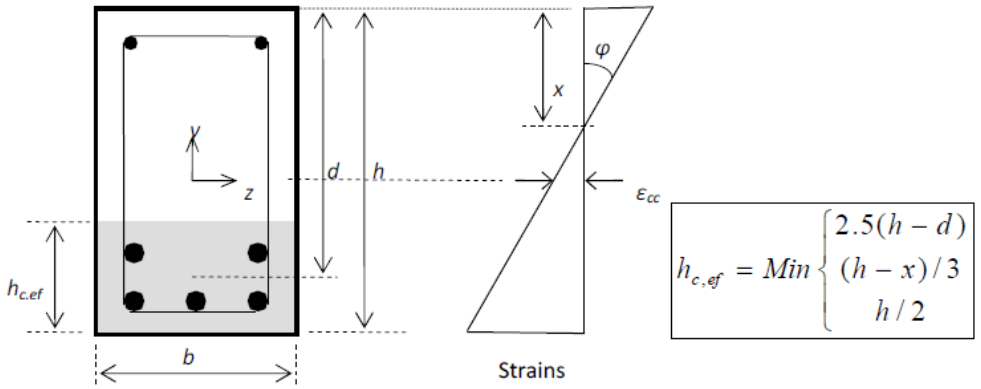

Figure 2- 8 Area of concrete effective in tension (Gil Martin et al, 2015)

- K_t – a factor which depends on the load duration: 0.6 for short-term loading condition and 0.4 for long term or cyclic loading.

Crack spacing ($s_{r,\,max}$): -

$$S_{r,\max} = K_3 c + K_1 K_2 K_4 \left(\frac{\phi_s}{\rho_{s,eff}} \right) \tag{2-11}$$

Where: -

- c is the cover depth (mm) and
- $Ø_s$ is the bar diameter (mm).
- k_3= 3.4 and k_4=0.425;
- k_1 is a coefficient which accounts for the bond properties of steel bars (= 0.8 for corrugated bars and = 1.6 for smooth bars);
- k_2 is a coefficient which takes account of the form of strain distribution along the cross section (= 0.5 for bending and = 1 for pure tension).

CHAPTER 3 FINITE ELEMENT MODEL AND ANALYSIS

The structural response of reinforced concrete element involves a wide range of effects such as strength difference, different bond character, internal cracking and also time dependent effects related with creep and shrinkage. These effects will result in a nonlinear structural behavior. Finite element modeling will help to evaluate the nonlinear structural behaviors of reinforced concrete material which are too complicated to be evaluated experimentally.

A proper model of material in finite element model will ultimately be capable of reflecting concrete's elastic and plastic behavior in compression and tension. The complete compressive behavior would involve both elastic and inelastic concrete behavior, including strain softening process. Tension softening, tension stiffening and local bonding effects should be part of the simulation of proper behavior under tension. Thus, finite element model (FEM) creation may involve rigorous material testing to integrate any of the finite element [FE] packages available into the material model (Wahalathantri et al, 2011).

3.1 Reinforced concrete element damage Models

ABAQUS simulation software can be listed among the commercial finite element packages which offer a very powerful and general analytical tool for reinforced concrete elements structural analysis.

This software offers the ability of simulating damage of reinforced concrete using any of the three crack models.

- Smeared crack model
- Brittle crack model
- Concrete damaged plasticity (CDP) model

Smeared model which was first developed by Rashid (1968) and Červenka & Gerstle (1971,1972) is focused on the development of suitable continuum material models, in which cracks are smeared over a distinct region, typically finite element or region corresponding to a finite element integration point. It builds up on equivalent continuum

concepts of elastic degradation and/or softening plasticity within the fixed mesh approach (L. Jendele et al).

In this kind of modeling, the reinforcement is assumed to be smeared in every element of the concrete. This means that the reinforcement will be transferred to an equivalent amount of concrete and the whole section of the reinforced concrete will be assumed as a homogenous material. This type of modeling is frequently used in practical works of design and analysis due to its simplicity of implementation. However, since the reinforcement is considered to be smeared in the concrete, the internal forces in the reinforcement will not be available to be analyzed.

Such model does not track individual cracks but distributes the effects of these cracks. It can only handle monotonic loading which limits the reach of its applicability.

The discontinuities of the displacement field resulting from the failure cycle are incorporated directly into the numerical model in the brittle crack model which was first applied to concrete structures by Saouma & Ingraffea (1981). This method is based explicitly on the fracture mechanics or the fictitious crack concepts. This method is theoretically more suitable to capture the failure localization (L.Jendele et al).

In this type of modeling, the concrete and the reinforcement will be modeled with two totally independent parts having different behavior. Therefore, in order to represent the bond between the two independent parts, a special element must be placed at the interface of the two parts. This type of modeling is very convenient to model irregular structures since it uses two independent parts in the model.

This model is very ‘user friendly’ and easy to calibrate in any loading scheme. The main disadvantage of this model is that it assumes linear elastic material behavior in compression (Vilnay, Chernin and Cotsovos, 2017).

The concrete damaged plasticity model implemented in Abaqus is by far the most complex concrete model which can be used in any loading regime. It is not ‘user friendly’ though, requires several parameters and can be very difficult to calibrate. Additionally, this model does not allow removing damaged elements from the analysis of finite element, which can contribute to the solution algorithms being numerically instable.

But this model has the potential to represent complete inelastic concrete behavior in both compression and tension including damage characteristics. Therefore, this model will be used for further reinforced concrete structures analysis since it can work under any loading type including static and dynamic loading.

In this type of modeling, the reinforcement is considered as an axial member in the concrete element. Both the reinforcement and the concrete will have the same displacement since they are considered to be embedded to one other. This shows that a perfect bond is considered between the two parts of the reinforced concrete element.

3.2 Bond Modeling on Finite Element

A reinforced concrete material consists of two different components with different mechanical and physical behaviors. An external load will be directly applied to the concrete. Whereas the reinforcement will receive part of this load from the surrounding concrete through bond.

The numerical modeling of the bond behavior is possible mainly at two levels:

- Detailed modeling in which the bar and concrete geometry is formed by three-dimensional elements and
- Phenomenological modeling based on the bar-concrete interface having a smeared or discrete formulation (J. Shafaie, Hosseini and Marefat, 2009).

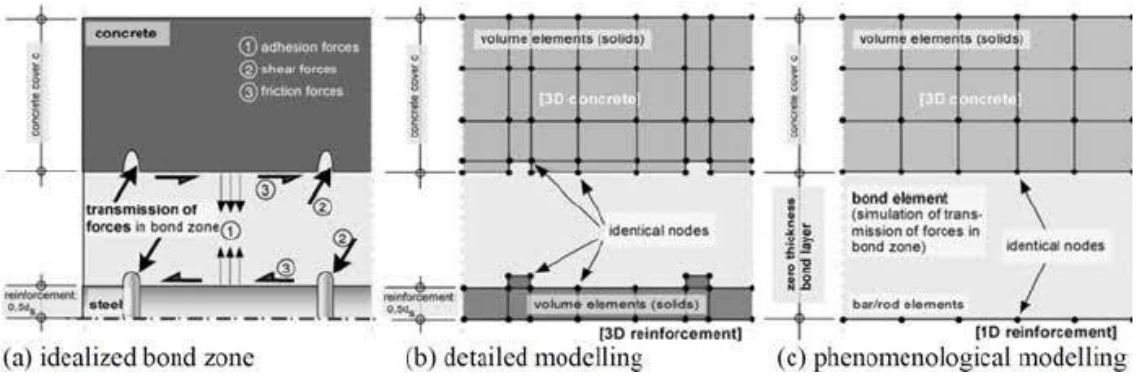

Figure 3- 1 Idealized bond zone schematic simulation (J. Shafaie et al, 2009)

In the phenomenological modelling of bond, the concrete and the reinforcement are discretized by three- or two- dimensional finite elements. A discontinuous approach, in which bond is defined by discrete, zero-thickness elements (springs) whose behavior is measured by the bond stress-slip relationship, can realize the link between the concrete

and the bar. This approach is only capable of predicting the bond behavior for different geometries and for different boundary conditions if a realistic constitutive model is used for the surrounding concrete. Nevertheless, the model cannot automatically predict a given bar geometry's bond behavior. Consequently, the effect of these parameters in the basic parameters of the bond model must be stored in advance. Therefore, one has the possibility to simulate reinforced concrete structures behavior with relatively low modeling and computation time effort in practical.

Through using detailed modeling, such as the modeling of the reinforcement ribs and the concrete lugs between the reinforcement ribs, a fairly fine finite element mesh must be produced. This again leads to a high effort in modelling work and in particular to a very long computation time, when conducting a finite element analysis on complex reinforced concrete structures (J. Shafaie, A Hosseini and Marefat, 2009).

3.3 Complete Analytical Procedure On Abaqus

The complete analytical procedure on Abaqus simulation software consists of three stages.

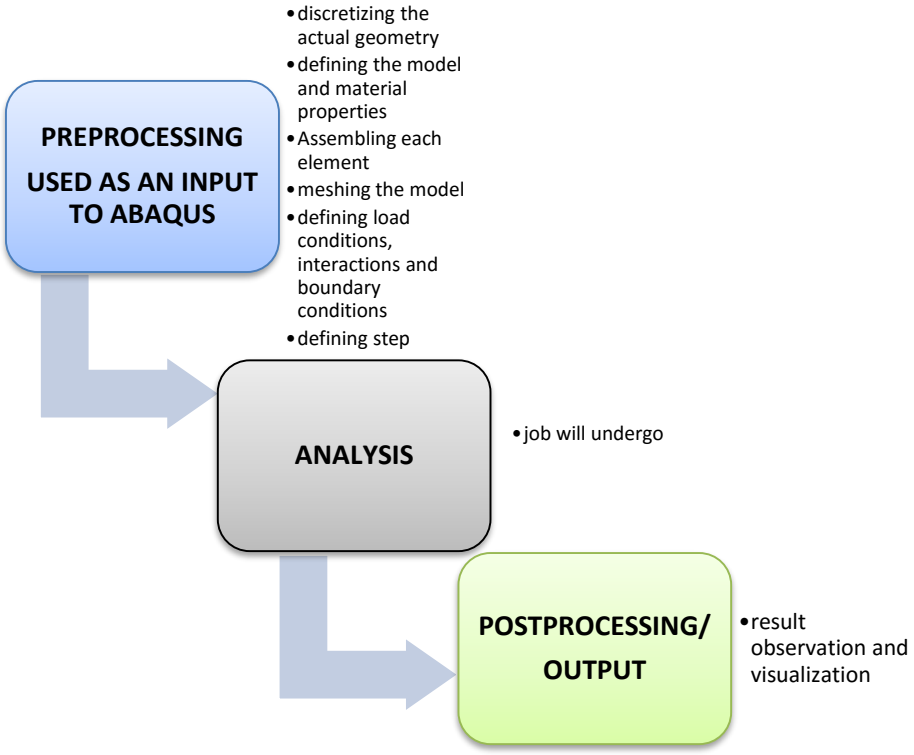

Figure 3- 2 Flow chart for the FEM numerical analysis

3.4 Material Property Model of Concrete

A proper material model should be capable of describing both the elastic and plastic behavior of concrete in tension and compression in finite element analysis. In order to attain a numerical result adequate to actual behavior of the element, a proper calibration of the model based on experimental tests is mandatory.

3.4.1 Compressive behavior of concrete

The concrete's complete compressive behavior would include both the concrete's elastic and inelastic behaviors including strain softening regimes. The complete stress-strain curve for concrete under compression is derived from the stress-strain relation for non-linear structural analysis using the ES EN 1992-1-1:2013 code.

As described in the code, the relation between stress and strain of concrete (compressive stress and shortening strain) for short term uniaxial loading is given by: -

$$\frac{\sigma_c}{f_{cm}} = \frac{K\eta - \eta^2}{1+(K-2)\eta} \tag{3-1}$$

Where: -

- $\eta = \frac{\varepsilon_C}{\varepsilon_{C1}}$
- ε_{c1} is the strain at the peak stress according to table 3.1 on the appendix c
- $K = 1.05E_{cm}\left(\frac{\varepsilon_{c1}}{f_{cm}}\right)$ (f_{cm} is according to table 3.1 on appendix c)
- f_{cm} is mean compressive strength

The above expression is valid for $0<|\varepsilon_c|<|\varepsilon_{cu1}|$ where ε_{cu1} is the nominal ultimate strain.

But experimental value of f_{cm} is directly used for the study purpose.

The code also allows other idealized stress-strain relations to be applied if they adequately represent the concrete's behavior under consideration.

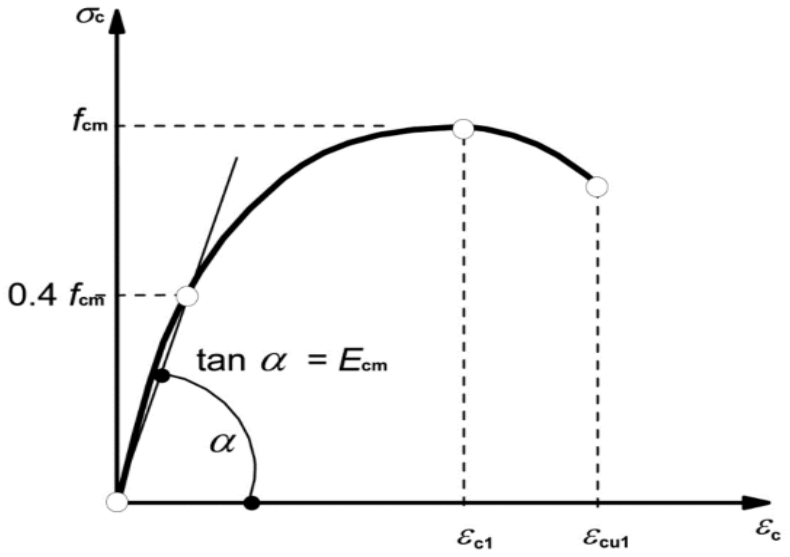

Figure 3- 3 Schematic representative of the stress strain relation of concrete (ES:EN 1992-1-1:2013)

According to the graph above: -

- $0.4*f_{cm}$- is the point where non-linearity starts.
- ε_{c1} is the peak strain and is defined by: -

$$\varepsilon_{c1} = 0.7\left(f_{cm}\right)^{0.31} \tag{3-2}$$

- ε_{cu1} is the ultimate strain and is equal to 3.5‰
- E_{cm} is secant modulus and is defined by: -

$$E_{cm} = 22\left(\frac{f_{cm}}{10}\right)^{0.3} \tag{3-3}$$

In order to describe the complete stress-strain relationship behavior on Abaqus considering the compressive behavior of concrete, one needs to enter the stresses (σ_c), inelastic strains (ε_c^{in}) corresponding the stresses, and damage properties (d_c) with inelastic strains.

Total strain values must be transformed into inelastic strains using (Chan et al, 2011): -

$$\varepsilon_c^{in} = \varepsilon_c - \varepsilon_{oc}^{el} \tag{3-4}$$

Where: -

- ε_{oc}^{el} –elastic strain corresponding undamaged material and is equal to σ_c/E_o
- ε_c – total strain

Furthermore, corrective steps should be taken to ensure that the values of plastic strain (ε_c^{pl}) are not negative nor declining with increasing stress values using: -

$$\varepsilon_c^{pl} = \varepsilon_c^{in} - \frac{d_c}{1-d_c}\frac{\sigma_c}{E_O} \tag{3-5}$$

3.4.2 Tensile behavior of concrete

The complete tensile behavior of concrete should include tension stiffening, tension softening and local bond effects considering the interaction between the reinforcement and the concrete in reinforced concrete elements.

The strain softening behavior of cracked concrete in tension was specified by tension stiffening in terms fracture energy criterion using exponential function as proposed by Cornelissen et al. 1986 and defined in Jawed Qureshi and Dennis Lam, 2010.

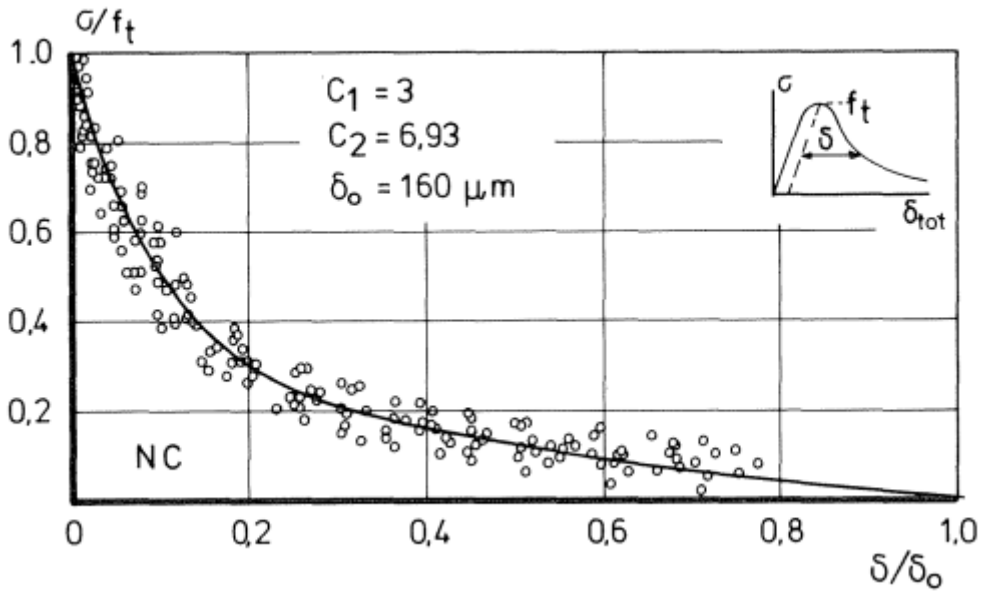

Figure 3- 4 Stress –crack opening relation for normal weight concrete (Cornelissen 1986)

The axial tensile strength is taken as 10% of compressive strength. The tensile stress and the cracking displacement have been obtained from: -

$$\frac{\sigma_t}{f_t} = f(w) - \frac{w}{w_c} f(w_c) \tag{3-6}$$

$$f(w) = \left[1 + \left(c_1 \frac{w}{w_c}\right)^3\right] \exp\left(\frac{-c_2 w}{w_c}\right) \tag{3-7}$$

Where: -

- W- crack opening displacement
- W_c- crack opening displacement where stress cannot be transferred anymore
- $W_c = 5.14 \frac{G_f}{f_t}$
- $C_1 = 3$ and $C_2 = 6.93$ for concrete having normal density

The tensile damage d_t is obtained using: -

$$d_t = 1 - \frac{\sigma_t}{f_t} \tag{3-8}$$

Fracture energy is an energy required to develop unit area of crack. As described in model code FIB, 2010, fracture energy (G_f) is obtained from: -

$$G_f = 73 f_{cm}^{0.18} \tag{3-9}$$

To develop this model, one should enter young's modulus (E_o), stress (σ_t), cracking displacement (u_t^{ck}) values and the damage parameter values (d_t) for the relevant grade of concrete.

Abaqus checks the accuracy of the damage curve using plastic cracking displacement calculation. Negative or decreasing tensile plastic cracking displacement values are indicative of incorrect damage curves which may lead to generate error message before the analysis is performed.

$$U_t^{pl} = U_t^{ck} - \frac{d_t}{1 - d_t} \frac{\sigma_t}{E_o} \tag{3-10}$$

In general, the concrete damaged plasticity model states that the tensile cracking and compressive crushing are the two major mechanisms of failure in concrete.

The mechanical property of concrete used for validation of the present study is taken from an experimental work by (Victor Gribniak et al, 2016).

Table 3- 1 Properties of concrete used [31]

Properties	Properties for Concrete grade 45.52 MPa
Young's modulus (MPa)	34664.37
Compressive strength (MPa)	45.52
Poisson ratio	0.2
Unit weight (kN/m^3)	25.65

Abaqus software needs the compressive and tensile damage of concrete property for analysis. These properties are based on the above theories of Ethiopian building construction code of standard and the Cornelissen et al 1986 theory and look like the table below. This table is taken from an excel sheet prepared for the purpose of this thesis which is attached on Appendix D.

Table 3- 2 Compressive and tensile damage values analyzed for 45.52 MPa concrete from an excel sheet attached on Appendix D.

Compressive damage of concrete			Tensile damage of concrete		
σ(MPa)	E_{in}	d_c	σt(MPa)	W (mm)	d_t
18.208	0	0	3.362	0	0
19.587	3.50E-05	0	3.170	0.0031	0.057
23.738	6.52E-05	0	2.977	0.0061	0.114
27.569	0.0001	0	2.785	0.0093	0.171
31.068	0.00015	0	2.594	0.0123	0.228
34.224	0.0002	0	2.401	0.0154	0.285
37.023	0.00028	0	2.209	0.0185	0.342
39.451	0.00036	0	2.017	0.0215	0.4
41.494	0.00045	0	1.825	0.0246	0.457
43.138	0.00055	0	1.633	0.0278	0.514
44.365	0.00067	0	1.441	0.0308	0.571
45.161	0.00079	0	1.248	0.0339	0.628
45.506	0.00093	0	1.056	0.0370	0.685
45.52	0.00097	0	0.864	0.0401	0.742
45.518	0.00098	4.32E-05	0.672	0.0431	0.8
45.234	0.00114	0.0063	0.605	0.0610	0.82
44.455	0.00132	0.0234	0.537	0.0789	0.84
43.160	0.00150	0.0518	0.471	0.0967	0.86
41.326	0.00171	0.0921	0.403	0.1146	0.88
38.931	0.00192	0.1447	0.336	0.1325	0.9
35.948	0.00216	0.2103	0.268	0.1503	0.92
32.352	0.00242	0.2892	0.202	0.1682	0.94
28.114	0.00268	0.3824	0.134	0.1861	0.96
			0.067	0.2040	0.98

3.4.3 Other material properties used in the analysis

The numerical values of parameters presented below involve intricate assumptions and mathematical derivations using the yield surface of the concrete damage plasticity model. Therefore, proposed values in other researchers' work have been used here, and the verification of the model is performed by comparing the numerical results with published experimental data.

3.4.3.1 Dilation Angle

Dilation angle is an angle of internal friction of the concrete material and has values that are recommended to oscillate between 30° and 40°. The best agreement of numerical results with experimental data was obtained in between these two degrees.

It is also associated with the growth of mechanisms of cracking that the concrete suffers during the inelastic period. A value of 31˚ is selected in this thesis work.

3.4.3.2 Flow potential eccentricity

The flow potential eccentricity is a small positive number that defines the rate at which the hyperbolic flow potential approaches its asymptote. The default value of 0.1 is used in this work.

3.4.3.3 Ratio of biaxial to uniaxial compressive yield stress (f_{bo}/f_{co})

Value of 1.16 is recommended for f_{bo}/f_{co}.

3.4.3.4 Ratio of the second stress invariant on the tensile meridian to that on the compression meridian for the yield function (k)

At initial yield for any given value of pressure invariant such that the maximum principal stress is negative, k is recommended between 0.5 and 1. Value of 0.667 is usually for k as a default value.

3.4.3.5 Viscosity parameter

Convergence is one of the problems arising in using nonlinear material models on Abaqus. Viscoplastic regularization is a common method used to overcome problems related with instabilities. It is used to get a converged result in static scheme accounting for brutal propagation.

It speeds up calculation time significantly. But it affects process forces and also the stiffness model. A low value of viscosity parameter should always be selected. Even though, results of the analysis show a converged result, the output may be inaccurate. Therefore, sensitivity analysis should be done in order to obtain proper results as experimental values.

Specimens with a value of viscosity parameter ranging from 0.00025 to 0.001 show a good agreement with experimental results (Sczecina Michal and Winnicki Andrzej, 2015).

A value of 0.001 is selected for this thesis work.

3.4.3.6 **Damage parameters**

Reduction of elastic constants is a characteristic of damage. In order to represent the nonlinear behavior of concrete the concept of plasticity should be combined with damage concept.

Damage parameters range from 0 to 1 or from no damage to full damage.

- Tensile damage parameter (d_t) = cracking strain/ total strain
- Compressive damage parameter (d_c) = inelastic strain/ total strain

3.4.3.7 **Stiffness recovery**

In the present analysis the default values are assumed for the stiffness recovery factors. The compressive stiffness recovery factor Wc= 1 is then used, assuming that compressive stiffness is completely restored at crack closure, when the load transitions from tension to compression.

The tensile stiffness recovery factor, W_t= 0 is used if the tensile stiffness is not recovered as the load switches from compression to tension once concrete crushing is initiated (Wahalathantri et al, 2011).

3.5 Tensile properties of steel

Steel has approximately linear elastic material behavior when its stiffness related with elastic modulus keeps constant at low strain magnitudes. Once the stress in the steel exceeds the yield stress, plastic or permanent deformation will start to occur. As a result, once the material yields its stiffness decreases.

The mechanical property of reinforcing bar used for validation is taken from an experimental work by (Victor Gribniak et al, 2016).

Table 3- 3 Properties of steel used (Victor Gribniak et al, 2016)

Properties	Longitudinal bar	Top and web reinforcement
Young's modulus (MPa)	199300	223500
Yield strength (MPa)	551.1	585.4
Tension rupture strength(MPa)	553	642.5
Poisson ratio	0.3	0.3
Unit weight (kN/m^3)	78.5	78.5

3.6 Finite element model development

3.6.1 Geometry of the model

In order to model concrete, solid element is selected. Modeling the concrete beam is rendered using the 3D 8-noded hexahedral (brick) elements with reduced integration (C3D8R) available in Abaqus element library. The steel bars are built using 3D linear truss element (T3D2). Stirrups are modeled using the same elements as longitudinal bars as well. All reinforcement elements are embedded in the concrete geometry, so that their degrees of freedom in translation are restricted to the corresponding degrees of concrete freedom.

The concrete element is modeled with a size of 1640mm x 284mm x 300mm in the longitudinal, transverse and on the height directions respectively. Since symmetry is considered in the model, half of the experimental beam is modeled. The top and bottom reinforcements on the other hand are modeled with a length of 1620mm considering concrete side cover of 20mm. Stirrups are modeled with size of 260mm x 244mm considering size of concrete side cover.

The beam end supports given in the experimental are modeled in a simplified way if boundary conditions are imposed on a line to avoid stress concentration. The end support of the beam was modeled using a rigid shell material with a diameter of 200mm and length of 284mm which is limited to a reference point lying on the center of the plates with a rigid body motion. All degrees of freedoms are blocked on the reference point and it is modeled as fixed support.

The loading plate which is used for loading the beam was also modeled in the same way. It is constrained with a reference point lying on its middle surface where the load will be applied.

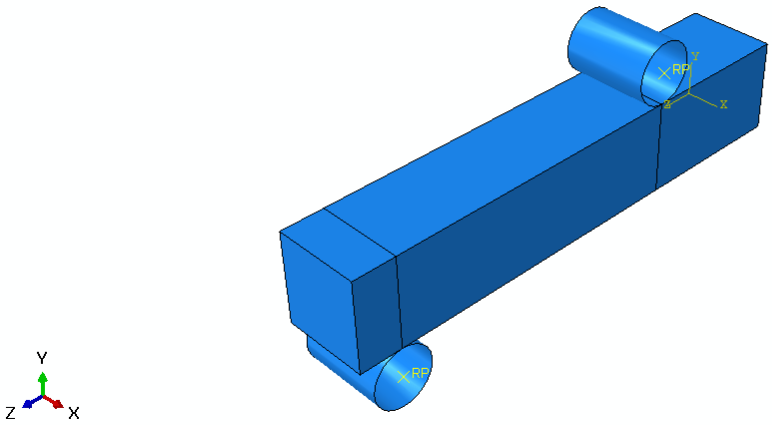

Figure 3- 5 Geometry of the beam model

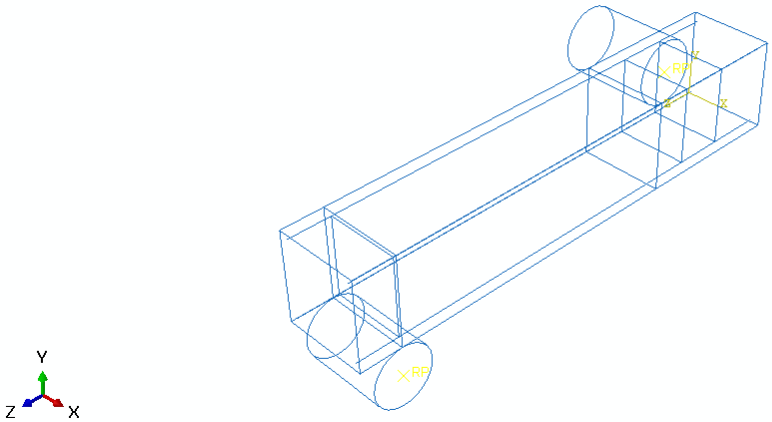

Figure 3- 6 Detail view of the beam model

3.6.2 Mesh

The finite element mesh size and type basically matters for the accuracy of the results from the analysis. Prior to concluding the final element mesh size, different sizes were tried on analyzing the model. The model is finally meshed with approximate element size of 25mm x 25 mm x 25 mm in the longitudinal, transversal and on the height direction respectively. According to mesh size convergence study, the above mesh size is finer enough to obtain a reliable result.

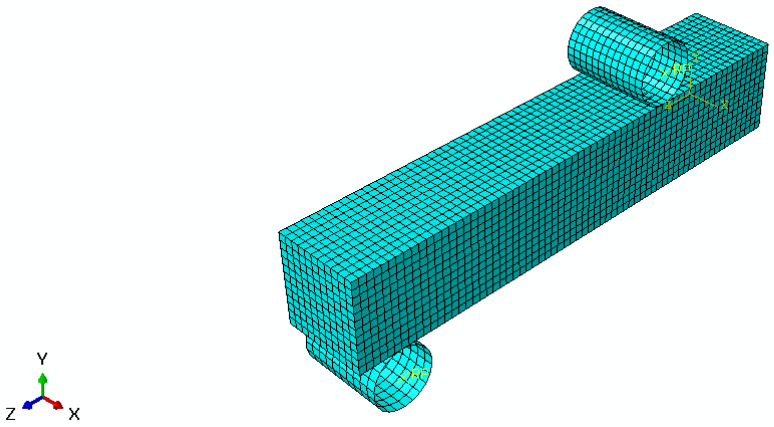

Figure 3- 7 Mesh of the model

3.6.3 Boundary Conditions

In order to save time of analysis, advantage of symmetry was used in the model. The beam in the experiment has a pin support with a 3000mm distance in between the supports. Due to advantage of symmetry, only one of the supports was modeled. It was specified with displacement boundary conditions where all degrees of freedom are blocked.

A load controlled analysis was performed by applying a downward load of 1 kN/min on the reference point of the loading plate for about 50-80 loading steps. According to the experiment, the testing equipment acting on the beam weighed 2.3 kN and summed up with the beam's own weight induced a 3.5 kNm bending moment at the mid-span.

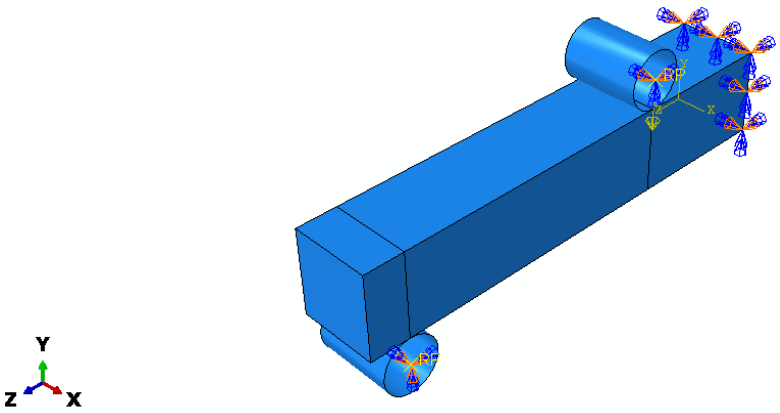

Figure 3- 8 Boundary conditions considered in the model

3.6.4 Step time used

A static general time step for a time period of 1 second is used on the finite element model. In order to model the non-linearity of the model accurately the geometric nonlinearity option (Nlgeom) is used.

Table 3- 4 Increments used on step time of the model

Maximum number of increments specified		100000
Initial time increment	Minimum time increment	Maximum time increment
0.01	$1*10^{-15}$	0.02

3.7 Validation of results of simulation

Finite element models are approximate and are not strong. Small errors in data input, modeling and boundary conditions can result in very large errors at the simulation's final output. Even though, the errors seem to be relatively small and difficult to identify, they will have significant impact on the service life or performance of the needed simulation.

The verification or validation process can take different forms depending on: -

- The type of analysis being conducted
- The accuracy required
- The part being analyzed
- The level of risk involved

Successful models of finite elements are those tests against sufficient test numbers, preferably from different sources. When validated, finite element modeling can be generalized to perform parametric studies exploring the effects of the various parameters affecting simulated model behavior.

The parametric studies in finite element modeling will provide the ability to assess effects, which are even too complex to be evaluated experimentally. They will also generate more data that will fill the gaps of test results and will help to understand the performance of the model under different geometries and scenarios.

3.7.1 Experimental output

The experimental work of [31] with four-point bending test to get the moment-curvature of a reinforced concrete beam with rectangular cross section will be compared with the results obtained using finite element simulation.

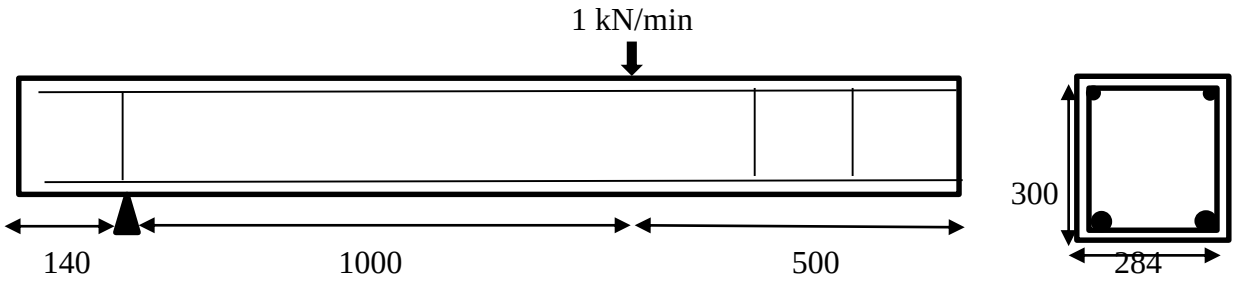

Figure 3- 9 Detail of experimental specimen considering symmetry

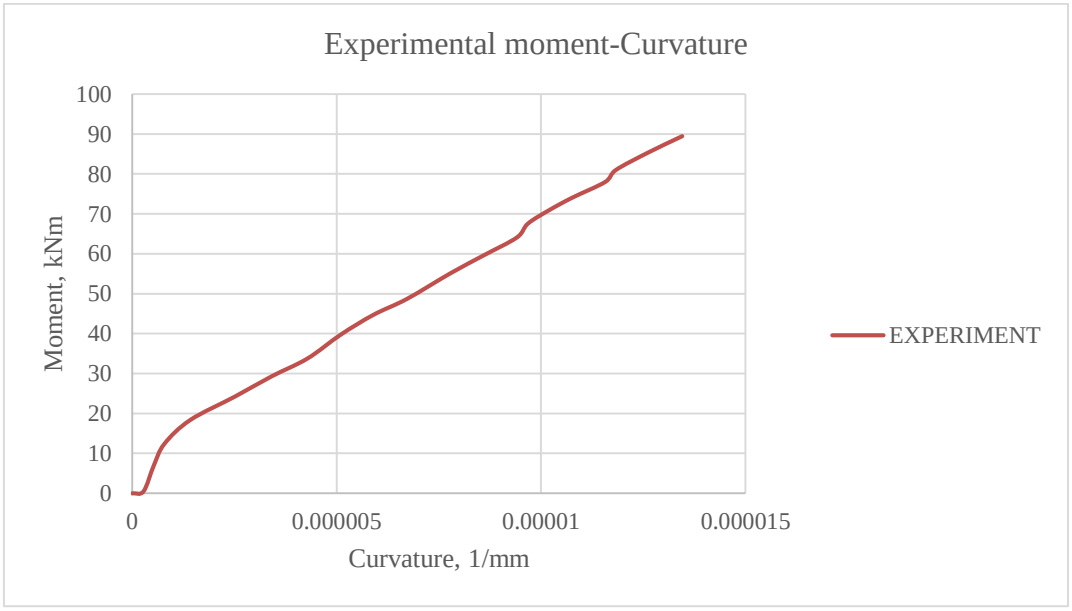

Figure 3- 10 Moment-curvature diagram of experimental specimen

3.7.2 Finite element model output

Half of the experimental beam was modeled. The output of the whole beam can be seen using mirror.

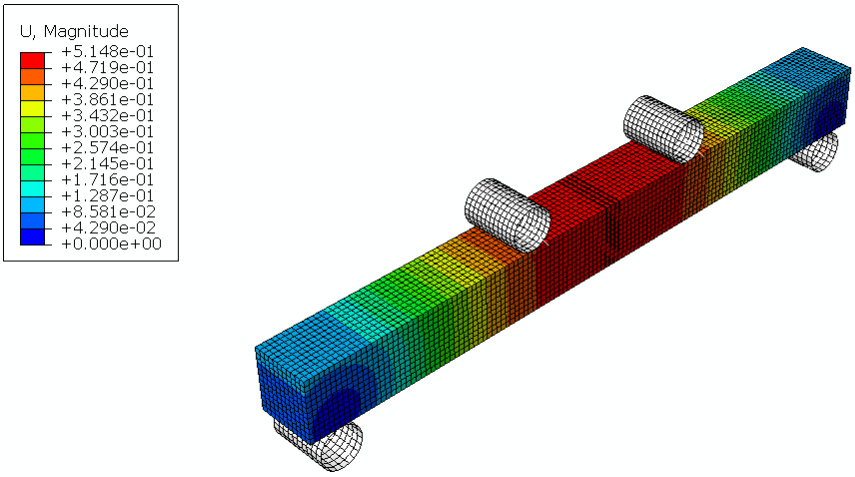

Figure 3- 11 Finite element model output of validation from Abaqus

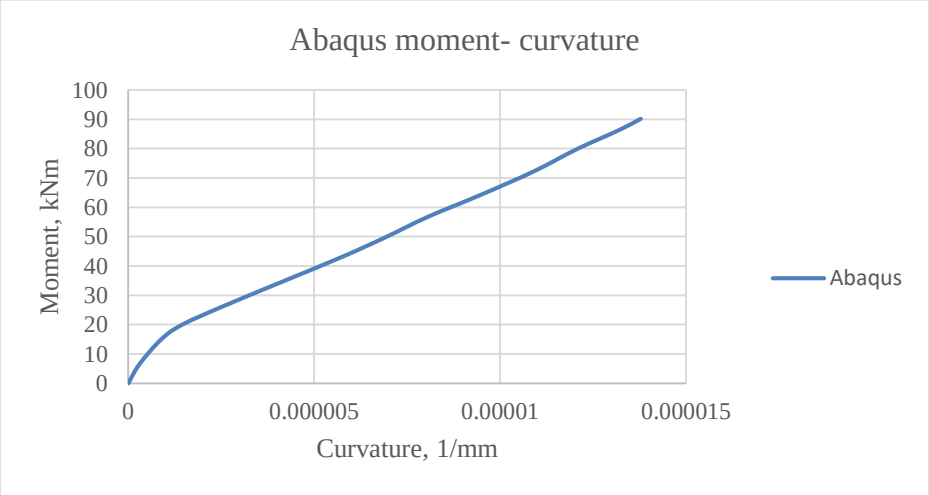

Figure 3- 12 Moment-curvature diagram of Abaqus specimen

Table 3- 5 Result comparison between experiment and numerical model

	Results	Moment(kNm)	Maximum curvature, (1/mm)	$C_{abaqus}/C_{experiment}$
1	Results from experiment	89.44	1.35E-05	0
2	Results from numerical model	90.15	1.38E-05	1.02

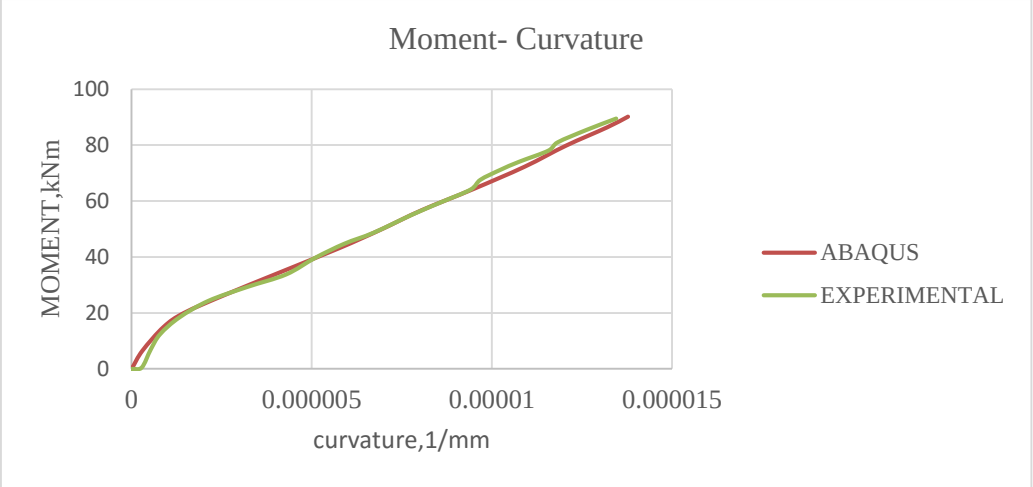

Figure 3- 13 Diagram of experimental and Abaqus moment-curvature output

From the above diagrams of the experimental and Abaqus moment-curvature output, it can be observed that the moment-curvature diagrams are almost identical. The maximum bending moment obtained from simulation is almost similar with that of the experimental output. But comparing the curvature outputs, the Abaqus result shows somehow a larger curvature as compared to the experimental output. This difference is primarily due to poor calibration of experimental results.

The results obtained from the Abaqus moment-curvature simulation are assumed to be accurate and computationally efficient.

CHAPTER 4 RESULTS AND DISCUSSIONS

This thesis focused on studying the effect of varying reinforcement bars arrangement on the cracking and deformation behavior of reinforced concrete beams. Even though there are different parameters which may affect the performance of concrete structures, it is reasonable to assume certain parameters will have a larger influence on cracking behavior than others.

4.1 Effect of arrangement of reinforcement bars on the cracking behavior of flexural elements

In order to study reinforcement arrangement effect, two types of arrangements were considered here. The first one holds reinforcement bars arranged in a single layer whereas, the second arrangement holds reinforcements in multiple layers but with similar reinforcement ratio. A beam with a single layer reinforcement arrangement will be compared with that of a beam with similar reinforcement ratio and multiple layer reinforcement arrangement.

Four flexural beams with different arrangement were considered and only half of the beams were modeled by taking advantage of symmetry. The beams were with the same size and length as that of the beam used for verification and were simulated with four-point bending. The load was applied under load control and Moment-curvature was used for evaluation.

Table 4- 1 Specimens description

Group	specimen	Bottom reinforcement	Top reinforcement	Reinforcement arrangement	Concrete grade (MPa)	Reinforcement ratio
A	A-1	2Ø22	2Ø6	Single layer	45.52	0.8
	A-2	3Ø14	2Ø6			0.5
B	B-1	9Ø10	2Ø6	Multiple layer	45.52	0.8
	B-2	15Ø6	2Ø6			0.5

Beams with single layer		Beams with multiple layer	
A-1	**A-2**	**B-1**	**B-2**
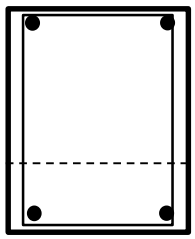	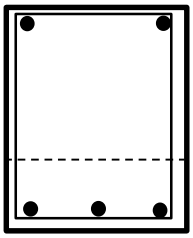	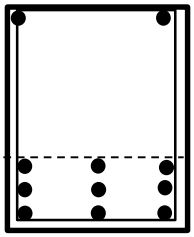	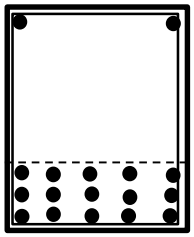

Figure 4- 1 Cross-section of beams

The moment-curvature diagrams are presented below for each group to compare the effect of arrangement of reinforcement with similar concrete strength and reinforcement ratio.

- From the first group: -

A-1: -

Actual model	Deformed shape
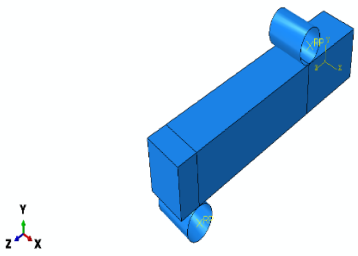	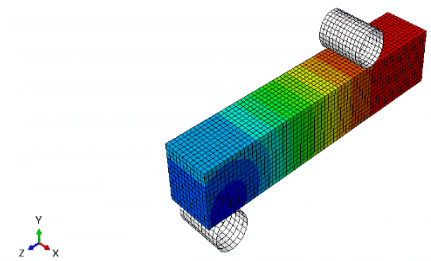

Figure 4- 2 Actual and deformed shape of A-1 from Abaqus finite element analysis

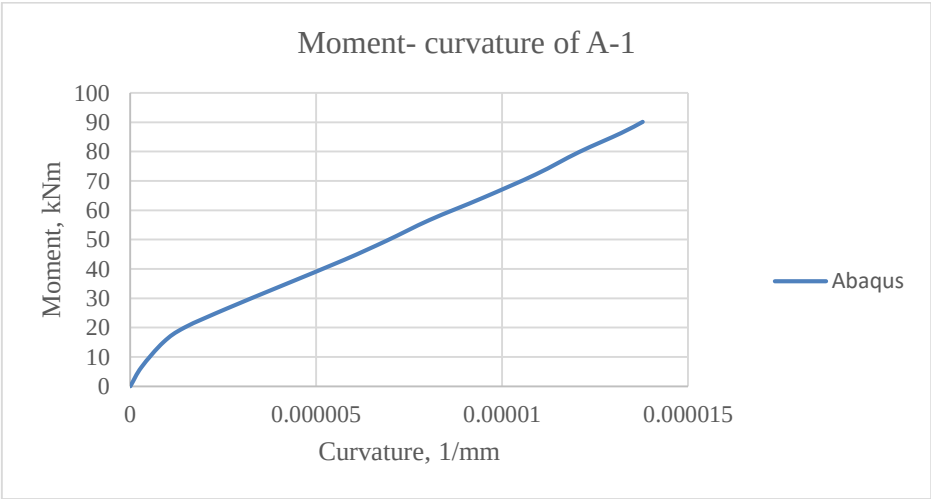

Figure 4- 3 Moment curvature graph of A-1

A-2: -

Actual model	Deformed shape
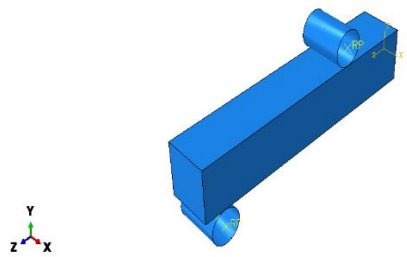	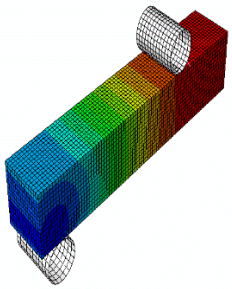

Figure 4- 4 Actual and deformed shape of A-2 from Abaqus finite element analysis

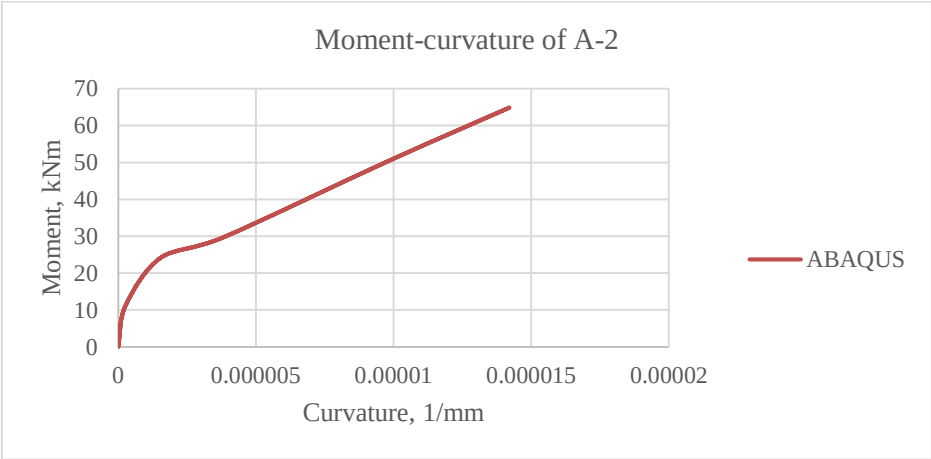

Figure 4- 5 Moment-curvature of A-2

- ❖ From the second group: -

B-1: -

Actual model	Deformed shape
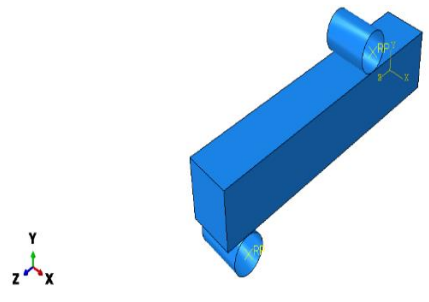	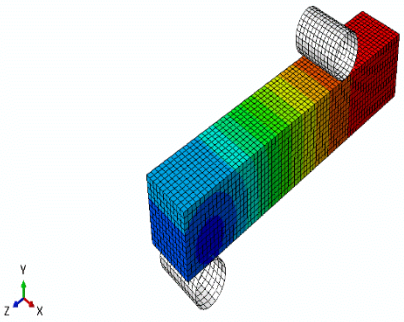

Figure 4- 6 Actual and deformed shape of B-1 from Abaqus finite element analysis

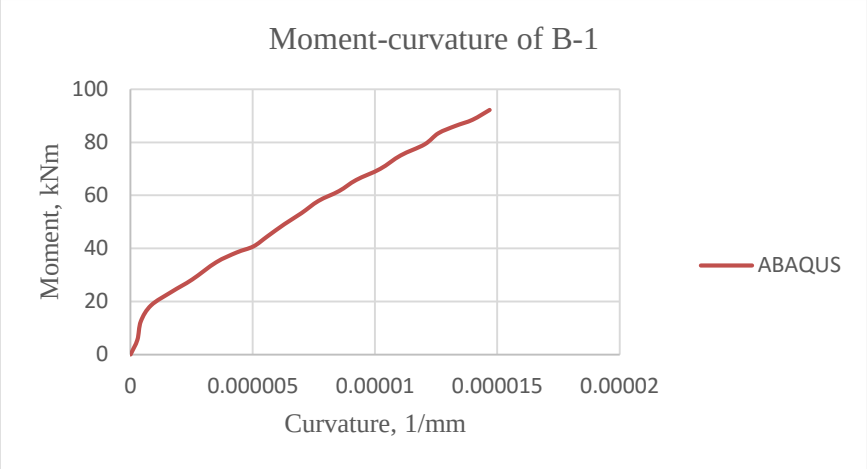

Figure 4- 7 Moment-curvature of B-1

B-2: -

Actual model	Deformed shape
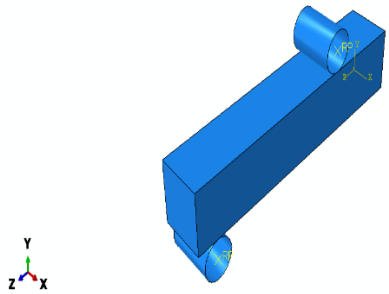	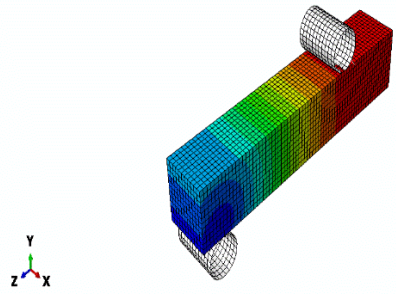

Figure 4- 8 Actual and deformed shape of B-1 from Abaqus finite element analysis

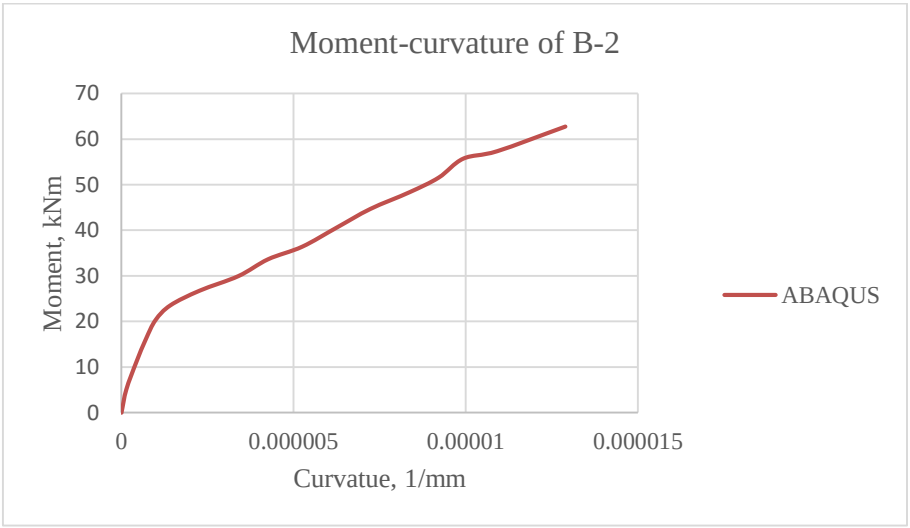

Figure 4- 9 Moment-curvature of B-2

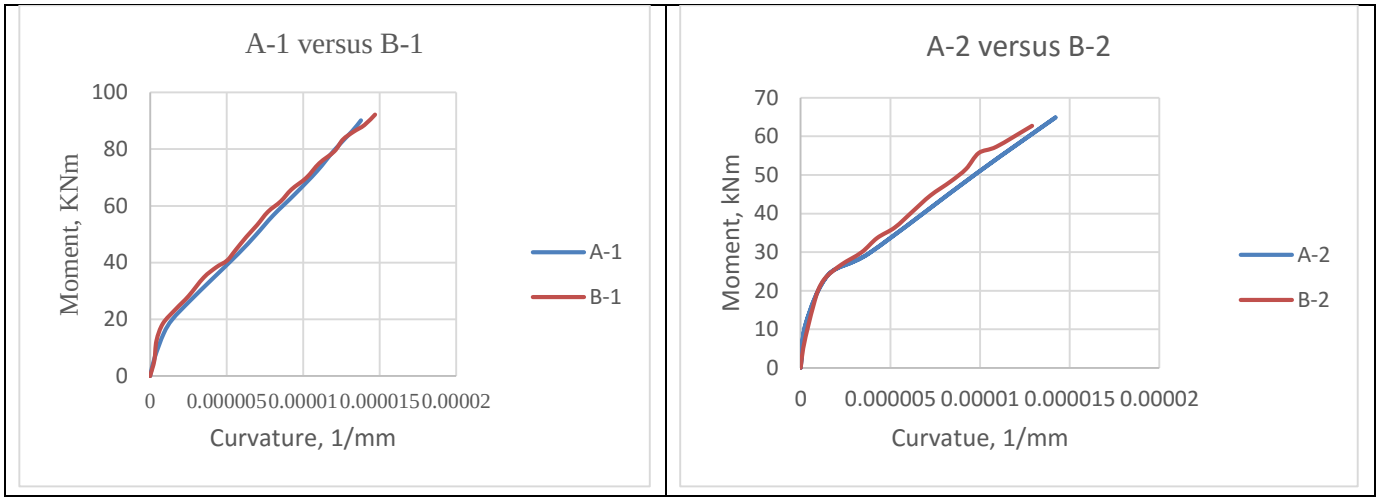

Figure 4- 10 Comparison of moment-curvature of the two groups

From the moment-curvature diagram of figure 4-10, comparing similar section having similar reinforcement ratio but with different reinforcement arrangements, it can be observed that B-1 and B-2 have more flexural stiffness than A-1 and A-2.

4.1.1 Moment-curvature prediction according to ES EN 1992-1-1:2013

Table 4- 2 Moment-curvature according to ES EN 1992-1-1:2013

MOMENT-CURVATURE OF THE FLEXURAL BEAMS								
	A				B			
	A-1		A-2		B-1		B-2	
X/L	M(x),KNm	α,1/mm	M(x),KNm	α,1/mm	M(x),KNm	α,1/mm	M(x),KNm	α,1/mm
0	0	0	0	0	0	0	0	0
0.25	22.5	2.36E-06	18.788	2.36E-06	12.023	1.96E-07	14.827	1.44E-06
0.5	45	5.99E-06	37.576	7.00E-06	48.092	8.08E-06	29.654	6.48E-06
0.75	67.5	9.34E-06	56.364	1.11E-05	72.138	1.25E-05	44.481	1.07E-05
1	90	1.26E-05	75.153	1.51E-05	96.184	1.69E-05	62.808	1.57E-05
1.25	90	1.26E-05	75.153	1.51E-05	96.184	1.69E-05	62.808	1.57E-05
1.5	90	1.26E-05	75.153	1.51E-05	96.184	1.69E-05	62.808	1.57E-05
1.75	90	1.26E-05	75.153	1.51E-05	96.184	1.69E-05	62.808	1.57E-05
2	90	1.26E-05	75.153	1.51E-05	96.184	1.69E-05	62.808	1.57E-05
2.25	67.5	9.34E-06	56.364	1.11E-05	72.138	1.25E-05	44.481	1.07E-05
2.5	45	5.99E-06	37.576	7.00E-06	48.092	8.08E-06	29.654	6.48E-06
2.75	22.5	2.36E-06	18.788	2.36E-06	12.023	1.96E-07	14.827	1.44E-06
3	0	0	0	0	0	0	0	0

The above moment-curvature calculation is based on equation 2-3 of chapter 2. Detail calculation is shown on Appendix A.

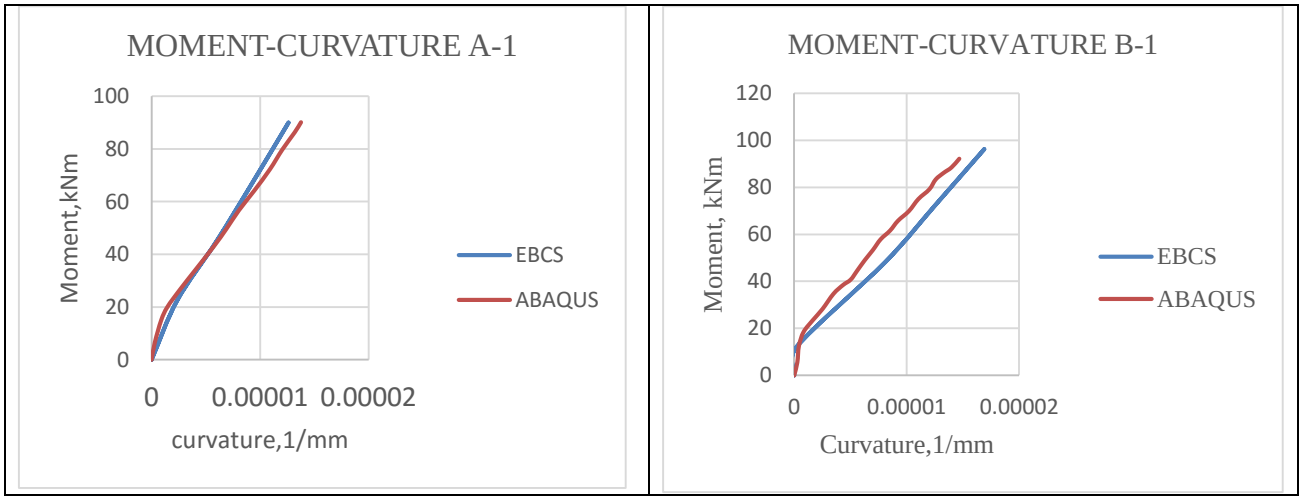

Figure 4- 11 Abaqus versus ES EN 1992-1-1:2013 moment curvature for A-1 and B-1

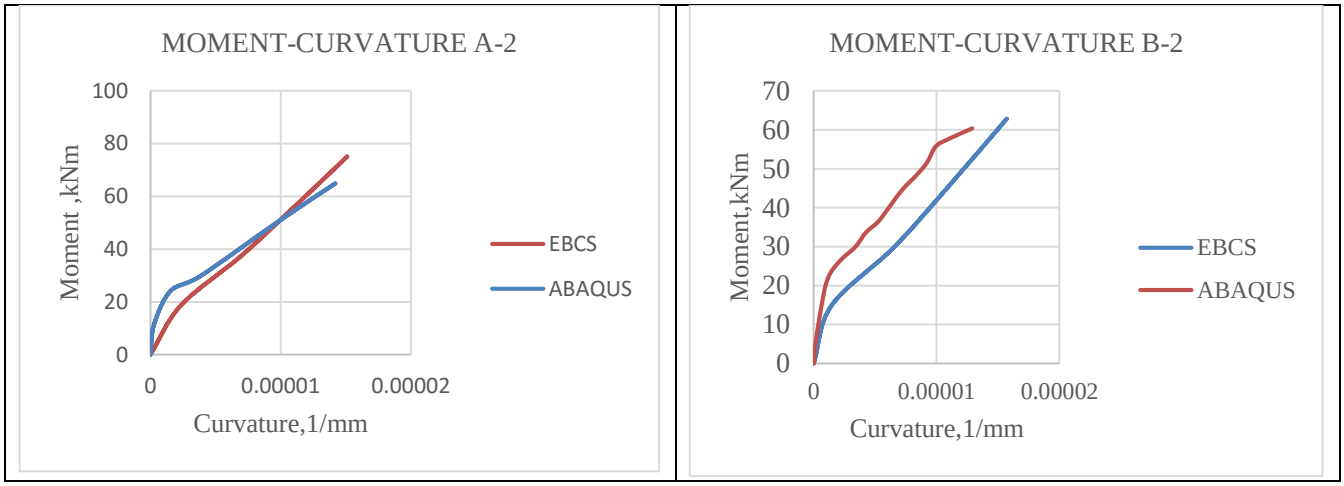

Figure 4- 12 Abaqus versus ES EN 1992-1-1:2013 moment curvature for A-2 and B-2

In figure 4-11 and 4-12, Abaqus moment-curvature results are compared with that of ES-EN moment-curvature predictions. By comparing the above code and Abaqus outputs, it can be observed that: -

- Beams in the first group, which are with one-layer reinforcement arrangement, show progressive degradation of flexural stiffness as the applied load increases.
- But beams in the second group, which are with multiple layer reinforcement arrangement, do not show such a degradation until failure.

The differences in the behavior of the beams under flexural load can be related with differences in their bond characteristics. The bond characteristics may be related with the bonded area and behavior of the reinforcement bars. Beams with multiple layers will have an increased bonded area which in turn will contribute in their resistance for development of cracks compared with the single layer reinforcement layout beams. Even once the beams with multiple layer reinforcements have cracked, the increased bonded area will maintain high relative stiffness throughout all loading steps.

4.1.2 Cracking analysis of the beams according to EBCS

In order to assess the differences in crack distances which are expected to potentially occur in both groups of beams, ES EN 1992-1-1:2013 code predictions were used.

The table below shows the calculated maximum crack distances according to equation 2-11 of chapter 2. The maximum crack distances are calculated taking the minimum effective height of the beams. Detail calculation is shown on Appendix B.

Table 4- 3 Calculated maximum crack distances based on code prediction

Calculated maximum distances between cracks determined according to EBCS code								
Group	beams	Ø, mm	P_{ef}, %	$A_{c,eff}$	h_{ef}*,mm			S_{max}, mm
					2.5(h-d)	(h-x)/3	h/2	
A	A-1	2Ø22	3.609	21053.7	82.5	74.13276	150	171.623
	A-2	3Ø14	2.3382	19740	70	78.27583	150	169.783
B	B-1	9Ø10	3.337	21170.02	127.5	75.071	150	118.939
	B-2	15Ø6	1.9092	22202.54	117.5	79.579	150	121.424

The maximum crack distances calculated from the code prediction also explained that the first groups have a larger crack distance which will be expected to potentially occur compared with that of the second groups. This can be related with the increased bonded area in the second groups which in turn is related with the effective concrete area in tension. The effective concrete area in tension will describe the bonded area related with force transfer between the surrounding concrete and the reinforcement itself.

Arrangement of reinforcement in reinforced concrete flexural elements will be related with their flexural stiffness. In addition to this, the complex nature of flexural elements will limit the ability to evaluate the reinforcement bar arrangement effect in tension zone on the reinforced concrete structures cracking behavior.

Therefore, in order to evaluate the cracking and deformation behavior of reinforced structures isolating uncertainties related with effective area of concrete in tension, analysis of a simplified structure will be very crucial. Reinforced concrete structures subjected to pure tension will help to assess reinforcement bar arrangement effect on cracking behavior in a good way.

4.2 Effect of arrangement of reinforcement bars on the cracking behavior of members subjected to pure tension

A concrete prism reinforced with a single bar in the center is a common test specimen used in order to analyze reinforced concrete structure cracking behavior.

Figure 4- 13 Tensile test layout

One of the drawbacks of such test layouts, is that such layouts do not allow to study the particular effects of characteristic parameters like diameter of reinforcement bars, cover, reinforcement ratio, reinforcement bars arrangement independently on the reinforced concrete structures cracking behavior. This limitation made invention of multiple reinforcement bar tensile test equipment possible. On the motivation of the experimental research by [19], multiple reinforcement bar tensile simulation is also used in the present study.

4.2.1 Verification for tensile element

Table 4- 4 Compressive and tensile damage values analyzed for 46.7 Mpa concrete from an excel sheet attached on Appendix D.

	f_{cm}, MPa			f_y, MPa	
concrete	46.7		Steel (4Ø10)		510.1
Compressive and tensile damage properties of concrete					
Compressive damage of concrete			Tensile damage of concrete		
σ	E_{in}	d_c	σ_t	W (mm)	d_t
18.68	0	0	3.432	0	0
19.822	3.254E-05	0	3.236	0.003	0.057
24.049	6.152E-05	0	3.040	0.006	0.114
27.962	9.9496E-05	0	2.843	0.0091	0.171
31.548	0.00015	0	2.647	0.0121	0.228
34.794	0.00020	0	2.451	0.0151	0.286
37.684	0.00027	0	2.255	0.0182	0.343
40.204	0.00034	0	2.059	0.0212	0.4
42.339	0.00043	0	1.863	0.0242	0.457
44.071	0.00053	0	1.667	0.0273	0.514
45.383	0.00065	0	1.471	0.0334	0.571
46.225	0.00077	0	1.274	0.0364	0.628
46.667	0.00091	0	1.078	0.0394	0.686
46.7	0.00096	0	0.882	0.0424	0.743
46.699	0.00096	4.812E-06	0.686	0.0600	0.8
46.466	0.00111	0.0049	0.617	0.0776	0.82
45.723	0.00129	0.0201	0.549	0.0952	0.84
44.443	0.00147	0.048	0.480	0.1128	0.86
42.602	0.00168	0.087	0.411	0.1304	0.88
40.172	0.00189	0.139	0.343	0.1480	0.9
37.122	0.00213	0.205	0.274	0.1655	0.92
33.422	0.00239	0.284	0.205	0.1832	0.94
29.036	0.00266	0.378	0.137	0.2007	0.96
			0.068	0.2183	0.98

Table 4- 5 Material properties used on Abaqus

Material properties used	
Dilation angle	35°
Flow potential eccentricity	0.1
fbo/fco	1.16
K	0.667
Viscosity parameter	0.002

Table 4- 6 property of experimental specimen used for verification

Beam	No of reinforcement	A_c,mm^2	A_s,mm^2	Cover,mm	P,%	f_{cm}, MPa
A-1	4Ø10	22186	314	30	1.415	46.7

4.2.2 Finite element model development for tensile element

4.2.2.1 Geometry of the model

In order to model the concrete and the steel member, solid element is selected. 3D 8-noded hexahedral (brick) elements with reduced integration (C3D8R) available in Abaqus element library was used to model both. Even if similar material is used to model both of them, they are each modeled with their own material properties.

The concrete element is modeled with a size of 500mm x 150mm x 150mm in the longitudinal, transverse and on the height directions respectively. The reinforcement on the other hand is modeled with a length of 600mm considering that the 500mm is embedded in the concrete and the rest 100 mm is left for the application of the load.

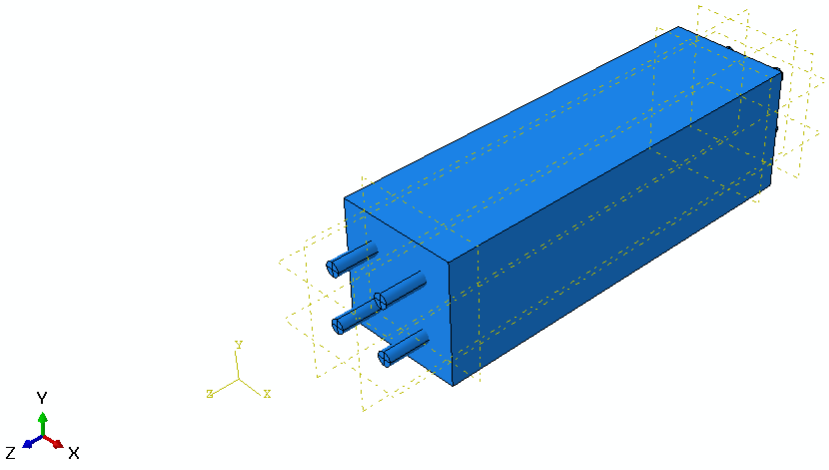

Figure 4- 14 Geometry of the tensile model

4.2.2.2 **Mesh**

Prior to concluding the final element mesh size, different sizes were tried on analyzing the model. The model is finally meshed with approximate element size of 15mm x 15 mm x 15 mm in the longitudinal, transversal and on the height direction respectively.

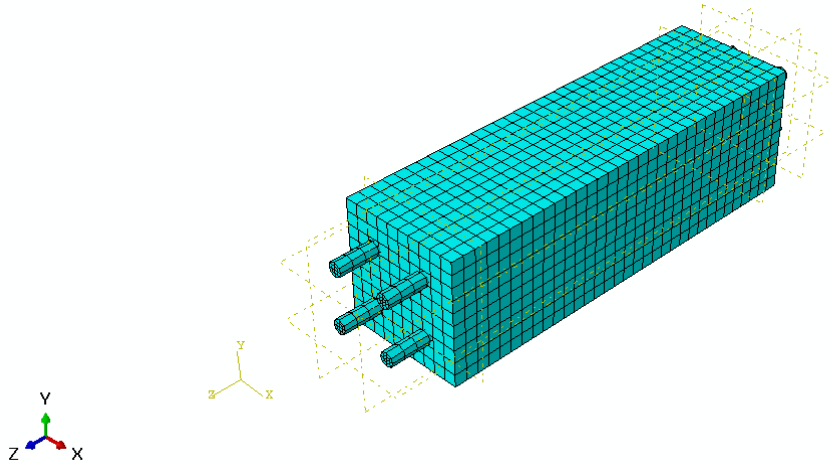

Figure 4- 15 Mesh of the model

4.2.2.3 **Boundary conditions**

A displacement controlled analysis was performed by applying a tensile displacement of 0.2mm/min on the steel member from both sides.

Figure 4- 16 Boundary conditions used in the model

4.2.2.4 **Step time used**

Table 4- 7 Increments used on step time of the model

Maximum number of increments specified		100000
Initial time increment	Minimum time increment	Maximum time increment
0.01	$1*10^{-15}$	0.02

4.2.2.5 **Experimental output**

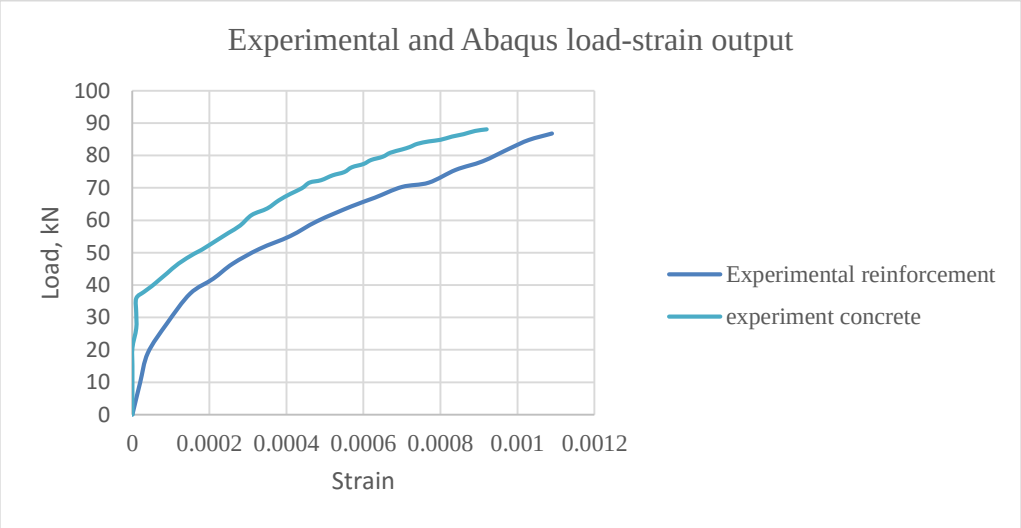

Figure 4- 17 Load-strain graph of experimental tensile beam

4.2.2.6 **Finite element model output compared with experiment**

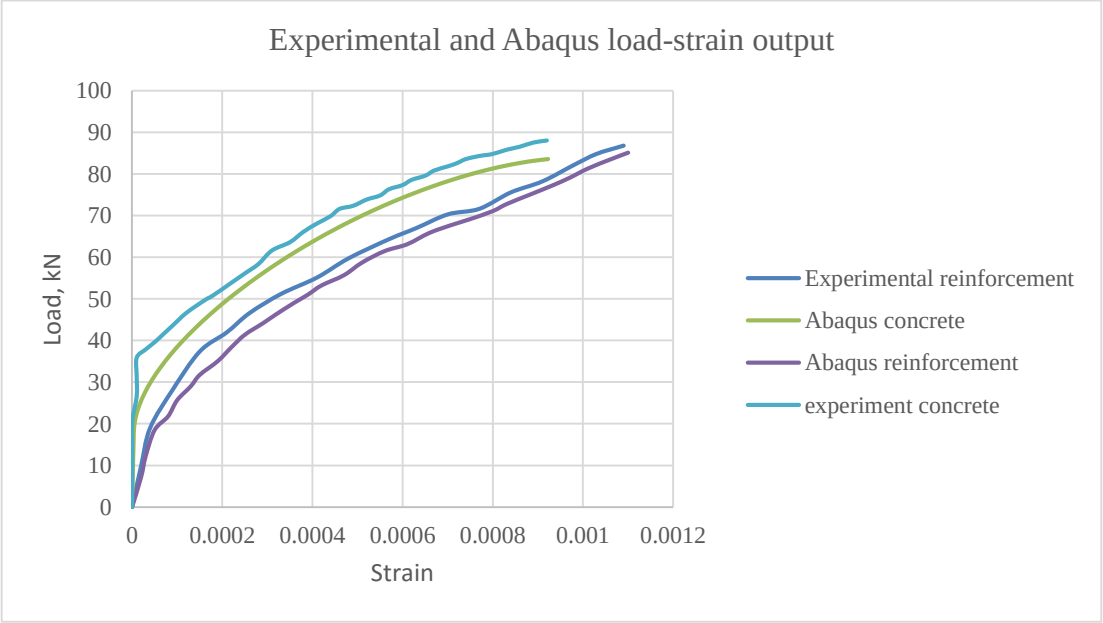

Figure 4- 18 Experimental and Abaqus load-strain output

Three multiple reinforcement bar tensile experimental tests were taken from [19]. The tensile specimen of the experiment has a length of 0.5m and 0.15m x 0.15m size. The load was applied under displacement control and load- strain was used for evaluation.

B-1, B-2 and B-3 are taken from the experiment and compared with the rest tensile equivalent beams.

The load-strain output of the concrete and reinforcement of B-1 was compared with B-1-1 and B-1-2 outputs from the first group. In similar way, outputs of B-2 were compared with B-2-1. And the same goes to the third group. Outputs of B-3 were compared with B-3-1. The same goes to the fourth and fifth groups used for the purpose of this study. Average surface strain of concrete and average strain of reinforcements are considered. Each specimen in each of the three groups have similar reinforcement ratio and size of concrete cross-section.

Table 4- 8 Properties of the multiple bar specimens

Group	Beams	No of reinforcement bars	A_c, mm^2	A_s , mm^2	p,%	f_{cm}, MPa	
1	B-1	4Ø10	22186	314	1.415	46.7	layout difference
	B-1-1	4Ø10	22186	314	1.415		
	B-1-2	16Ø5	22186	314	1.415		
2	B-2	4Ø12	22047.84	452.16	2.051	54	
	B-2-1	16Ø6	22047.84	452.16	2.051		
3	B-3	4Ø14	21884.56	615.44	2.812	43.5	
	B-3-1	12Ø8	21897.12	602.88	2.753		
4	B-4	4Ø10	22186	314	1.415	38	
	B-4-1	16Ø5	22186	314	1.415		
5	B-5	4Ø14	21884.56	615.44	2.812	54	
	B-5-1	12Ø8	21897.12	602.88	2.753		

It should be noted that diameter five (Ø5) reinforcement bar is considered only for equivalent number of bars having similar reinforcement ratio.

❖ **From the first group: -**

B-1: -

Actual model	Deformed shape of concrete
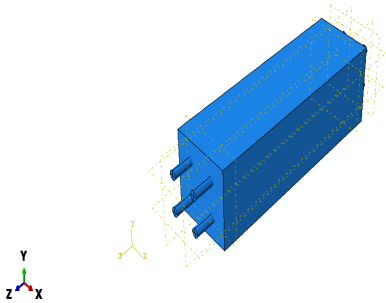	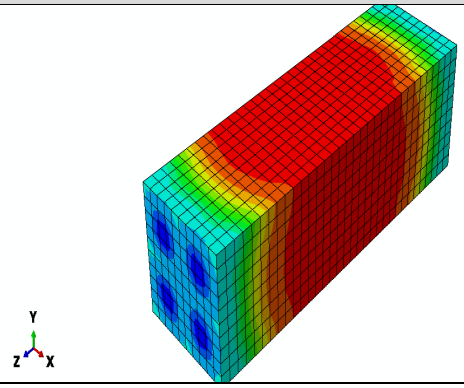

Figure 4- 19 Actual model and deformed shape of concrete for B-1

Deformed shape of reinforcement	Load-strain graph
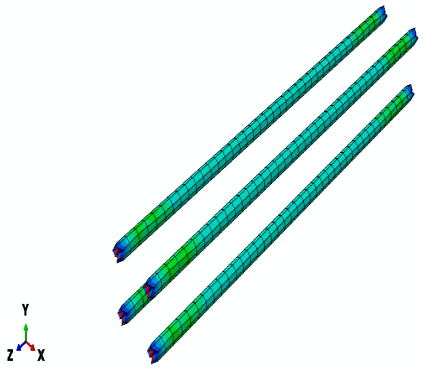	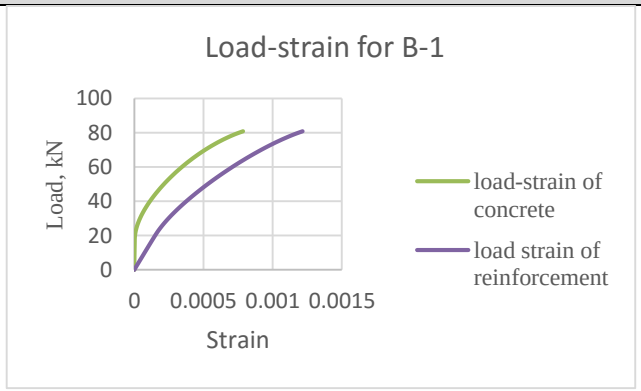

Figure 4- 20 Deformed shape of reinforcement and load-strain diagram for B-1

B-1-1: -

Actual model	Deformed shape of concrete
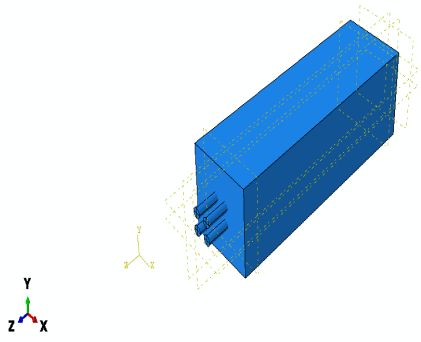	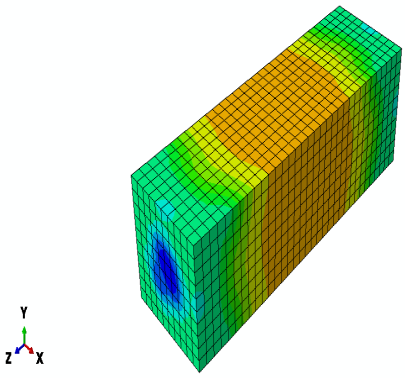

Figure 4- 21 Actual and deformed shape of concrete for B-1-1

Deformed shape of reinforcement	Load strain graph
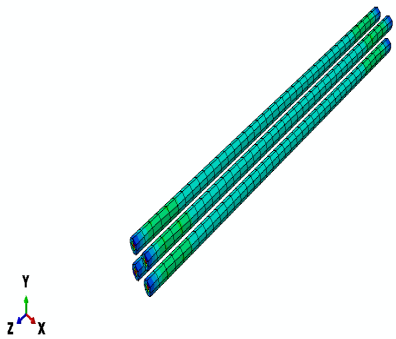	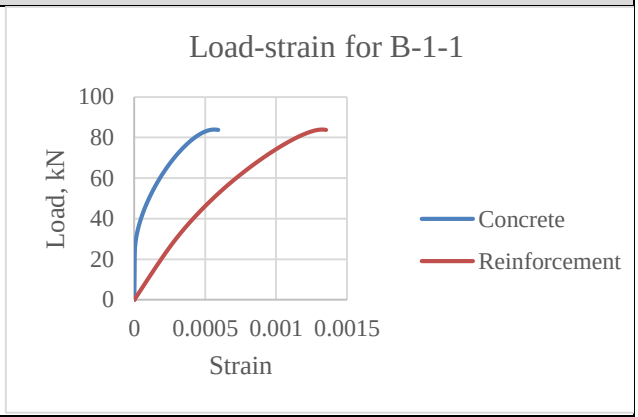

Figure 4- 22 Deformed shape of reinforcement and load-strain of B-1-1

B-1-2: -

Actual model	Deformed shape of concrete
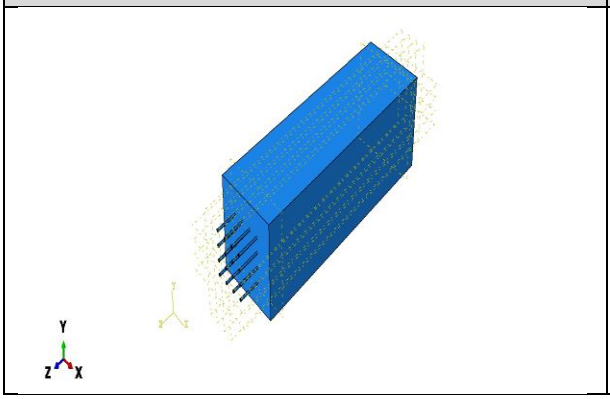	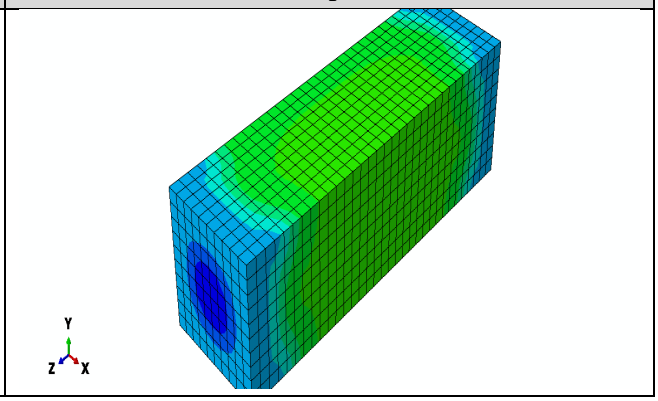

Figure 4- 23 Actual and deformed shape of concrete for B-1-2

Deformed shape of reinforcement	Load-strain graph
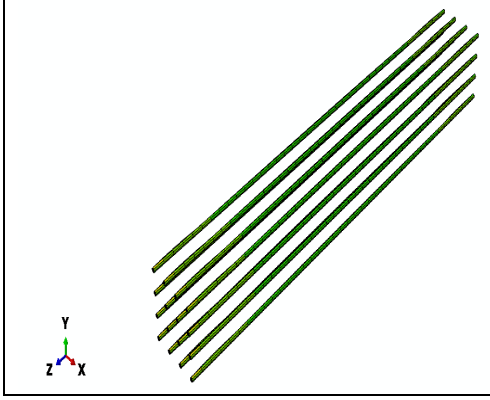	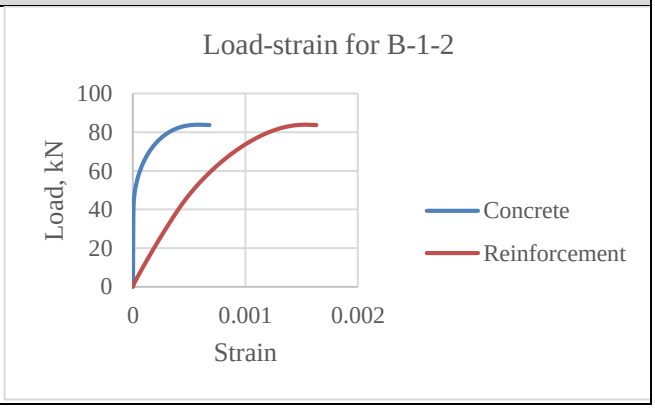

Figure 4- 24 Deformed shape of reinforcement and load strain graph of B-1-2

The above figures from figure 4-19 to 4-24 show the load-strain of concrete and reinforcement for each of the specimens in the first group. The results show that the reinforcement and concrete will not have similar strain under similar increment of load.

The load-strain outputs of concrete and reinforcement of each specimen were compared.

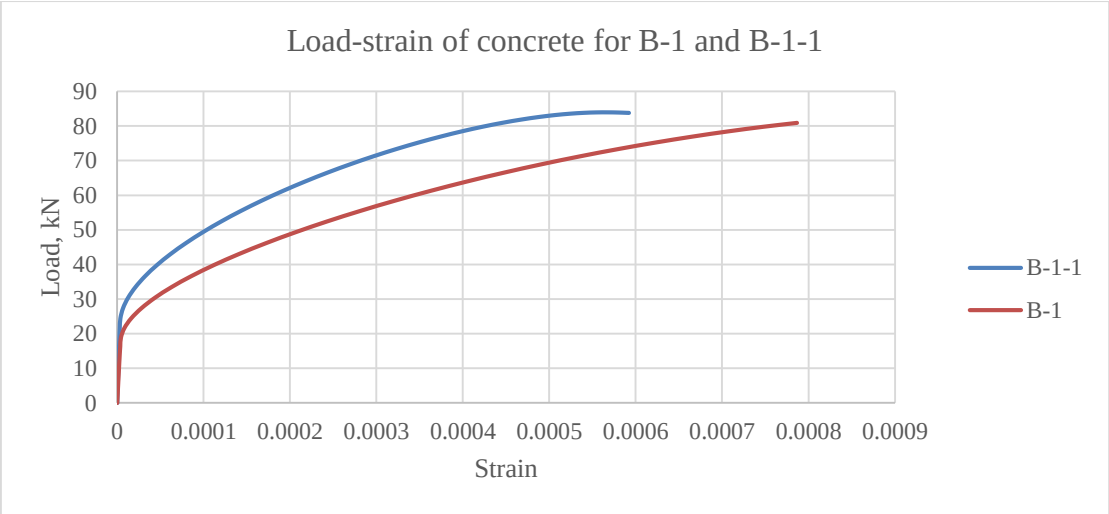

Figure 4- 25 Load-strain diagram of concrete for B-1 and B-1-1

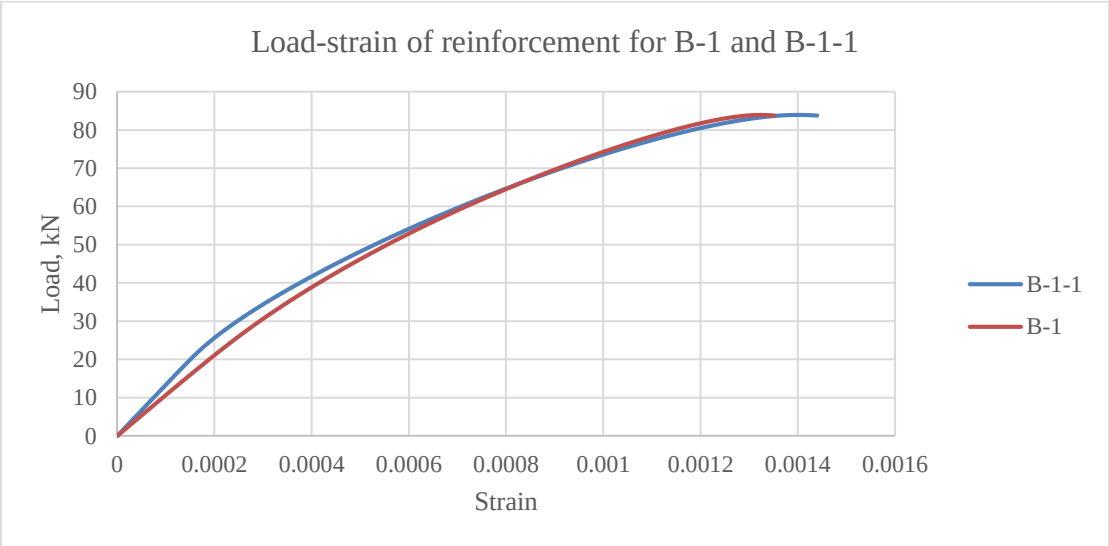

Figure 4- 26 Load-strain diagram for reinforcement of B-1 and B-1-1

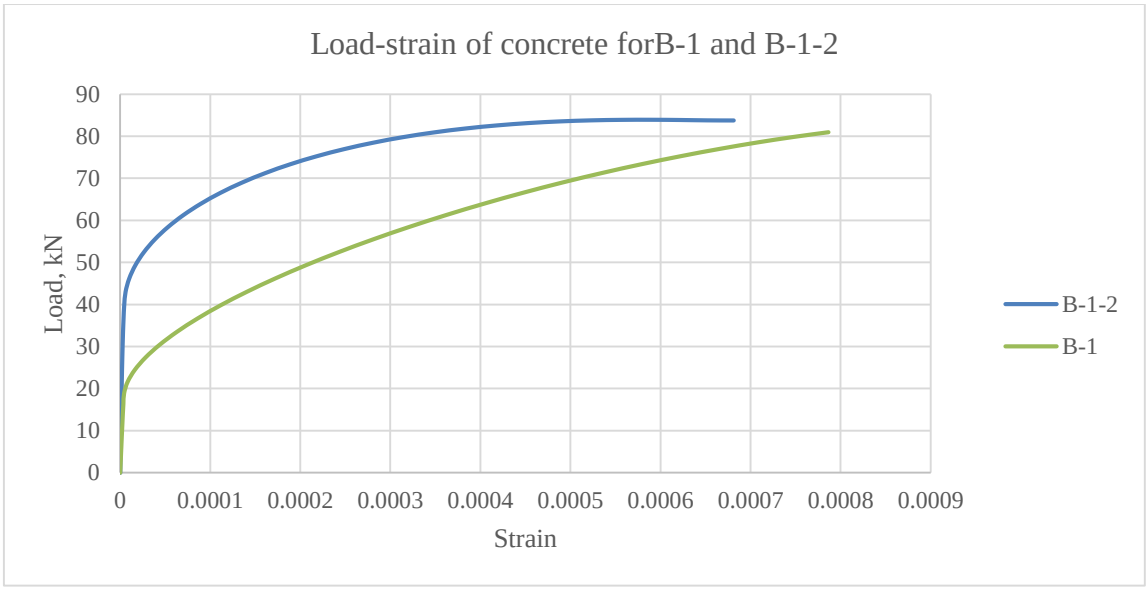

Figure 4- 27 Load-strain diagram of concrete for B-1 and B-1-2

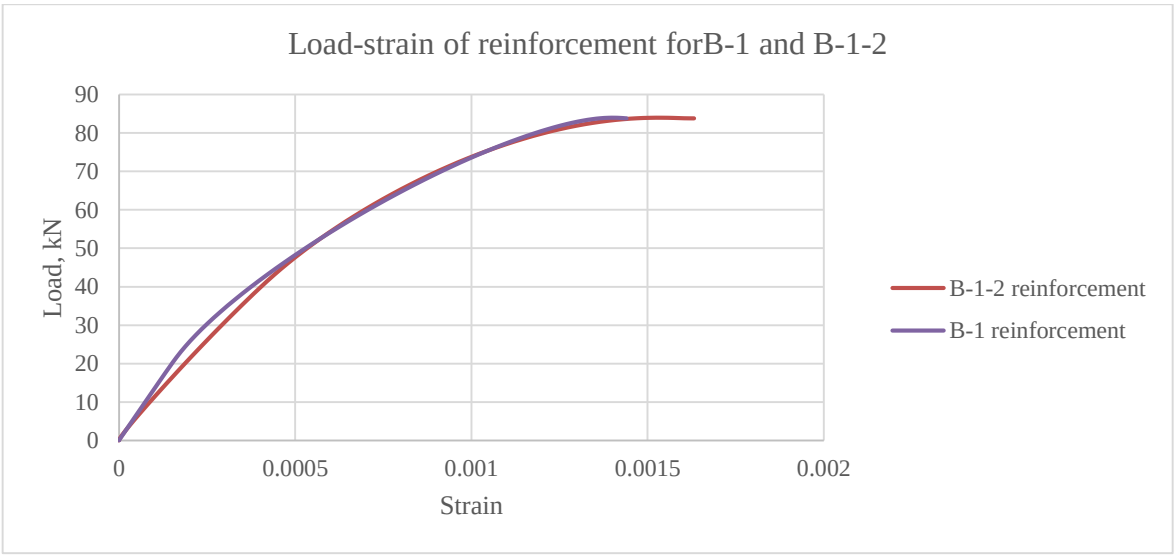

Figure 4- 28 Load-strain diagram of reinforcement for B-1 and B-1-2

Comparing the load-strain outputs of concrete and reinforcement in B-1 with that of B-1-1 and B-1-2, it can be observed that: -

- The load-strain output of concrete in B-1 is different compared with B-1-1, which have a wider cover. Even if they have similar reinforcement, the position of the bars made difference in their response to the applied load.
- The load-strain output of reinforcement in B-1 is almost similar to that of the output in B-1-1. The arrangement of the bars does not put any effect on their response.

- In similar way, the load-strain output of concrete in B-1 is different from that of B-1-2. Comparing the two results, B-1-2 is stiffer than B-1 due to the increased bonded area in case of B-1-2.
- The load-strain output of reinforcement in B-1 is similar to that of the output in B-1-2. This again shows that for specimens with bars having similar reinforcement ratio, reinforcement bar arrangement has no effect in the response of reinforcement.
- In addition to this, from figure 4-19 up to figure 4-24, it can be observed that arrangement of reinforcement will have an effect on the deformed shape or cracking behavior of the specimens under similar load application.

❖ **From the second group**: -

B-2 and B-2-1 were compared.

B-2: -

Actual model	Deformed shape of concrete
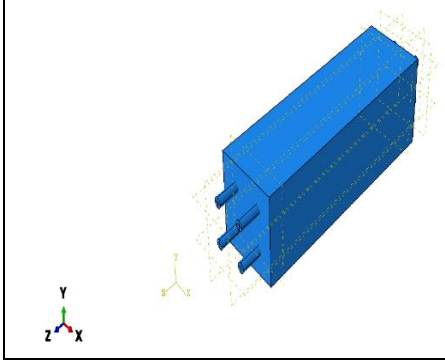	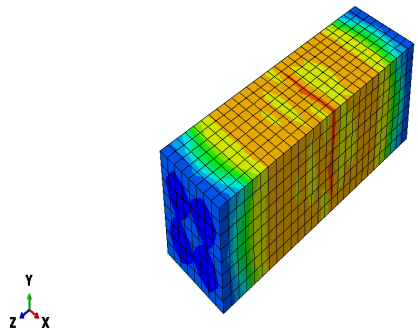

Figure 4- 29 Actual and deformed shape of concrete for B-2

Deformed shape of reinforcement	Load-strain graph
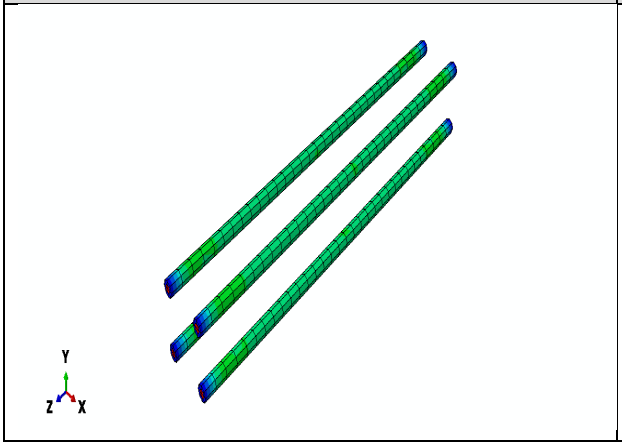	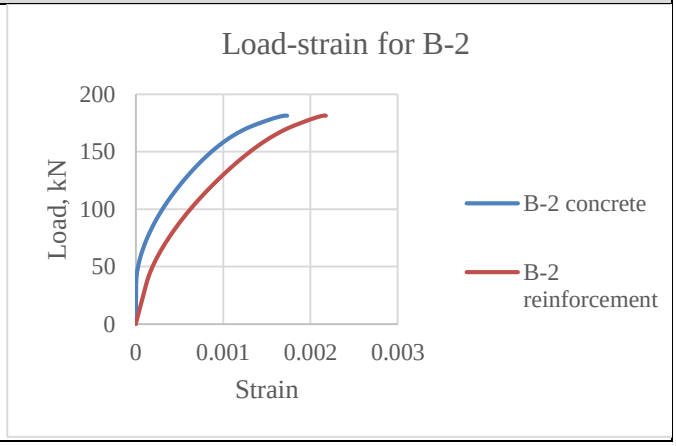

Figure 4- 30 Deformed shape of reinforcement and load-strain diagram of B-2

B-2-1: -

Actual model	Deformed shape of concrete
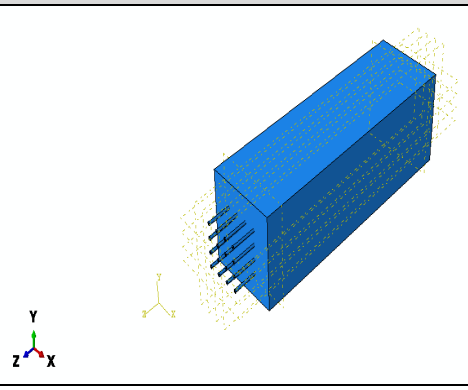	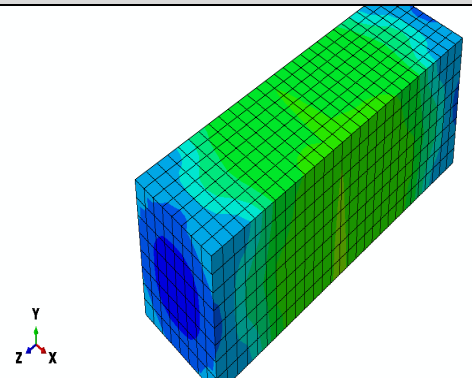

Figure 4- 31 Actual model and deformed shape of concrete for B-2-1

Deformed shape of reinforcement	Load-strain graph
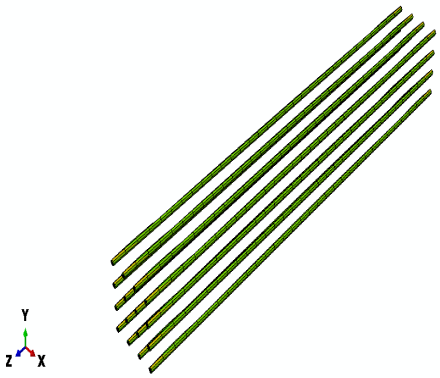	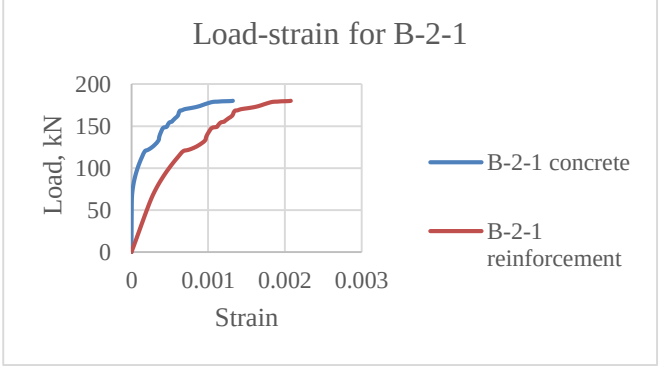

Figure 4- 32 Deformed shape of reinforcement and load-strain diagram for B-2-1

The above figures from figure 4-29 to 4-32 show the load-strain of concrete and reinforcement for each of the specimens in the second group. The results show that the reinforcement and concrete will not have similar strain under similar increment of load.

The load-strain outputs of concrete and reinforcement of each specimen in this group were compared.

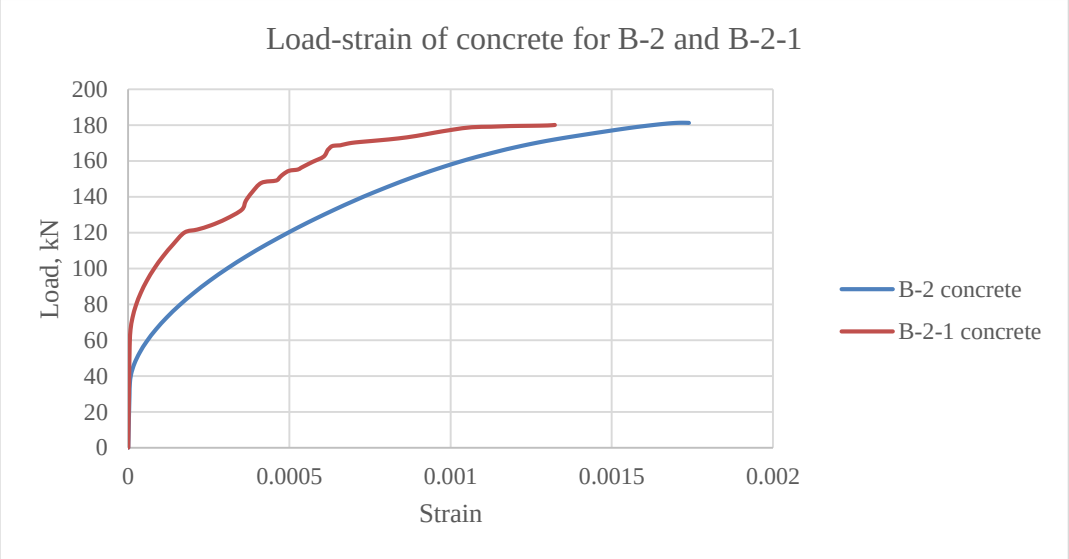

Figure 4- 33 Load-strain of concrete for B-2 and B-2-1

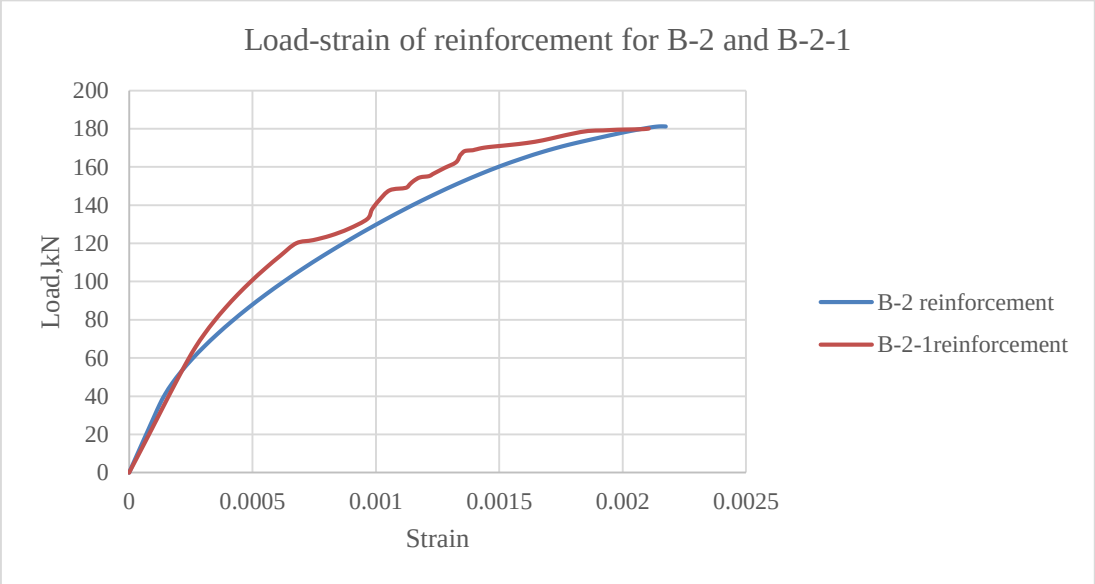

Figure 4- 34 Load-strain of reinforcement for B-2 and B-2-1

Comparing the load-strain outputs of concrete and reinforcement in B-2 with that of B-2-1, it can be observed that: -

- The load-strain output of concrete in B-2 is different compared with B-2-1. Even if they have similar reinforcement ratio, the position and difference in number of reinforcement bars made difference in their response to the applied load.
- The load-strain output of reinforcement in B-2 is similar to that of the output in B-2-1. This shows that for specimens with bars having similar reinforcement ratio, reinforcement bar arrangement has no effect in the response of reinforcement.

- In addition to this, from figure 4-29 up to figure 4-32, it can be observed that arrangement of reinforcement will have an effect on the deformed shape or cracking behavior of the specimens under similar load application.

❖ **From the third group:** -

B-3 and B-3-1 were compared.

B-3: -

Actual model	Deformed shape of concrete
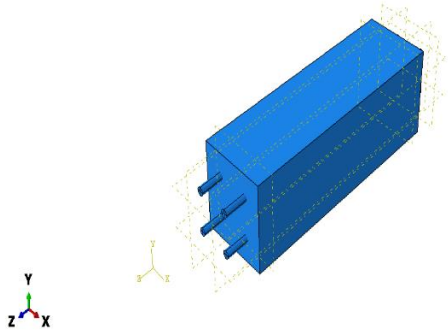	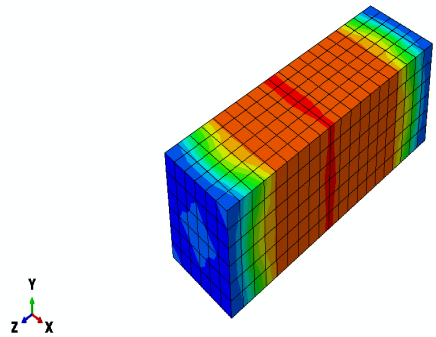

Figure 4- 35 Actual model and deformed shape of concrete for B-3

Deformed shape of reinforcement	Load-strain graph
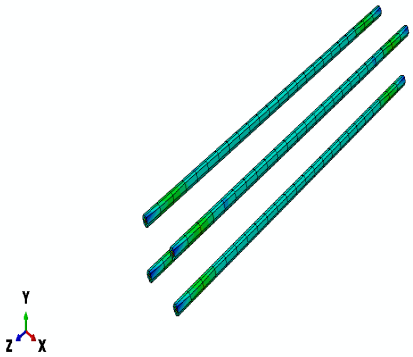	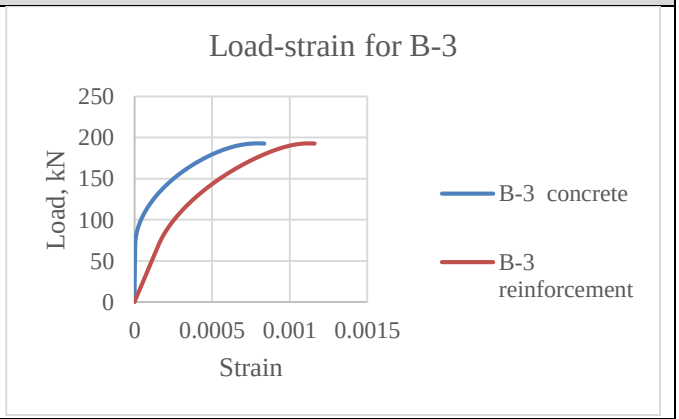

Figure 4- 36 Deformed shape of reinforcement and load-strain graph of B-3

B-3-1: -

Actual model	Deformed shape of concrete
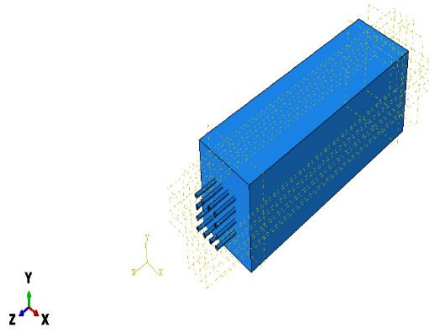	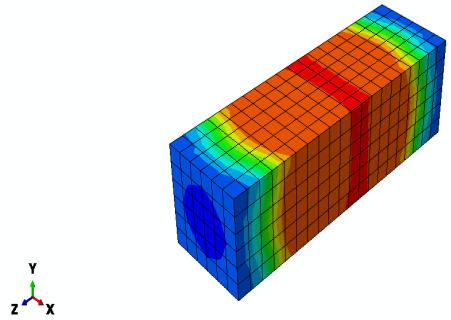

Figure 4- 37 Actual model and deformed shape of concrete for B-3-1

Deformed shape of reinforcement	Load-strain graph
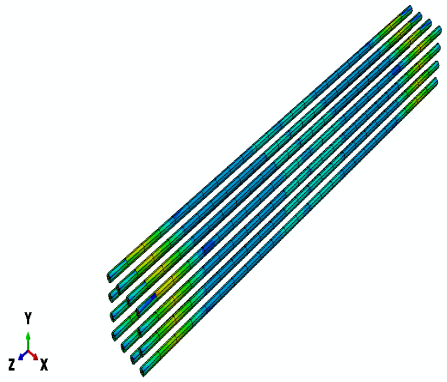	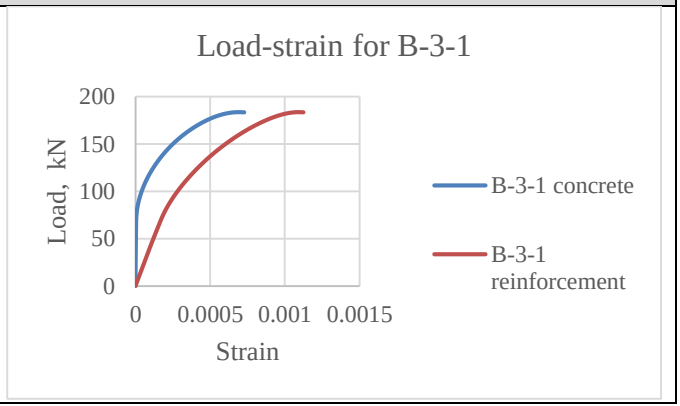

Figure 4- 38 Deformed shape of reinforcement and load-strain diagram of B-3-1

The above figures from figure 4-35 to 4-38 show the load-strain of concrete and reinforcement for each of the specimens in the third group. The results show that the reinforcement and concrete will not have similar strain under similar increment of load.

The load-strain outputs of concrete and reinforcement of each specimen in this group were compared.

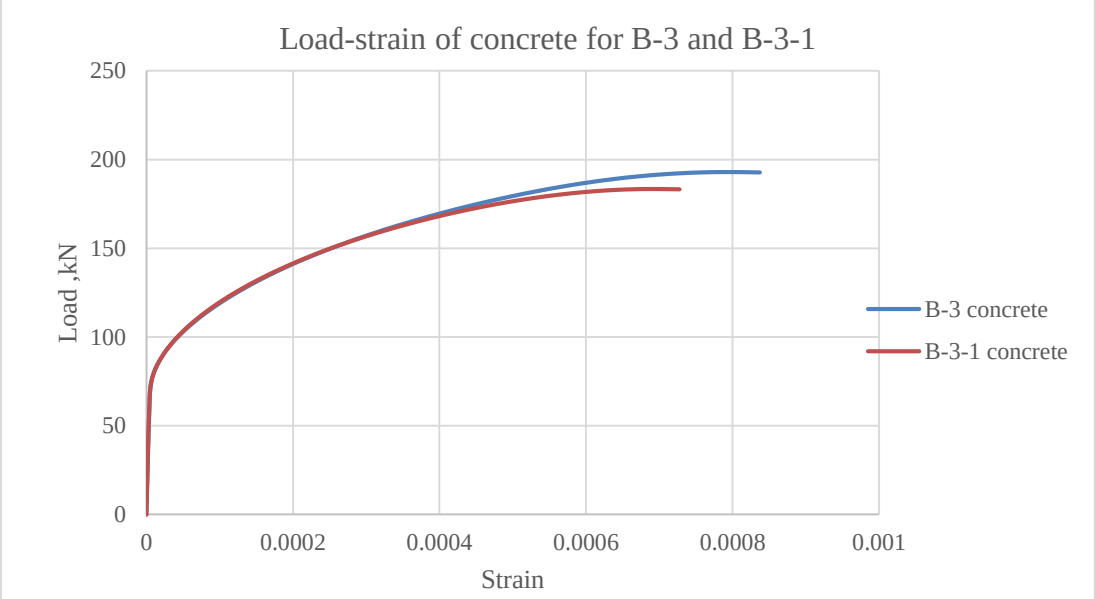

Figure 4- 39 Load-strain of concrete for B-3 and B-3-1

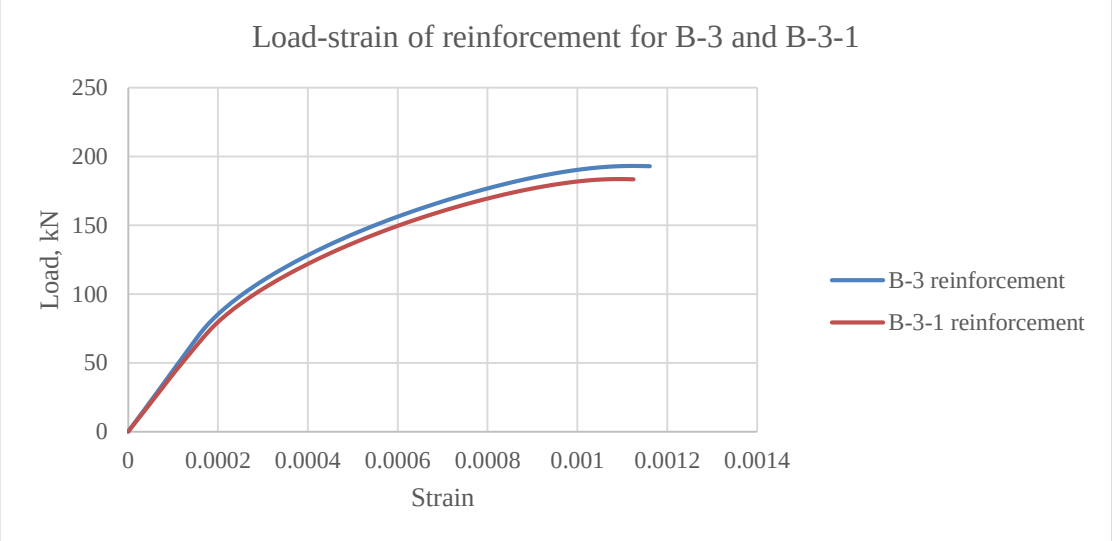

Figure 4- 40 Load-strain of reinforcement for B-3 and B-3-1

Comparing the load-strain outputs of concrete and reinforcement in B-3 with that of B-3-1, it can be observed that: -

- The load-strain output of reinforcement in B-3 is almost similar to that of the output in B-3-1. This shows that for specimens with bars having almost similar reinforcement ratio, reinforcement bar arrangement has no effect in the response of reinforcement.

- The load-strain output of concrete in B-3 is similar to that of B-3-1. This is due to the reduced reinforcement ratio in B-3-1. But comparing the two results, B-3-1 is stiffer than B-3 due to the increased bonded area in case of B-3-1.
- In addition to this, from figure 4-35 up to figure 4-38, it can be observed that arrangement of reinforcement will have an effect on the deformed shape or cracking behavior of the specimens under similar load application.

❖ **From fourth to fifth group: -**

Tensile beams of earlier groups were simulated with a different concrete compressive strength.

B-4: -

Actual model	Deformed shape of concrete
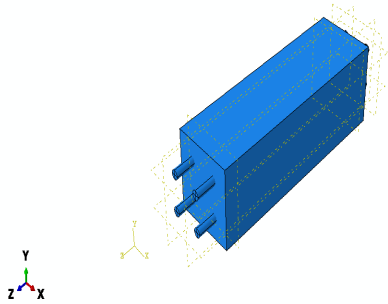	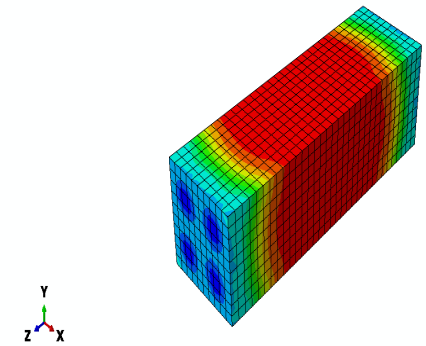

Figure 4- 41 Actual model and deformed shape of concrete for B-4

Deformed shape of reinforcement	Load-strain graph
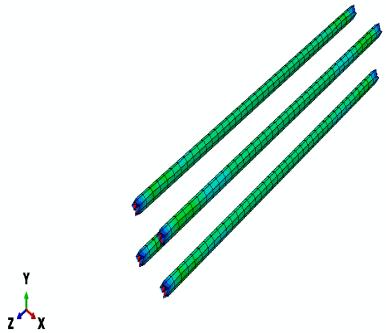	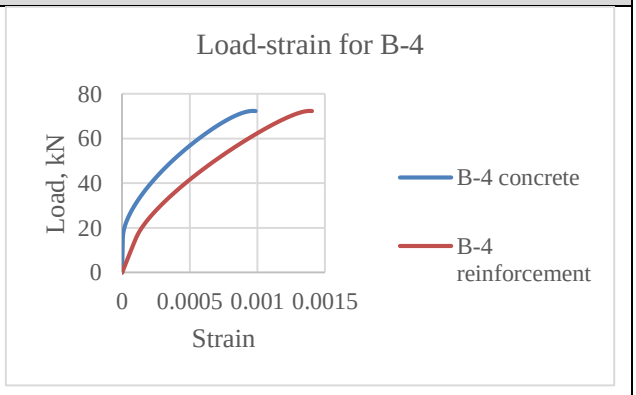

Figure 4- 42 Deformed shape of reinforcement and load-strain graph of B-4

B-4-1: -

Actual model	Deformed shape of concrete
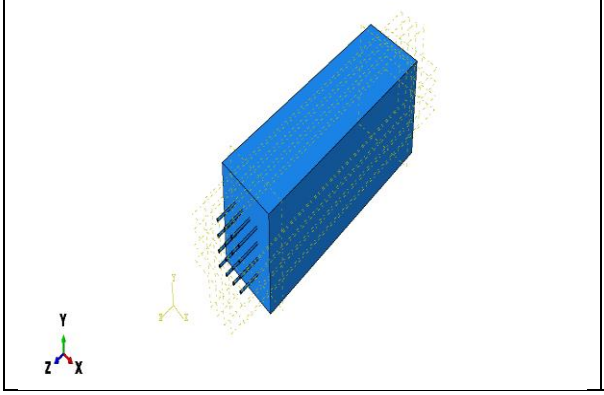	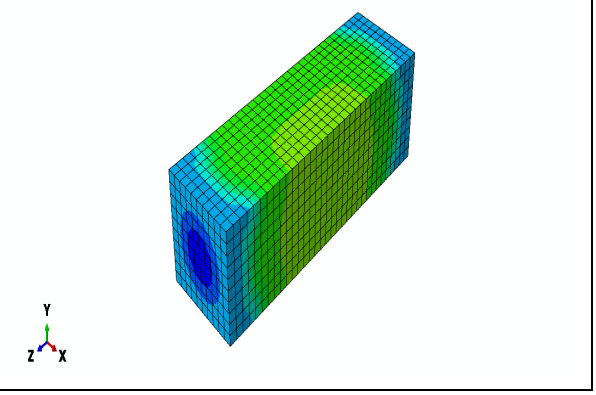

Figure 4- 43 Actual model and deformed shape of concrete for B-4-1

Deformed shape of reinforcement	Load-strain graph
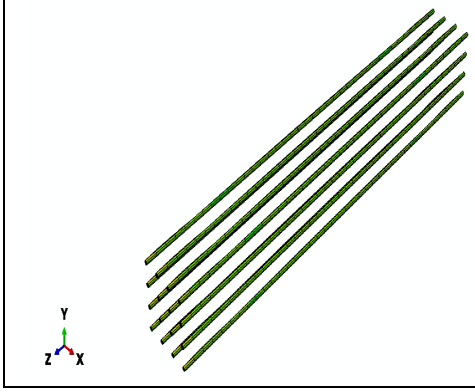	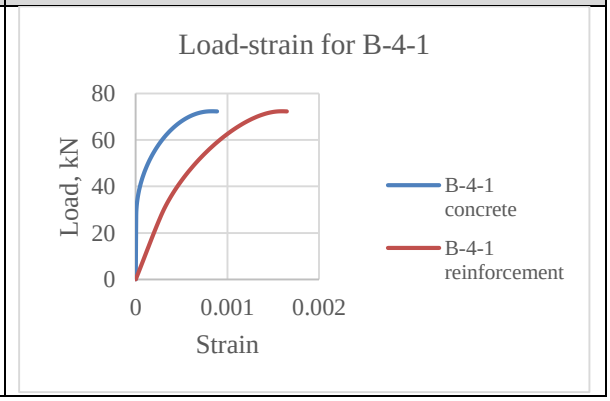

Figure 4- 44 Deformed shape of reinforcement and load-strain graph for B-4-1

The above figures from figure 4-41 to 4-44 show the load-strain of concrete and reinforcement for each of the specimens in the fourth group. The results show that the reinforcement and concrete will not have similar strain under similar increment of load.

The load-strain outputs of concrete and reinforcement of each specimen in this group were compared.

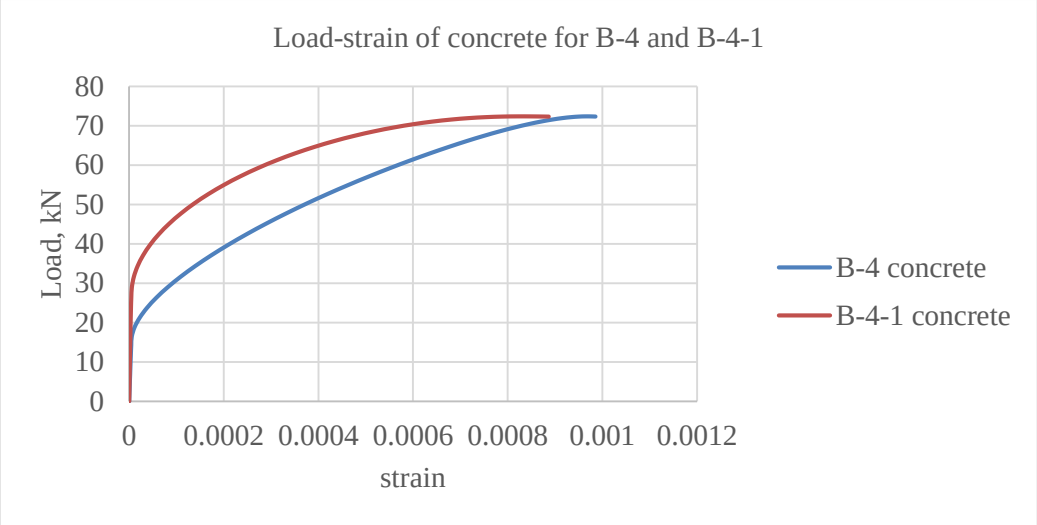

Figure 4- 45 Load-strain of concrete for B-4 and B-4-1

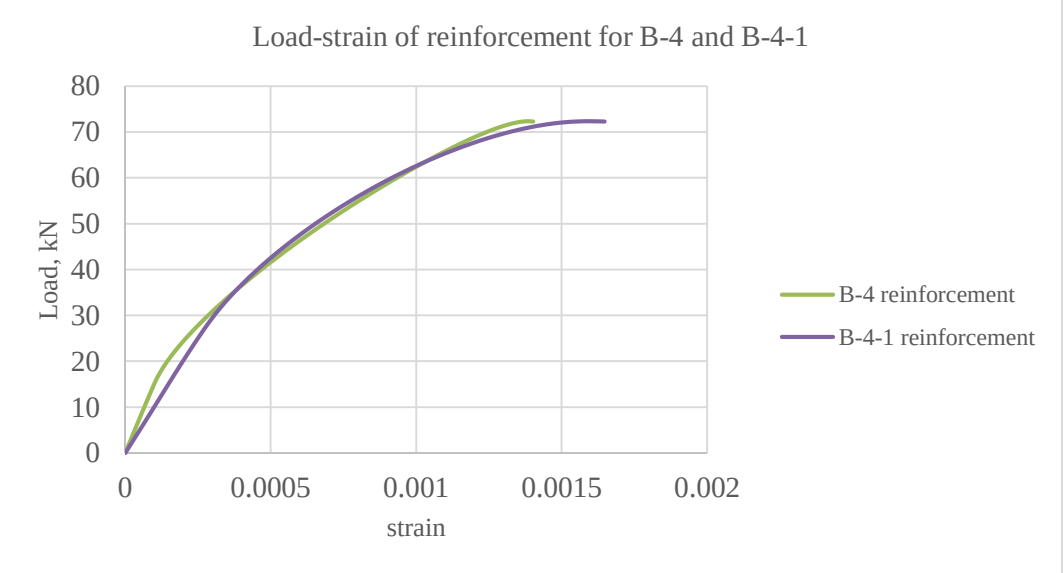

Figure 4- 46 Load-strain of concrete for B-4 and B-4-1

Comparing the load-strain outputs of concrete and reinforcement in B-4 with that of B-4-1, it can be observed that: -

- The load-strain output of concrete in B-4 is different compared with B-4-1. Even if they have similar reinforcement ratio, the position and difference in number of reinforcement bars made difference in their response to the applied load.
- The load-strain output of reinforcement in B-4 is similar to that of the output in B-4-1. This shows that for specimens with bars having similar reinforcement ratio, reinforcement bar arrangement has no effect in the response of reinforcement.

- In addition to this, from figure 4-41 up to figure 4-44, it can be observed that arrangement of reinforcement will have an effect on the deformed shape or cracking behavior of the specimens under similar load application.

B-5: -

Actual model	Deformed shape of concrete
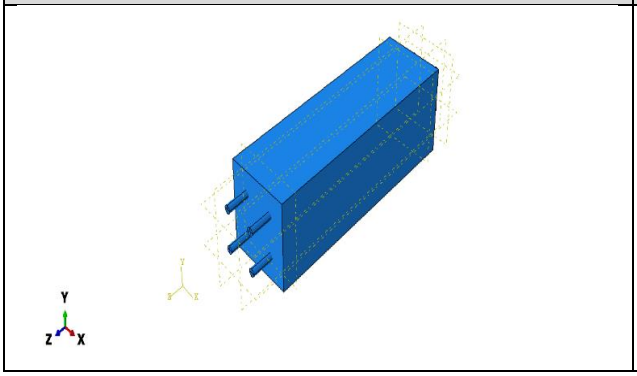	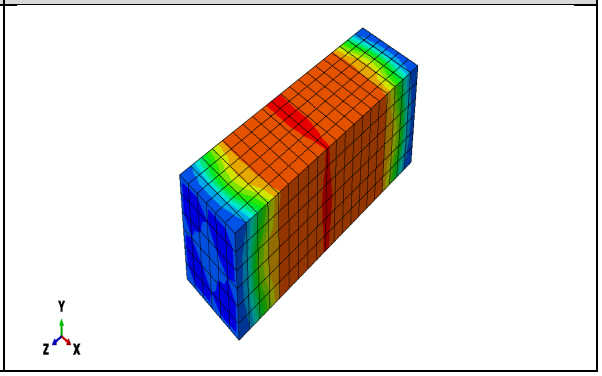

Figure 4- 47 Actual model and deformed shape of concrete for B-5

Deformed shape of reinforcement	Load-strain graph
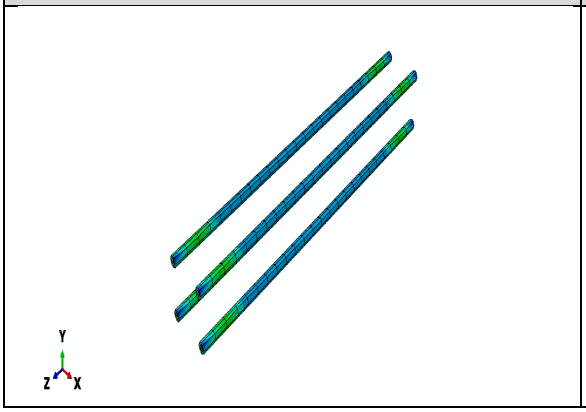	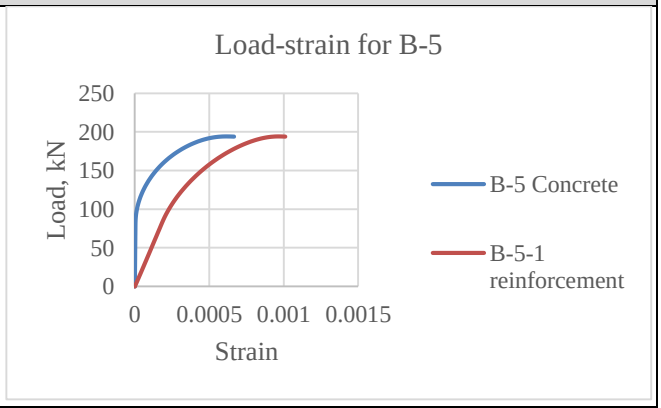

Figure 4- 48 Deformed shape of reinforcement and load-strain graph of B-5

B-5-1: -

Actual model	Deformed shape of concrete
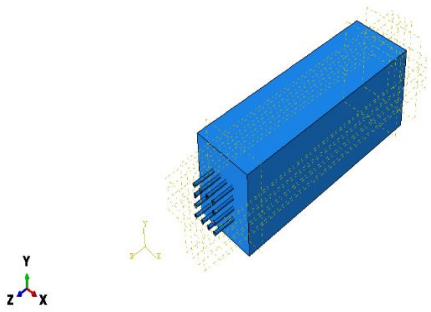	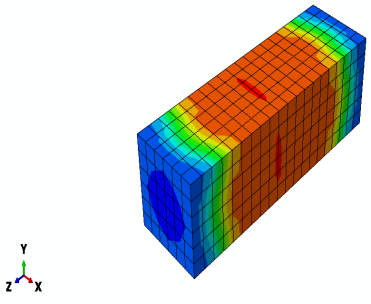

Figure 4- 49 Actual and deformed shape of concrete for B-5-1

Deformed shape of reinforcement	Load-strain graph
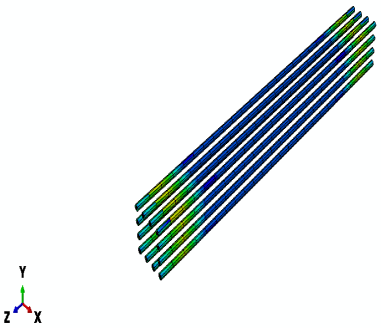	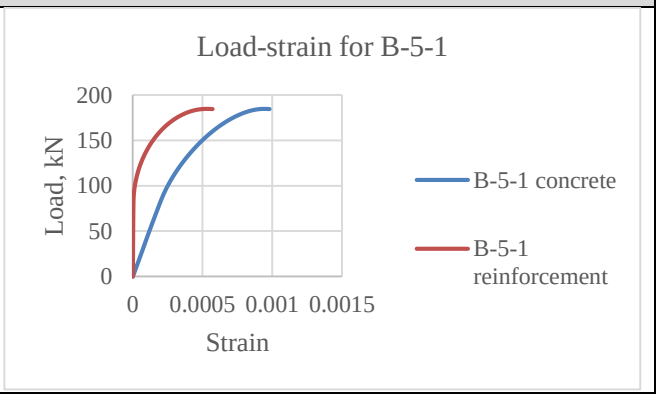

Figure 4- 50 Deformed shape of reinforcement and load- strain for B-5-1

The above figures from figure 4-47 to 4-50 show the load-strain of concrete and reinforcement for each of the specimens in the fifth group. The results show that the reinforcement and concrete will not have similar strain under similar increment of load.

The load-strain outputs of concrete and reinforcement of each specimen in this group were compared.

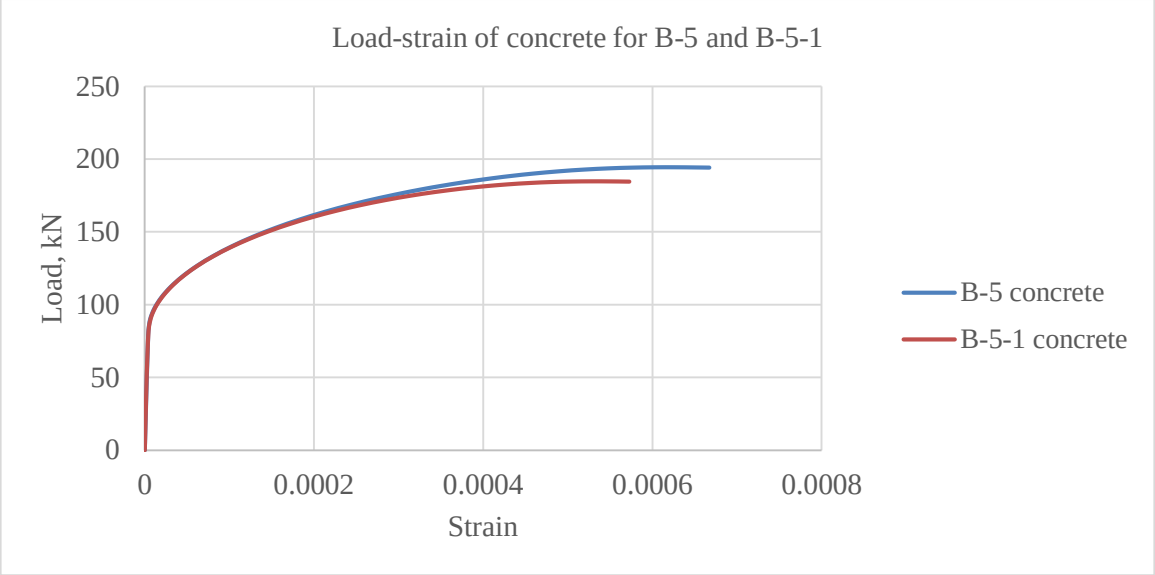

Figure 4- 51 Load-strain of concrete for B-5 and B-5-1

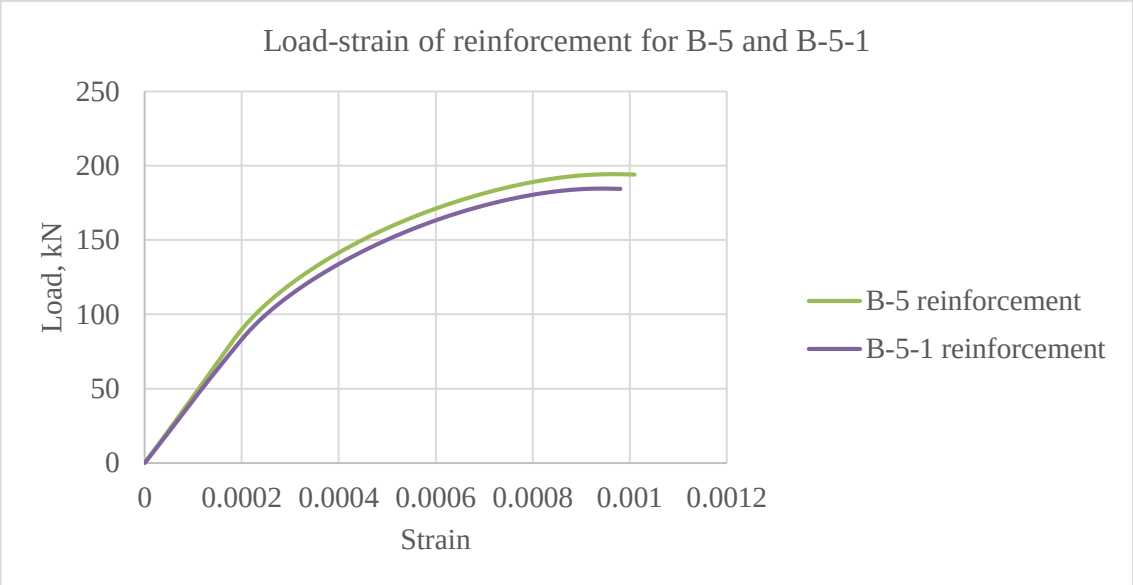

Figure 4- 52 Load-strain of reinforcement for B-5 and B-5-1

Comparing the load-strain outputs of concrete and reinforcement in B-5 with that of B-5-1, it can be observed that: -

- The load-strain output of reinforcement in B-5 is similar to that of the output in B-5-1. This shows that for specimens with bars having similar reinforcement ratio, reinforcement bar arrangement has no effect in the response of reinforcement.

- The load-strain output of concrete in B-5 is similar to that of B-5-1. This is due to the reduced reinforcement ratio in B-5-1. But comparing the two results, B-5-1 is stiffer than B-5 due to the increased bonded area in case of B-5-1.
- In addition to this, from figure 4-47 up to figure 4-50, it can be observed that arrangement of reinforcement will have an effect on the deformed shape or cracking behavior of the specimens under similar load application.

In the above cases of tensile members, differences were observed in the strain of concrete in each group related with arrangement of reinforcement. Whereas, the strain in the reinforcements were almost similar in each of the cases. This showed that reinforcement bars arrangement will have an effect on the reinforced concrete structures cracking behavior.

4.2.3 Cracking analysis of the tensile beams according to ES EN 1992-1-1:2013

In order to assess the differences in crack distances which are expected to potentially occur in groups of tensile beams, ES EN 1992-1-1:2013 code predictions were used.

The table below shows the calculated maximum crack distances according to equation 2-11 of chapter 2. Detail calculation is shown on Appendix E.

Table 4- 9 Calculated maximum crack distances based on code prediction

Group	Beams	No of reinforcement bars	p,%	Ø/p	c,mm	$S_{r,max}$
1	B-1	4Ø10	1.415	706.714	30	342.283
	B-1-1	4Ø10	1.415	706.714	50	410.283
	B-1-2	16Ø5	1.415	353.357	30	222.141
2	B-2	4Ø12	2.051	585.080	30	300.927
	B-2-1	16Ø6	2.051	292.540	30	201.464
3	B-3	4Ø14	2.812	497.866	30	271.274
	B-3-1	12Ø8	2.753	290.592	30	200.801

The maximum crack distances calculated from the code prediction explained that crack distances which will be expected to potentially occur in tensile beams with larger number of reinforcements are smaller as compared with that of tensile beams with smaller number of reinforcements. This can be related with the increased bonded area between the reinforcement and concrete.

The tables below show the result comparison for both flexural and tensile beams considering under this study.

Table 4- 10 Result comparison for flexural beams

Result comparison for flexural beams			
Groups	Specimens	Curvature obtained, 1/mm	Change in curvature,%
1	A-1	1.59E-05	
	B-1	1.47E-05	7.55
2	A-2	1.42E-05	
	B-2	1.29E-05	9.154

Table 4-10 shows a decrease in curvature as the number of reinforcement with similar reinforcement ratio increases. In flexural elements, an increase in reinforcement number will be related with flexural stiffness.

Table 4- 11 Result comparison for tensile beams

Result comparison for tensile beams				
Groups	Specimens	Strain in concrete	Strain in reinforcement	Change in strain of concrete,%
1	B-1	0.001047	0.0014	
	B-1-1	0.000592	0.00135	43.48
	B-1-2	0.000681	0.0014	34.95
2	B-2	0.00174	0.0021	
	B-2-1	0.001324	0.0021	23.91
3	B-3	0.000838	0.0011	
	B-3-1	0.000728	0.0011	13.13
4	B-4	0.000985	0.0014	
	B-4-1	0.000887	0.0016	9.95
5	B-5	0.000667	0.001	
	B-5-1	0.000573	0.001	14.09

As can be seen from table 4-11, the strain in reinforcement of each group is similar. Differences are observed in strain of concrete in each group. As the number of reinforcement is increased for a similar reinforcement ratio in each group of specimen, the bonded area will also increase. This affected the response in the concrete of each specimen.

In addition to this, from table 4-3 and table 4-9 maximum crack distance predictions from code showed that an increase in reinforcement number for similar reinforcement ratio will decrease crack distances in both tensile and flexural elements.

CHAPTER 5 CONCLUSIONS AND RECOMMENDATIONS

5.1 Conclusions

In this research, effect of layered reinforcement bar arrangement on the deformation and cracking behavior of reinforced concrete beams has been studied by reviewing different literatures, codes, experimental researches and through analytical simulation of fifteen beam specimens, four under flexural loading and eleven beams considered under pure tension. After examining these analyses, the following points are put forward.

1. Numerical models, calibrated with carefully collected experimental results, are capable of assessing effects which are too complicated to be evaluated experimentally. Such numerical models are capable in predicting reinforced concrete structures cracking behavior with different arrangements of reinforcement.
2. In flexural elements, different reinforcement layouts show correlation with flexural stiffness and do not show direct relationship with reinforced concrete structures cracking behavior.
3. The complex nature of flexural elements will limit the ability to evaluate the effect of reinforcement bar arrangement in tension zone on the reinforced concrete structures cracking behavior. But reinforced concrete structures exposed to pure tension will help to assess the effects of reinforcement bar arrangement on cracking behavior in a good way by isolating uncertainties related with effective area of concrete in tension.
4. The differences in the deformed shape of tensile members with similar size of concrete cross-section and reinforcement ratio are related with differences related with concrete cover and bonded area with different diameter of reinforcement bars.
5. The strain observed in the specimens varies not only along the bar but also with in the surface of the concrete section.
6. Beams with larger number of reinforcements are capable of safeguarding the cracking behavior of the beams than beams with smaller number of reinforcements even if they have identical reinforcement ratios and size of concrete cross-section.

7. Considering the tensile members, adequacy of evaluating the cracking behavior in the members is closely associated with assessing the strain in the concrete since the strain in the reinforcement is similar in the cases considered.

5.2 Recommendations

This research focused on the cracking and deformation behavior of reinforced concrete beams considering the effect of layered reinforcement bar arrangement under flexural loading and pure tension. The results and conclusions are limited by the parameter that was studied.

1. Additional parameters that have an effect on the cracking behavior of reinforced concrete structures like effects related with diameter of bar, concrete strength, concrete cover, embedment length, confinement effect, aggregate size effect, loading effect should be studied.
2. Experimental tests should be conducted to see the accuracy of the numerical models.
3. Multiple bar tensile tests should be encouraged to study different parameters independently. Since the usual type of tensile test can only study limited effects related with diameter of bar and does not support studying parameters independently.
4. Further study should be done in relation with effects of different fibers and reinforcement bar arrangement on reinforced concrete structures cracking behavior.

REFERENCES

[1] D. Floros, A. Ingason, "Modeling and simulation of reinforced concrete beams: Coupled analysis of imperfectly bonded reinforcement in fracturing concrete" Goteborg, Sweden, 2013

[2] Saurabh Dhanmeher, "Crack pattern observations to finite element simulation: An Exploratory Study for Detailed Assessment of Existing Reinforced Concrete Structures" November, 2017

[3] Gerd-Jan Schreppers, Chantal Frissen, Hee-Jeong Kang, "Prediction of Crack-width and Crack-pattern", November 2011

[4] George C. Sih, A. DiTommaso, "Fracture mechanics of concrete: Structural application and numerical calculation", 1985

[5] Nuraziz Handika, "Multi-cracking of Reinforced Concrete Structures: Image Correlation Analysis and Modeling", INSA de Toulouse, 2017.

[6] R. I. Gilbert and S. Nejadi, "An experimental study of flexural cracking in reinforced concrete members under short term loads", The University of New South Wales, April 2015.

[7] Task Group Bond Models, fib Bulletin 10: "Bond of reinforcement in concrete, State of the art report.", International Federation for Structural Concrete, Lausanne, Switzerland, 2000

[8] Pieter Desnerck, Janet M. Lees, Chris T. Morley, "Bond behavior of reinforcing bars in cracked concrete", 2015

[9] k. Holschemacher and D. Weibe, "Bond of reinforcement in ultra-strength reinforced concrete", September 2004

[10] Simon Hang Chi Chan, "Bond and Cracking of Reinforced Concrete", PhD Thesis, March 2012

[11] Tepfers R., "cracking of concrete cover along anchored deformed reinforcing bars", magazine of concrete research 31(106), Pp.3-12, 1979

[12] Yun Lin, "Tension stiffening model for reinforced concrete based on bond stress slip relation", Aug.2010

[13] Graham Dean Roberts, "Simplified method to nonlinear analysis of reinforced concrete in pure flexure", Johannesburg 2015

[14] Gintaris Kaklauskas, Vytautas Tamulenas, Viktor Gribniak, Pui Lam Ng, and Rimantas Kupliauskas, "Tension-stiffening behavior of reinforced concrete ties of various strength classes", Pp. 582-590, Dec 2015

[15] Francesco Morelli, Cosimo Amico, Walter Salvatore, Nunziante Squeglia and Stefano Stacul, "Influence of Tension Stiffening on the Flexural Stiffness of Reinforced Concrete Circular Sections", 2017

[16] Eurocode 2: Design of Concrete Structures –Part 1: General Rules and Rules for Buildings, EN 1992-1-1:2004. Brussels: CEN, 2004

[17] ES EN 1992-1-1:2013: Design of Concrete Structures: final Draft

[18] Kaklauskas et al, "Tension-stiffening relationships based on design code provisions", 3rd *fib* International Congress – May, 2010

[19] Arvydas Rimkus, "Effects of bar reinforcement arrangement on deformations and cracking of concrete elements" PhD thesis, 2017

[20] Bischoff, P. H., "Effects of shrinkage on tension stiffening and cracking in reinforced concrete". Canadian Journal of Civil Engineering, 28(3), Pp 363–374, 2001

[21] Gudonis, E., Kacianauskas, R., Gribniak, V., Weber, A., Jakubovskis, R. & Kaklauskas, G., "Mechanical properties of the bond between GFRP reinforcing bars and concrete" Mechanics of Composite Materials, 50(4), Pp 457–466, 2014

[22] Gil Martín L.M., Carbonell-Márquez J.F., Hernández-Montes E., "Upper bound to the effective area of concrete in tension", 3rd international conference on mechanical model in structural engineering, Spain, June 2015

[23] Wahalathantri, B.L., Thambiratnam, D.P., Chan, T.H.T., & Fawzia, S., "A material model for flexural crack simulation in reinforced concrete elements using Abaqus" Queensland University of Technology, Brisbane, Australia, Pp 260-264, 2011

[24] L. Jendele, J. Červenka, V. Saouma and R. Pukl, "On the choice between discrete or smeared approach in practical structural FE analyses of concrete structures", U.S.A

[25] Vilnay, M., Chernin, L., and Cotsovos, D., "Advanced material modeling of concrete in Abaqus", paper presented at CONFAB 2017, London, United Kingdom

[26] Cornelissen, HAW., Hordijk, DA. And Reinhardt HW, "Experimental determination of crack softening characteristics of normal weight and light weight concrete", Heron; 31(2): 45-56, 1986

[27] Jawed Qureshi and Dennis Lam, “Finite element modeling of shear connection behavior in push test using profiled sheeting”, September 2010

[28] Mr. Abhay Gujar, Dr. Sachin Pore and Dr. Vipul Prakash, “Modeling in ABAQUS for Experimental investigation of multi-linear bond-slip properties in reinforced concrete”, Pp. 155-163, March-2019

[29] Mekdes Tadesse, “Effects of spacing and configuration of web reinforcement on shear behavior of reinforced concrete beams”, 2015

[30] J. Shafaie, A. Hosseini, M. S. Marefat, “3D finite element modelling of bond-slip between Rebar and concrete in pull-out test”, The 3rd International Conference on Concrete and Development, Tehran, I.R. Iran, 2009

[31] Victor Gribniak, Alejandro perez Caldentey, Gintaris Kaklauskas and Alexandr Sokolov, “Effect of arrangement of tensile reinforcement on flexural stiffness and cracking”, Pp. 418-428, April 2016

[32] Sczecina Michal and Winnicki Andrzej, “Calibration of CDP model parameters in Abaqus”, Korea, August 25-29, 2015

APPENDIX A

MOMENT CURVATURE CALCULATION FOR FLEXURAL BEAMS LOADED WITH FOUR-POINT BENDING

For conventional beams,

- **A-2**

The moment curvature calculation for a 3.28m span simply supported experimental beam is shown below.

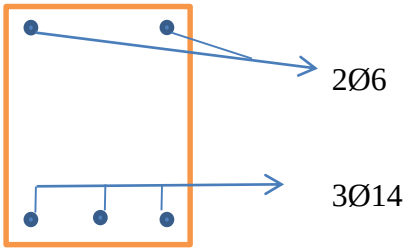

Figure A- 1 Cross section of the beam

According to the Ethiopian building code standard (ES EN 1992-1-1:2013) section 7.4.3, two limiting conditions are assumed to exist for the deformation of concrete sections.

1. Uncracked condition
2. Cracked condition

Members who are not supposed to be loaded above the point which would cause the concrete's tensile strength to be surpassed anywhere in the member shall be considered uncracked.

Members, required to crack, may behave in an intermediate manner between conditions that are uncracked and fully cracked.

$\alpha = \zeta\alpha_{II} + (1 - \zeta)\,\alpha_{I}$

Where: -

- α_I- for uncracked condition
- α_{II}- for cracked condition
- $\alpha_I = M/EI_1$-------region 1
- $\alpha_{II}=M/EI2$--------region 2
- $\zeta=1-\beta(M_{cr}/M)^2$

- β- 1 for short term loading
- M- applied moment by the four-point bending test plus induced moment due to equipment weight and beam's own weight
- M_{cr}- cracking moment
- I_1---moment of inertia of uncracked section
- I_2 ---moment of inertia of cracked section

Table A- 1 From the experimental beam considered

Beams	Ø	top Ø	c, mm	p,%	$A_{c,\,ef}$
A-2	3Ø14	2Ø6	20	0.548595992	19740

Experimentally applied moment- four-point bending

Nominal length of the beam- 3280 mm

Shear span- 1000 mm

Capacity of the hydraulic jack used– 1000 kN

Weight of loading equipment- 2.3 kN

Moment induced by beam's own weight and weight of equipment – 3.5 kNm

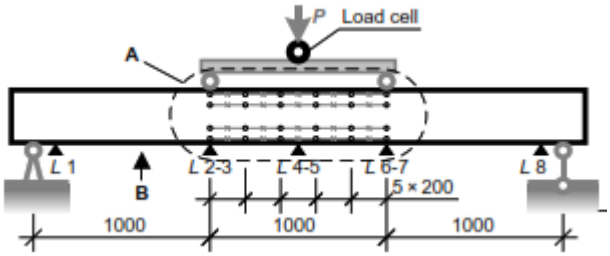

Figure A- 2 Four- point bending test loading system

Table A- 2 Size of the beam considered

Beam	H	d	B	d'
A-2	300	272	282	29

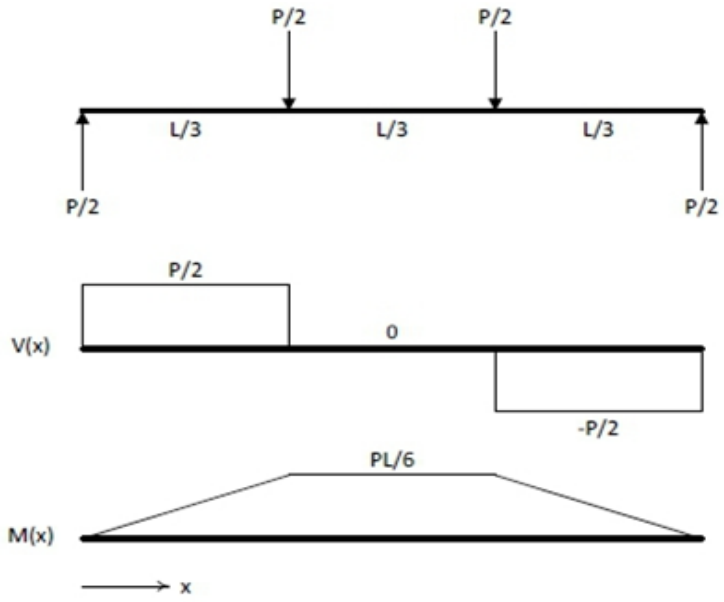

Figure A- 3 Free body, shear force, and bending moment diagrams for a simply supported beam in four-point bending mode

Taking sections in order to calculate bending moment,

Table A- 3 Sections for calculating moment

Regions	L, m	M(X)
0-L/3	0-1m	1/2PX
L/3-2/3L	1m-2m	1/6(PL)
2/3L-L	2m-3m	1/2P(L-X)

L- is considered from support to support only = 3 m

Moment in the pure bending zone: - M= 1/6*PL

=1/6*150.30637 kN*3m = 75.153186 kNm

The induced moment = 3.5 kNm

M total = **75.153186 kNm**

Area of top and bottom reinforcements for the beam under consideration,

As'-- (2Ø6) = (2*3.14* 6^2)/4 = 56.52 mm^2

As---- (3Ø14) = (3*3.14*14^2)/4 = 461.58 mm^2

From the experimental data used: - taking results from 28 days

For C30/37…...F_{ck}=45.52 N/mm^2

F_{yk} = 578.1 MPa

Reinforcement ratio calculation: -

P= As /bd = 461.58 mm^2/ (282*272) mm^2 = 0.0066

P'= As'/bd =56.52 mm^2/ (282*272) mm^2 = 0.000808

CURVATURE CALCULATION

According to ES EN 1992-1-1:2013: -

- Effective modulus of elasticity, $E_{c,eff}$ = Ecm/(1+Ø)
- Ecm= 22*(0.1*fcm)$^{0.3}$ = 22* (0.1 * 45.52)$^{0.3}$ = 34.664 kN/mm^2
- Fcm= fck+8 = 45.52 MPa (considering experimental results)
- $E_{c,eff}$ = Ecm-------when creep is ignored!
- $E_{c,eff}$ = 34.664 kN/mm^2
- Effective modular ratio, α_e =Es/ $E_{c,eff}$
- Es = 200kN/mm^2, (design value of modulus of elasticity from ES EN 1992-1-1:2013 section 3.2.7.4)
- α_e =200/34.664 = 5.769

UNCRACKED SECTION

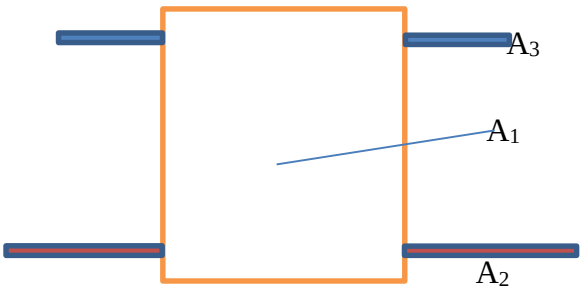

Figure A- 4 Equivalent transformed cross section

To calculate neutral axis depth of the uncracked section: -

- A_1=b*h= 282*300 = 84600 mm^2
- A_2= (α_e-1) *As = (5.769-1) * 461.58 = 2201.557 mm^2
- A_3 = (α_e-1) *As' = (5.769-1) *56.52 = 269.578 mm^2

Considering the top fiber as reference for the neutral axis,

- X_1=h/2 = 300/2 =150 mm
- X_2= d = 272 mm
- X_3= d' = 29 mm

$X= ((A1 * X1) + (A2 * X2) + (A3 * X3))/(A1 + A2 + A3)$

X= **152.7761mm**

- **Second moment of area of the uncracked section**: -
  - I1 = bh^3/12= 282*300^3/12= 634500000 mm^4
  - I2= 0
  - I3= 0
- Y_1= x-(h/2)= 152.7761mm-150mm = 2.7761 mm
- Y_2= d-x= 272mm-152.7761mm= 119.2239 mm
- Y_3= x-d'= 152.7761mm-29mm= 123. 7761 mm

Therefore: - $I_{uncraked} = I1 + I2 + I3 + (A1 * Y1^2) + (A2 * Y2^2) + (A3 * Y3^2)$

=634500000 + (84600 *2.7761^2) + (2256.77997*119.2239^2) + (276.3404044*123. 7761^2)

I_{unc} =**671464303mm^4**

CRACKED SECTION

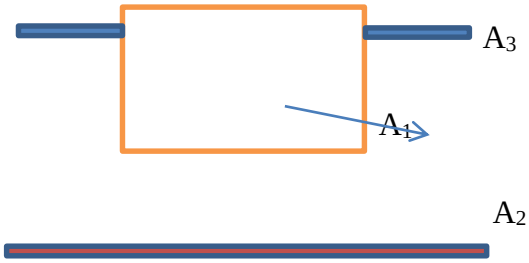

Figure A- 5 Equivalent transformed cracked cross section

Neutral axis depth can be considered by taking the static moments of the shaded areas about the centroidal axis.

1/2b*(kx*d) ^{2}+(αe-1) As'(kx*d-d') =V=αe*As(d-kx*d)

Dividing this by bd^2 and taking P=As/bd and P' =As'/bd, then: -

kx=x/d=-[α_ep+(α_e-1) *p'] + sqrt[(α_ep+(α_e-1) p')^2+2*(α_ep+(α_e-1) p'*d'/d]

Kx= X/d = 0.2406732

X= 0.2406732d

X= **59.686962mm**

❖ **Second moment of area of the cracked section: -**

- $I1 = bh^3/12 = 282*59.686962^3/12 = 4943805.55\ mm^4$
- $I2 = 0$
- $I3 = 0$
- $A1 = b*h = 282*59.686962 = 16831.72\ mm^2$
- $A2 = \alpha_e * As = 5.889249902*461.58 = 2718.36\ mm^2$
- $A_3 = (\alpha_e - 1) * As' = (5.889249902-1) *56.52 = 276.3404044\ mm^2$

- $Y_1 = x-(x/2) = 59.686962mm-(59.686962mm/2) = 29.84348mm$
- $Y_2 = d-x = 272mm-59.686962mm = 212.313mm$
- $Y_3 = x-d' = 59.686962mm-29mm = 30.68696\ mm$

Therefore: - $I_{cracked} = I1 + I2 + I3 + (A1 * Y1^2) + (A2 * Y2^2) + (A3 * Y3^2)$

$= \mathbf{142729966.3mm^4}$

Cracking moment calculation: -

$Mcr = f_{ctm} * I_{un}/Y_t$

For C 30/37-----$f_{ctm} = 2.9\ N/mm^2$……. (EBCS table 3.1)

Yt= h-x= 300-152.776 = 147.2239mm

$Mcr = (2.9N/mm^2 * 671464303mm^4)/ 147.2239mm = 13226429Nmm$

Mcr= 13.226429KNm

- Applied moment M= 75.153186 kNm
- Cracking moment Mcr= 13.226429KNm

Mcr<M---------section has cracked!

❖ Curvature of the uncracked section

$\alpha_l = M/ (E_{c,eff} * I_{uncracked}) = (75.153186*10^6)/(33.96018225*10^3*671464303)$

$= 3.2957*10^{-6}\ mm^{-1}$

❖ Curvature of the cracked section

$\alpha_2 = M/ (E_{c,eff} * I_{cracked}) = (75.153186*10^6)/(33.96018225*10^3*142729966.3)$

$=1.5504*10^{-5}\ mm^{-1}$

- Intermediate curvature values of the section

$\alpha = \zeta\alpha_{II} + (1 - \zeta)\ \alpha_{I}$

Mcr/M= (13.226429KNm/75.153186 KNm) = 0.17599

Taking the whole section, the next table shows the moment and curvature of the whole section.

Table A- 4 Moment curvature table according to ES EN 1992-1-1:2013

x/L	M(x),kNm	αl[*10^-6]	αll[*10^-6]	(Mcr/M)^2	ζ	α[*10^-6]
0	0	0	0	0	1	0
0.25	18.788	0.823	3.876	0.495	0.504	2.363
0.5	37.576	1.647	7.752	0.123	0.876	6.996
0.75	56.364	2.471	11.628	0.055	0.944	11.124
1	75.153	3.295	15.504	0.031	0.969	15.126
1.25	75.153	3.295	15.504	0.031	0.969	15.126
1.5	75.153	3.295	15.504	0.031	0.969	15.126
1.75	75.153	3.295	15.504	0.031	0.969	15.126
2	75.153	3.295	15.504	0.031	0.969	15.126
2.25	56.364	2.471	11.628	0.055	0.944	11.124
2.5	37.576	1.647	7.752	0.123	0.876	6.996
2.75	18.788	0.823	3.876	0.495	0.504	2.363
3	0	0	0	0	1	0

- Having this, the moment curvature graph of the experimental beam as evaluated with the Ethiopian building code standard ES EN 1992-1-1:2013: -

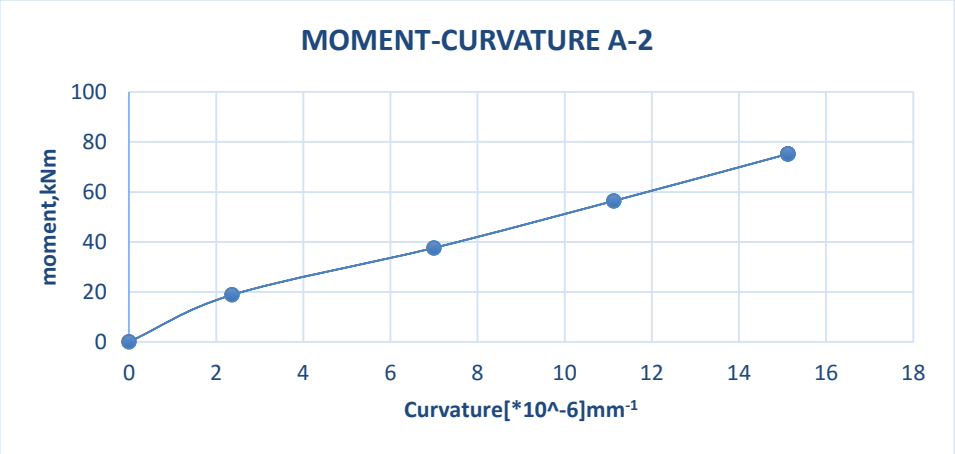

Figure A- 6 Moment curvature graph of the beam

APPENDIX B

CRACKING ANALYSIS ACCORDING TO ES EN 1992-1-1:2013 CODE

FOR B-1

Cover-20mm

Table B- 1 Cross section of the beam

Beam	H	D	b	d'
B-1	299	248	282	25

According to ES EN 1992-1-1:2013: -

Crack spacing ($s_{r,max}$): -

$$s_{r,\max} = k_3 \cdot c + k_1 \cdot k_2 \cdot k_4 \cdot \frac{\varnothing_s}{\rho_{s,eff}}.$$

Where: -

- c is the cover depth (mm) and
- $\varnothing_s$ is the bar diameter (mm).
- k_3= 3.4 and k_4=0.425;
- k_1 is a coefficient which accounts for the bond properties of steel bars (= 0.8 for corrugated bars and = 1.6 for smooth bars);
- k_2 is a coefficient which takes account of the form of strain distribution along the cross section (= 0.5 for bending and = 1 for pure tension).

$P_{ef} = A_s/A_{ce}$

$A_{ce}=h_{c,ef}$*b(width)

Table B- 2 Properties of the section

Beam	Ø,mm	As_1	As_2	E_s	E_{cm}
B-1	9Ø10	707	56.52	209.5	34.664

$n= E_s/E_{cm}$

=209.5/34.664= 6.0437

$\rho_1 = A_{s1}/(b*d)$ = 707/(282*248)= 0.010102

$\rho_2 = A_{s2}/(b*d)$ =56.52/(282*248)= 0.00081

$h_{c,ef}$ = min { 2.5*(h-d) ; (h-x)/3 ; h/2 }

$$X = n\rho_1\left(1+\frac{\rho_2}{\rho_1}\right)\left[-1+\sqrt{1+2\left(1+\frac{\rho_2 d'}{\rho_1 d}\right)/\left(n\rho_1\left(1+\frac{\rho_2}{\rho_1}\right)^2\right)}\right]d$$

X=6.0437*0.010102(1+0.00081/0.010102)*[-1+sqrt(1+2(1+(0.00081*25)/ (0.010102*248)) / (6.0437*0.010102*(1+0.00081/0.010102)^2)]*248

X=72.1805 mm

$h_{c,ef}$= 2.5* (299-248)=127.5 mm

min { (299-72.1805)/3= 75.6065 mm ; 299/2= 149.5 mm }

$h_{c,ef}$= 75.6065mm

$A_{c,ef}$= $h_{c,ef}$*b= 75.6065mm* 282mm =21321.033 mm^2

$P_{s,ef}$ =A_s/$A_{c,ef}$

= (707/21321.033) *100 = 3.3159%

$S_{r,max}$= 3.4*20+ 0.8*0.5*0.425*(10/0.033159)

=**<u>119.268 mm</u>**

APPENDIX C

Table C- 1 Strength and deformation characteristics of concrete according to ES EN 1992-1-1:2013

Strength classes for concrete																Analytical relation / Explanation
f_{ck} (MPa)	12	16	20	25	30	35	40	45	50	55	60	70	80	90		
$f_{ck,cube}$ (MPa)	15	20	25	30	37	45	50	55	60	67	75	85	95	105		
f_{cm} (MPa)	20	24	28	33	38	43	48	53	58	63	68	78	88	98		$f_{cm} = f_{ck} + 8$ (MPa)
f_{ctm} (MPa)	1.6	1.9	2.2	2.6	2.9	3.2	3.5	3.8	4.1	4.2	4.4	4.6	4.8	5.0		$f_{ctm} = 2.12 \ln(1+(f_{cm}/10)) \geq C50/60$
$f_{ctk,0.05}$ (MPa)	1.1	1.3	1.5	1.8	2.0	2.2	2.5	2.7	2.9	3.0	3.1	3.2	3.4	3.5		$f_{ctk,0.05} = 0.7 \times f_{ctm}$ 5 % fractile
$f_{ctk,0.95}$ (MPa)	2.0	2.5	2.9	3.3	3.8	4.2	4.6	4.9	5.3	5.5	5.7	6.0	6.3	6.6		$f_{ctk,0.95} = 1.3 \times f_{ctm}$ 95 % fractile
E_{cm} (GPa)	27	29	30	31	33	34	35	36	37	38	39	41	42	44		$E_{cm} = 22[(f_{cm})/10]^{0.3}$ (f_{cm} in MPa)
ε_{c1} (‰)	1.8	1.9	2.0	2.1	2.2	2.25	2.3	2.4	2.45	2.5	2.6	2.7	2.8	2.8		See Figure 3.2 ε_{c1} (‰) = $0.7 f_{cm}^{0.31} \leq 2.8$
ε_{cu1} (‰)	3.5									3.2	3.0	2.8	2.8	2.8		See Figure 3.2 for $f_{ck} \geq 50$ MPa ε_{cu1} (‰) = $2.8 + 27[(98 - f_{cm})/100]^4$
ε_{c2} (‰)	2.0									2.2	2.3	2.4	2.5	2.6		See Figure 3.3 for $f_{ck} \geq 50$ MPa ε_{c2} (‰) = $2.0 + 0.085[(f_{ck}-50)^{0.53}$
ε_{cu2} (‰)	3.5									3.1	2.9	2.7	2.6	2.6		See Figure 3.3 for $f_{ck} \geq 50$ MPa ε_{cu2} (‰) = $2.6 + 35[(90 - f_{ck})/100]^4$
n	2.0									1.75	1.6	1.45	1.4	1.4		for $f_{ck} \geq 50$ MPa $n = 1.4 + 23.4\,[(90 - f_{ck})/100]^4$
ε_{c3} (‰)	1.75									1.8	1.9	2.0	2.2	2.3		See Figure 3.4 for $f_{ck} \geq 50$ MPa ε_{c3} (‰) = $1.75 + 0.55[(f_{ck} - 50)/40]$
ε_{cu3} (‰)	3.5									3.1	2.9	2.7	2.6	2.6		See Figure 3.4 for $f_{ck} \geq 50$ MPa ε_{cu3} (‰) = $2.6 + 35[(90 - f_{ck})/100]^4$

Table 3.1 Strength and deformation characteristics for concrete

APPENDIX D

COMPRESSIVE AND TENSILE BEHAVIOR OF CONCRETE

This excel sheet can work for any concrete grade.

$f_{ck,\ MPa}$	37.52	
f_{cm}	45.52	Taking experimental value
E_{cm}	34.6643736	
ε_{c1}	2.2863396	
K	1.82814711	
$0.4f_{cm}$	18.208	
K-2	-0.1718529	
$\frac{(k-2)*\sigma_c}{fcm}$	-0.0687412	
Str/f_{cm}	0.4	

$$\frac{\sigma_c}{f_{cm}} = \frac{k\eta - \eta^2}{1+(k-2)\eta}$$

Where:

$\eta = \varepsilon_c / \varepsilon_{c1}$

ε_{c1} is the strain at peak stress according to Table 3.1

$k = 1.05\, E_{cm} \times |\varepsilon_{c1}| / f_{cm}$ (f_{cm} according to Table 3.1)

E_{cm}	f_{cm}	σ=0.4*f_{cm}
34.6643736	45.52	0.4*45.52=18.208
ε_c	$\boldsymbol{\sigma}/E_{cm}$	0.525265

Compressive behavior of concrete

	$\boldsymbol{\varepsilon_c}$	$\boldsymbol{\eta}$		$\boldsymbol{\sigma}$	$\boldsymbol{\varepsilon_{oc}}$	$\boldsymbol{\varepsilon_c/1000}$
@ yield stress	0	0		0	0	0
ε_c	0.525265	0.2297405		18.208	0.52526551	0.0002414
Shall be equally spaced with small gaps	0.6	0.26242821		19.587014	0.56504739	0.0006
	0.75	0.32803526		23.7381262	0.68479894	0.00075
	0.9	0.39364231		27.5693412	0.79532207	0.0009
	1.05	0.45924936		31.0689117	0.89627789	0.00105
	1.2	0.52485641		34.224508	0.98731073	0.0012
	1.35	0.59046346		37.0231812	1.06804703	0.00135
	1.5	0.65607052		39.4513248	1.13809426	0.0015
	1.65	0.72167757		41.4946313	1.1970397	0.00165
	1.8	0.78728462		43.1380472	1.24444906	0.0018
	1.95	0.85289167		44.3657235	1.27986514	0.00195
@ultimate stress	2.1	0.91849872		45.1609624	1.30280624	0.0021
	2.25	0.98410577		45.5061598	1.31276452	0.00225
ε_{c_1}	2.2863396	1		45.52	1.31316378	0.002286
Shall be equally spaced with small gaps	2.3	1.00597479		45.5180354	1.31310711	0.0023
	2.45	1.07158184		45.2341093	1.30491639	0.00245
	2.6	1.13718889		44.4551808	1.28244581	0.0026
	2.75	1.20279594		43.160144	1.24508651	0.00275
	2.9	1.268403		41.3266762	1.19219452	0.0029
	3.05	1.33401005		38.9311481	1.12308818	0.00305
	3.2	1.3996171		35.9485276	1.03704536	0.0032
	3.35	1.46522415		32.3522736	0.93330039	0.00335
Crushing strain	3.5	1.5308312		28.1142205	0.81104078	0.0035

Table D- 1 Inputs for Abaqus considering compressive behavior of concrete

Inputs for ABAQUS (stress vs inelastic strain)		Inputs for ABAQUS (damage vs inelastic strain)	
σ	ε_{in}	d_c	ε_{in}
18.208	0	0	0
19.58701399	3.50E-05	0	3.50E-05
23.73812616	6.52E-05	0	6.52E-05
27.56934123	0.000104678	0	0.000104678
31.06891174	0.000153722	0	0.000153722
34.22450795	0.000212689	0	0.000212689
37.02318124	0.000281953	0	0.000281953
39.4513248	0.000361906	0	0.000361906
41.49463131	0.00045296	0	0.00045296
43.13804724	0.000555551	0	0.000555551
44.36572353	0.000670135	0	0.000670135
45.16096241	0.000797194	0	0.000797194
45.50615976	0.000937235	0	0.000937235
45.52	0.000973176	0	0.000973176
45.51803538	0.000986893	4.32E-05	0.000986893
45.2341093	0.001145084	0.00628055	0.001145084
44.45518076	0.001317554	0.02339234	0.001317554
43.16014403	0.001504913	0.05184218	0.001504913
41.32667619	0.001707805	0.09212047	0.001707805
38.93114814	0.001926912	0.14474631	0.001926912
35.94852764	0.002162955	0.2102696	0.002162955
32.35227358	0.0024167	0.28927343	0.0024167
28.11422054	0.002688959	0.38237653	0.002688959

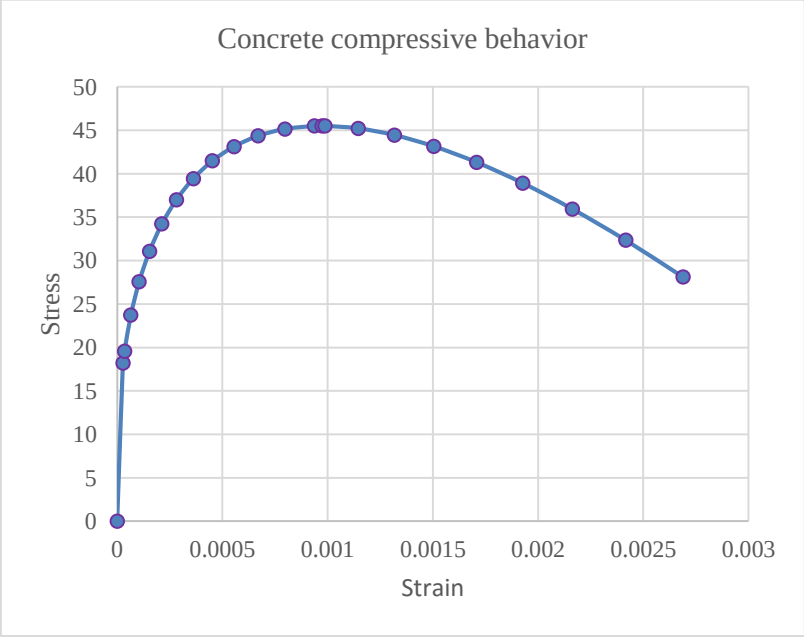

Figure D- 1 Compressive behavior of concrete

Tensile Behavior of concrete

f_{cm} (MPa)	45.52
f_{ck} (MPa)	37.52
f_{ctm} (MPa)	3.362248
G_f (N/m)	145.14406

w(m)	σ_t(MPa)	w(mm)	d_t
0	3.362248	0	0
4.3169E-05	0.6724497	0.043168	0.8
0.00022189	0	0.221887	1

Table D- 2 Inputs for Abaqus considering tensile behavior of concrete

w(m)	σ_t(MPa)	d_t	w(mm)	
0	3.362248495	0	0	0.19212849
3.08348E-06	3.17012001	0.057142857	0.003083482	
6.16696E-06	2.977991524	0.114285714	0.006166964	
9.25045E-06	2.785863039	0.171428571	0.009250446	
1.23339E-05	2.593734553	0.228571429	0.012333928	
1.54174E-05	2.401606068	0.285714286	0.01541741	
1.85009E-05	2.209477582	0.342857143	0.018500892	
2.15844E-05	2.017349097	0.4	0.021584374	
2.46679E-05	1.825220612	0.457142857	0.024667856	
2.77513E-05	1.633092126	0.514285714	0.027751338	
3.08348E-05	1.440963641	0.571428571	0.03083482	
3.39183E-05	1.248835155	0.628571429	0.033918302	
3.70018E-05	1.05670667	0.685714286	0.037001784	
4.00853E-05	0.864578184	0.742857143	0.040085266	
4.31687E-05	0.672449699	0.8	0.043168748	0.06724497
6.10406E-05	0.605204729	0.82	0.06104061	
7.89125E-05	0.537959759	0.84	0.078912472	
9.67843E-05	0.470714789	0.86	0.096784334	
0.000114656	0.403469819	0.88	0.114656196	
0.000132528	0.336224849	0.9	0.132528058	
0.0001504	0.26897988	0.92	0.15039992	
0.000168272	0.20173491	0.94	0.168271782	
0.000186144	0.13448994	0.96	0.186143643	
0.000204016	0.06724497	0.98	0.204015505	
0.000221887	0	0.99	0.22188737	

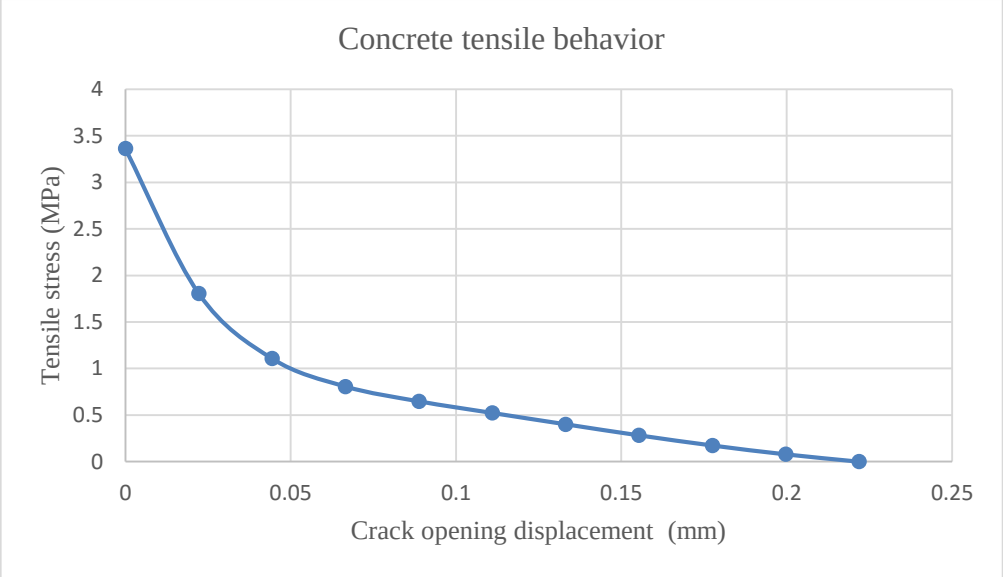

Figure D- 2 Tensile behavior of concrete

To check the adequacy of the damage curve in the tensile behavior

$$\tilde{\varepsilon}_t^{pl} = \tilde{\varepsilon}_t^{ck} - \frac{d_t}{(1-d_t)} \frac{\sigma_t}{E_0}$$

If this result is negative/decreasing---it will generate an error on Abaqus

w(mm)	d_t	σ_t(Mpa)	E_o	ε_{pl}	
0	0	3.362248495	34664.37361	0	
0.003083482	0.057142857	3.17012001	34664.37361	0.003077939	0.003077939
0.006166964	0.114285714	2.977991524	34664.37361	0.006155879	0.003077939
0.009250446	0.171428571	2.785863039	34664.37361	0.009233818	0.003077939
0.012333928	0.228571429	2.593734553	34664.37361	0.012311758	0.003077939
0.01541741	0.285714286	2.401606068	34664.37361	0.015389697	0.003077939
0.018500892	0.342857143	2.209477582	34664.37361	0.018467637	0.003077939
0.021584374	0.4	2.017349097	34664.37361	0.021545576	0.003077939
0.024667856	0.457142857	1.825220612	34664.37361	0.024623516	0.003077939
0.027751338	0.514285714	1.633092126	34664.37361	0.027701455	0.003077939
0.03083482	0.571428571	1.440963641	34664.37361	0.030779395	0.003077939
0.033918302	0.628571429	1.248835155	34664.37361	0.033857334	0.003077939
0.037001784	0.685714286	1.05670667	34664.37361	0.036935274	0.003077939
0.040085266	0.742857143	0.864578184	34664.37361	0.040013213	0.003077939
0.043168748	0.8	0.672449699	34664.37361	0.043091153	0.003077939
0.06104061	0.82	0.605204729	34664.37361	0.060961075	0.017869922
0.078912472	0.84	0.537959759	34664.37361	0.078830997	0.017869922
0.096784334	0.86	0.470714789	34664.37361	0.096700919	0.017869922
0.114656196	0.88	0.403469819	34664.37361	0.114570841	0.017869922
0.132528058	0.9	0.336224849	34664.37361	0.132440763	0.017869922
0.15039992	0.92	0.26897988	34664.37361	0.150310685	0.017869922
0.168271782	0.94	0.20173491	34664.37361	0.168180607	0.017869922
0.186143643	0.96	0.13448994	34664.37361	0.186050529	0.017869922
0.204015505	0.98	0.06724497	34664.37361	0.203920451	0.017869922
0.221887367	0.99	0	34664.37361	0.221887367	0.017966916

Table D- 3 Adequacy of the damage curve in the tensile behavior

To check the adequacy of the damage curve in the compressive behavior

$$\tilde{\varepsilon}_c^{pl} = \tilde{\varepsilon}_c^{in} - \frac{d_c}{(1-d_c)} \frac{\sigma_c}{E_0}$$

If this result is negative/decreasing---it will generate an error on Abaqus

σ	ε_{in}	d_c	E_o	ε_{pl}	
0	0	0	34664.37361	0	
18.208	2.72473E-05	0	34664.37361	2.72473E-05	2.72473E-05
19.58701399	3.49526E-05	0	34664.37361	3.49526E-05	7.70528E-06
23.73812616	6.52011E-05	0	34664.37361	6.52011E-05	3.02485E-05
27.56934123	0.000104678	0	34664.37361	0.000104678	3.94769E-05
31.06891174	0.000153722	0	34664.37361	0.000153722	4.90442E-05
34.22450795	0.000212689	0	34664.37361	0.000212689	5.89672E-05
37.02318124	0.000281953	0	34664.37361	0.000281953	6.92637E-05
39.4513248	0.000361906	0	34664.37361	0.000361906	7.99528E-05
41.49463131	0.00045296	0	34664.37361	0.00045296	9.10546E-05
43.13804724	0.000555551	0	34664.37361	0.000555551	0.000102591
44.36572353	0.000670135	0	34664.37361	0.000670135	0.000114584
45.16096241	0.000797194	0	34664.37361	0.000797194	0.000127059
45.50615976	0.000937235	0	34664.37361	0.000937235	0.000140042
45.52	0.000973176	0	34664.37361	0.000973176	3.59403E-05
45.51803538	0.000986893	4.31595E-05	34664.37361	0.000986836	1.36604E-05
45.2341093	0.001145084	0.006280551	34664.37361	0.001136836	0.00015
44.45518076	0.001317554	0.023392338	34664.37361	0.001286836	0.00015
43.16014403	0.001504913	0.051842179	34664.37361	0.001436836	0.00015
41.32667619	0.001707805	0.09212047	34664.37361	0.001586836	0.00015
38.93114814	0.001926912	0.144746306	34664.37361	0.001736836	0.00015
35.94852764	0.002162955	0.210269604	34664.37361	0.001886836	0.00015
32.35227358	0.0024167	0.289273428	34664.37361	0.002036836	0.00015
28.11422054	0.002688959	0.382376526	34664.37361	0.002186836	0.00015

Table D- 4 Adequacy of the damage curve in the compressive behavior

APPENDIX E

CRACKING ANALYSIS FOR TENSILE BEAM ACCORDING TO EBCS CODE

FOR B-1

Cover-30mm

Crack spacing ($s_{r,max}$): -

$$s_{r,\max} = k_3 \cdot c + k_1 \cdot k_2 \cdot k_4 \cdot \frac{\emptyset_s}{\rho_{s,eff}}.$$

Where: -

- c is the cover depth (mm) and
- $\emptyset_s$ is the bar diameter (mm).
- k_3= 3.4 and k_4=0.425;
- k_1 is a coefficient which accounts for the bond properties of steel bars (= 0.8 for corrugated bars and = 1.6 for smooth bars);

k_2 is a coefficient which takes account of the form of strain distribution along the cross section (= 0.5 for bending and = 1 for pure tension).

Table E- 1 Properties of the tensile beam

Beam	Ø,mm	P%	Ø/P	C,mm
B-1	4Ø10	1.415	706.7138	30

Sr,max = 3.4*30 + (0.8*1*0.425*706.7138)

=342.28mm